

DeceFL: A Principled Decentralized Federated Learning Framework

Ye Yuan^{1,2,*}, Jun Liu^{3,*}, Dou Jin^{1,*}, Zuogong Yue^{1,*}, Ruijuan Chen¹, Maolin Wang¹, Chuan Sun¹, Lei Xu⁴, Feng Hua², Xin He², Xinlei Yi⁵, Tao Yang⁴, Hai-Tao Zhang^{1,2}, Shaochun Sui⁶, Han Ding²

Abstract

Traditional machine learning relies on a centralized data pipeline, i.e., data are provided to a central server for model training. In many applications, however, data are inherently fragmented. Such a decentralized nature of these databases presents the biggest challenge for collaboration: sending all decentralized datasets to a central server raises serious privacy concerns. Although there has been a joint effort in tackling such a critical issue by proposing privacy-preserving machine learning frameworks, such as federated learning, most state-of-the-art frameworks are built still in a centralized way, in which a central client is needed for collecting and distributing model information (instead of data itself) from every other client, leading to high communication pressure and high vulnerability when there exists a failure at or attack on the central client. Here we propose a principled decentralized federated learning algorithm (DeceFL), which does not require a central client and relies only on local information transmission between clients and their neighbors, representing a fully decentralized learning framework. It has been further proven that every client reaches the global minimum with zero performance gap and achieves the same convergence rate $O(1/T)$ (where T is the number of iterations in gradient descent) as centralized federated learning when the loss function is smooth and strongly convex. Finally, the proposed algorithm has been applied to a number of applications to illustrate its effectiveness for both convex and nonconvex loss functions, demonstrating its applicability to a wide range of real-world medical and industrial applications.

¹School of Artificial Intelligence and Automation, Huazhong University of Science and Technology. ²School of Mechanical Science and Engineering, Huazhong University of Science and Technology. ³Department of Applied Mathematics, University of Waterloo. ⁴State Key Laboratory of Synthetical Automation for Process Industries, Northeastern University. ⁵School of Electrical Engineering and Computer Science, and Digital Futures, KTH Royal Institute of Technology. ⁶AVIC Chengdu Aircraft Industrial (Group) Co., Ltd.. *Equal contributions. Email: yye@hust.edu.cn.

An urgent challenge for AI application today consists of the following dilemma concerning data privacy: on one hand, a large number of sophisticated algorithms have been proposed to broaden the applicability of AI to various applications such as medicine, manufacturing and more [1], [2], [3]; on the other hand, regulations such as General Data Protection Regulation (GDPR) restrict data sharing, thus limiting the performance of AI algorithms [4]. As a result, models that are trained and evaluated on a limited amount of data due to privacy could have biases [5]. This has become a well-known bottleneck in medical AI [6].

Promising privacy-preserving methods such as federated learning can help maintain the performance of AI algorithms, while preserving the data stored locally [7]. Inspired by this, there has been a surge of interests in both the theory and applications of federated learning [8]. Federated averaging (FedAvg), the leading algorithm in the field of federated learning, was proposed in 2016 by researchers at Google [9], [10]. Through crowded efforts and comprehensive surveys [11], [12], [13], [14], widely used federated learning methods were established, the challenges and related applications of federated learning were introduced, and a large number of valuable research directions were outlined. A notable example has been demonstrated in a report by Kaassis et al. [15], in which a convolutional neural network was trained over the public Internet with encryption from medical images using a secure federated learning framework.

Despite these breakthrough, classical federated learning algorithms have a major drawback: the need for a central client, which could cause privacy, communication, computation, and resilience issues [16]. Much effort, therefore, has been invested to reduce the communication and computational complexity of centralized federated learning algorithms. In order to deal with the challenge of system constraints, the authors of [17] applied sparse technology to reduce the communication and computing costs in the training process. In addition, the authors in [18] proposed an optimal tradeoff control algorithm between local update and global parameter aggregation in the resource constrained system. Recently, federated schemes can be extended to a time-varying centralized scheme, where a changing leader is selected based on certain rules, which is a firm step to full decentralization [19].

Here we propose the first principled decentralized federated learning algorithm, in which each client is guaranteed to achieve the same performance as the centralized algorithm in terms of training/test accuracy, when the global objective function is smooth and strongly convex. Empirical experiments have also demonstrated that the same claim holds for nonconvex global objective functions, thus revealing its potential to be applied to a wider class of applications such as those using deep learning. In addition to desirable features that other state-of-the-art federated learning and swarm learning algorithms possess, DeceFL has additional desirable features beyond classical centralized federated learning and swarm learning, namely: 1) full decentralization: at any iteration, there is no central

client that can receive all other clients' information, therefore avoiding data leakage; 2) principled: it has been proved that zero performance gap can be achieved when the loss function is strongly convex; 3) flexible communication topology design: any connected network structure suffices to achieve the training task; 4) all clients in the network can have the trained model, incentivizing clients to participate.

THE PROPOSED DECENTRALIZED FEDERATED LEARNING FRAMEWORK

A. Problem formulation

We first formulate the decentralized federated learning problem theoretically: assuming that there are K clients with local data in the form for standard machine learning tasks: \mathcal{D}_k for $k \in \{1, 2, \dots, K\}$. The training of AI models can be formulated as the following global learning problem (let $\mathcal{D} \triangleq \cup_k \mathcal{D}_k$ and $\cap_k \mathcal{D}_k = \emptyset$):

$$\mathcal{M}_c \triangleq \arg \min_{\mathcal{M}} F(\mathcal{D}; \mathcal{M}).$$

Such an optimization problem cannot be directly solved without centralized information \mathcal{D} . However, clients would like to collaboratively train a model \mathcal{M}_d using the same objective function F , in which the k -th client does not send its data \mathcal{D}_k to others. We define the performance gap as a nonnegative metric, which quantifies the degenerative performance between a centralized model and a decentralized one:

$$\Delta \triangleq F(\mathcal{D}; \mathcal{M}_c) - F(\mathcal{D}; \mathcal{M}_d).$$

The goal is to make Δ as small as possible, in the ideal case $\Delta = 0$.

B. The proposed DeceFL algorithm

To solve the optimization problem in a decentralized way, we model the communication network between clients as an undirected connected¹ graph $\mathcal{G} = (\mathcal{N}, \mathcal{E}, W)$, where $\mathcal{N} := \{1, 2, \dots, K\}$ represents the set of clients, and $\mathcal{E} \subseteq \mathcal{N} \times \mathcal{N}$ represents the set of communication channels, each connecting two distinct clients. For each edge $(i, j) \in \mathcal{E}$, the corresponding element in the adjacency matrix W , i.e., W_{ij} indicates whether there is a communication channel between the i -th client and the j -th client. Specifically, when $W_{ij} > 0$, there is information communication between clients i and j , while $W_{ij} = 0$ means none. For client i , when $W_{ij} > 0$, then client j is called a neighbor of client i . The set of all such clients j is represented as \mathcal{N}_i , i.e., $\mathcal{N}_i = \{j | W_{ij} > 0, \forall j \in \mathcal{N}\}$. Define the local loss function

¹In this work, we consider that the information communication between clients is mutual for notational simplicity; therefore, the adjacency matrix $W = [W_{kj}] \in \mathbb{R}^{K \times K}$ is symmetric. Further we assume that the underlying topology is connected, i.e., for any two clients k and j , there is at least one path from k to j .

$F_k(w) \triangleq F(\mathcal{D}_k; \mathcal{M})$ as the user-specified loss function on the dataset \mathcal{D}_k with model parameters w in \mathcal{M} , then $F(\mathcal{D}; \mathcal{M})$ can be rewritten as $F(w) \triangleq \frac{1}{K} \sum_{k=1}^K F_k(w)$. Let the client k hold a local copy of the global variable w , which is denoted by $w_k \in \mathbb{R}^n$, and $\mathbf{w} = [w_1; \dots; w_K] \in \mathbb{R}^{Kn}$. Specifically, the update rule of DeceFL is, for each client $k = 1, \dots, K$,

$$w_k(t+1) = \underbrace{\sum_{j=1}^K W_{kj} w_j(t)}_{\text{average of neighbors' estimates}} - \underbrace{\eta_t \nabla F_k(w_k(t))}_{\text{gradient descent}}, \quad (1)$$

where $\eta_t > 0$ is the learning rate, and the initial condition $w_k(0) \in \mathbb{R}^n$ can be arbitrarily chosen. Every client is sharing with its neighbors (which is a subset of all other clients) their model parameters rather than their data. Specifically, every client is running its local training algorithm, e.g., gradient descent, and it only communicates its own estimate of the global parameter with its neighbors. Once a client receives other estimates from neighboring clients, it averages out other estimates, adds to its local gradient and generates its estimate in the next iteration. The above process will be repeated until convergence. As shown in Figure 1, in DeceFL, each client completes the update by receiving and transmitting directly with neighbor clients and local gradient calculation, without needing the aggregation and transmission of a third-party central client at any iteration. Thus, it is fully decentralized.

We stack the $w_k(t)$ and $\nabla F_k(w_k(t))$ in (1) into vectors, i.e., define $\mathbf{w}(t) = [w_1(t)^T, \dots, w_K(t)^T]^T \in \mathbb{R}^{Kn}$ and $\nabla F(\mathbf{w}(t)) = [\nabla F_1(w_1(t))^T, \dots, \nabla F_K(w_K(t))^T]^T \in \mathbb{R}^{Kn}$. Then, we can compactly rewrite (1) as

$$\mathbf{w}(t+1) = (W \otimes \mathbf{I}_n) \mathbf{w}(t) - \eta_t \nabla F(\mathbf{w}(t)), \quad (2)$$

where $W = [W_{ij}] \in \mathbb{R}^{K \times K}$ and $\mathbf{I}_n \in \mathbb{R}^{n \times n}$ is the identity matrix. Next, we analyze the convergence of DeceFL under the following assumptions about the global cost function, which is consistent with those made in the convergence analysis of FedAvg [20].

Assumption 1: For each $k = 1, \dots, K$, assume that F_k is L_k -smooth and μ_k -strongly convex, where $L_k, \mu_k > 0$. That is, F_k is differentiable and the gradient is L_k -Lipschitz continuous, i.e., for any $x, y \in \mathbb{R}^n$,

$$\|\nabla F_k(x) - \nabla F_k(y)\| \leq L_k \|x - y\|, \quad (3)$$

and

$$F_k(x) \geq F_k(y) + \langle \nabla F_k(y), x - y \rangle + \frac{\mu_k}{2} \|x - y\|^2. \quad (4)$$

When Assumption 1 holds, the global objective function $F(\cdot)$ is L -smooth and μ -strongly convex, where $L = \max\{L_1, \dots, L_K\}$ and $\mu = \min\{\mu_1, \dots, \mu_K\}$. Clearly, $\mu \leq L$.

Assumption 1 is standard and satisfied by typical loss functions in machine learning, including l_2 -regularized linear regression and l_2 -regularized logistic regression. In order to analyze the convergence

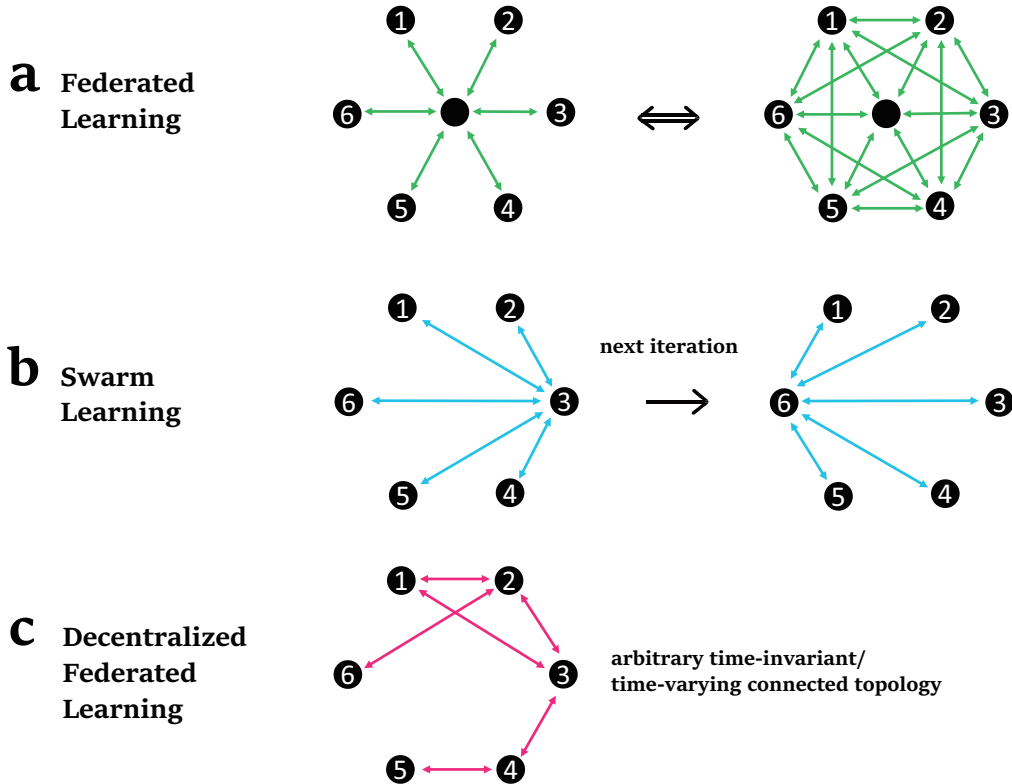


Fig. 1. Illustration of key concepts in different state-of-the-art federated learning frameworks. **a**, Classical Federated Learning: a central client is needed to receive and transmit all essential information to other clients. It is equivalent to an all-to-all network without such a central center, i.e., every client in the network can receive information from all other clients. **b**, Swarm Learning: there is no such a universal central client, but a potentially different central client is selected in every iteration. Mathematically, it is equivalent to FedAvg with varying central clients. **c**, The proposed Decentralized Federated Learning: there is no need for a central client in any iteration. Any connected time-invariant/time-varying topology would work, therefore unifying the classical federated learning and swarm learning.

of the algorithm, we define the average sequence $\bar{w}(t) = \frac{1}{K}(\mathbf{1}_K^T \otimes \mathbf{I}_n)\mathbf{w}(t) = \frac{1}{K}\sum_{k=1}^K w_k(t)$, where $\mathbf{1}_K \in \mathbb{R}^K$ is a vector in which all elements are 1. Denote λ as the spectral norm of $W - \frac{1}{K}\mathbf{1}\mathbf{1}^T$, where $\lambda \in (0, 1)$ from algebraic graph theory (Supplementary Information).

Theorem 1: Consider algorithm (1), where the learning rate chosen by $\eta_t = \frac{\delta}{t+\Gamma}$, in which $\delta > \frac{1}{\mu}$ and $\Gamma > \frac{\lambda}{1-\lambda}$ satisfying $\frac{\delta}{\Gamma} \leq \frac{1}{L}$. Denote the gap between the average local optimal value and the local function value at the initial point $\mathbf{w}(0)$, as $\varepsilon_0 \triangleq \sum_{k=1}^K (F_k(w_k(0)) - F_k(w_k^*)) \geq 0$, where $w_k^* = \arg \min_{w_k} F_k(w_k)$. Then the following inequality can be obtained under Assumption 1:

$$\|\mathbf{w}(t) - \mathbf{1} \otimes \bar{w}(t)\| \leq \frac{\zeta}{t + \Gamma}, \quad (5)$$

and

$$\|\bar{w}(t) - w^*\| \leq \frac{\tilde{\zeta}}{t + \Gamma}, \quad (6)$$

where $\zeta \triangleq \max \left\{ \Gamma \|\mathbf{w}(0) - \mathbf{1}\bar{w}(0)\|, \frac{\delta\sqrt{2L\epsilon_0}}{\frac{\Gamma}{\Gamma+1} - \lambda} \right\}$ and $\tilde{\zeta} \triangleq \max \left\{ \Gamma \|\bar{w}(0) - w^*\|, \frac{1}{\mu\delta-1} \frac{L\delta\zeta}{\sqrt{K}} \right\}$.

Proof: See Supplementary Information. ■

In [21], the authors studied the convergence of FedAvg and established the convergence rate $O(1/T)$ (where T is the number of iterations in gradient descent) for strongly convex and smooth problems. Theorem 1 guarantees the convergence of the proposed DeceFL algorithm under time-invariant connected communication topologies with the same convergence rate. In the Supplementary Information, it has been further demonstrated that the proposed DeceFL converges even for time-varying topologies, in which case the underlying topology does not need to be connected for all iterations.

C. An illustrative example

We use a simple yet important example to illustrate the problem and demonstrate the advantages of the proposed decentralized framework as compared with centralized learning, federated learning and swarm learning (SL). Consider the case where K clients would like to compute the average of every client's private value $\mathcal{D}_k = w_k(0)$, i.e., $w^* \triangleq \frac{\sum_{k=1}^K w_k(0)}{K}$. This task is simple if there exists a central client. However, it becomes challenging when a central client is not available. This is the well-known decentralized consensus problem [22], [23], [24], which has many engineering applications including synchronization, PageRank, state estimation, load balancing, and more.

We can convert the consensus problem to the following optimization problem

$$\min_{w \in \mathbb{R}} F(\mathcal{D}; w) \triangleq \frac{1}{2} \sum_{k=1}^K (w - w_k(0))^2, \quad (7)$$

with its optimal value coincided with w^* . Rather than computing the mean, we convert it to solve the optimization problem (7) using algorithms FedAvg, SL and the proposed DeceFL respectively.

1) *FedAvg algorithm:* In the classical federated learning algorithm, i.e., FedAvg, there is a central server to collect the local parameter information of each client for average aggregation, and to assign it to each client, which is equivalent to a complete graph of K clients without a central server after simple derivation (Figure 1A):

$$w_k(t+1) = \frac{1}{K} \sum_{k=1}^K w_k(t) - \eta_t (w_k(t) - w_k(0)), \quad (8)$$

where t represents the t -th iteration, $w_k(t)$ represents the estimate of global optimum for the k -th client at iteration t , and η_t is learning rate in the gradient descent algorithm. In essence, every client iteratively updates its estimate based on all others' estimates together with its current gradient. Using derivation in the Supplementary Information based on dynamical system and algebraic graph theory, it can be shown that the system reaches the steady-state, i.e., $\lim_{t \rightarrow \infty} \|w_k(t) - w^*\| = 0$, if $\eta_t = \frac{\gamma}{t+\Gamma}$ and $\frac{\gamma}{\Gamma} < 1$ is satisfied for any $\gamma, \Gamma > 0$.

2) *SL algorithm*: The SL algorithm considers the situation where there is no central server: in each iteration, a random leader is dynamically selected from the members to aggregate the model parameters from all clients (including itself) and assign them to each client shown in Figure 1B. Mathematically, this is exactly the same as centralized federated learning as shown in the Supplementary Information.

3) *DeceFL algorithm*: Each client communicates parameters through the topology of the undirected connected graph shown in Figure 1C. According to the weighted aggregation of information obtained from neighbor clients, the local update is completed according to the following iteration,

$$w_k(t+1) = \sum_{j=1}^K W_{kj}(t) w_k(t) - \eta_t(w_k(t) - w_k(0)), \quad (9)$$

where $W(t) \in \mathbb{R}^{K \times K}$ is the weighted matrix of the undirected connected graph at iteration t . Using derivation in the Supplementary Information based on dynamical system and algebraic graph theory, it can be shown that the system reaches the steady-state, i.e., $\lim_{t \rightarrow \infty} \|w_k(t) - w^*\| = 0$, if $\eta_t = \frac{\gamma}{t+\Gamma}$ and $\frac{\gamma}{\Gamma} < 1 - \sigma'^2$ are satisfied for any $\gamma, \Gamma > 0$.

4) *Summary*: It can be shown that all methods can reach consensus with zero performance gap, i.e., $\Delta = 0$. The convergence speeds of all methods are $O(1/T)$. As shown in the Supplementary Information Figure 1, these methods converge to the consensus value exponentially. This is consistent with the theoretical results. The information used in three different algorithms is however distinct: FedAvg and SL need global information at every iteration, while DeceFL only needs local information from clients' neighbors. In addition, the first two algorithms can be viewed as special cases of the proposed DeceFL algorithm by setting W to the corresponding adjacency matrix correspondingly. Specifically, when $W(t) = \frac{1}{k}\mathbf{1}_K\mathbf{1}_K^T$ for all t , the proposed DeceFL algorithm becomes to FedAvg and SL. Therefore, the proof of convergence in this paper also warrants that of centralized federated learning and SL.

EXPERIMENTS

Experiments were carried out on real-world biomedical and industrial applications, which demonstrate the effectiveness and the wide applicability of DeceFL, as a fully decentralized framework. We benchmarked the performance of DeceFL, in comparison with FedAvg and SL that demand much more communication costs and strongly rely on a restricted communication topology. Furthermore, the superiority of DeceFL on robustness in the presence of communication topology interference (random node or edge malfunction) was shown in two experiments with time-varying communication topologies. The overall performance of DeceFL was corroborated by these practical applications.

²Let us sort the eigenvalues of W in a non-increasing order as $1 = \lambda_1(W) > \lambda_2(W) \geq \dots \geq \lambda_n(W) > -1$, denoted σ' as the second largest eigenvalue of the weighting matrix W , i.e., $\sigma' = \max\{|\lambda_2(W)|, |\lambda_n(W)|\} \in (0, 1)$.

A. Application to medicine: collaborative prediction of leukaemias

First, we used the dataset of peripheral blood mononuclear cell (PBMC) transcriptomes from [19], named “dataset A2”, as a benchmark example to compare three federated learning frameworks: DeceFL, FedAvg and SL. Samples were split into non-overlapping training datasets associated with each node, and a global test dataset that was reserved for testing the models built on these frameworks. The experiment setup is consistent with that of SL: the dataset is divided into a training set and a test set at the ratio of 8:2, and the dataset owned by each node was obtained from the training set. The logistic regression model with l_2 regularization and the 8-layer fully connected deep neural network (as in [19]) were selected for our experiments detailed in the Materials and Methods Section.

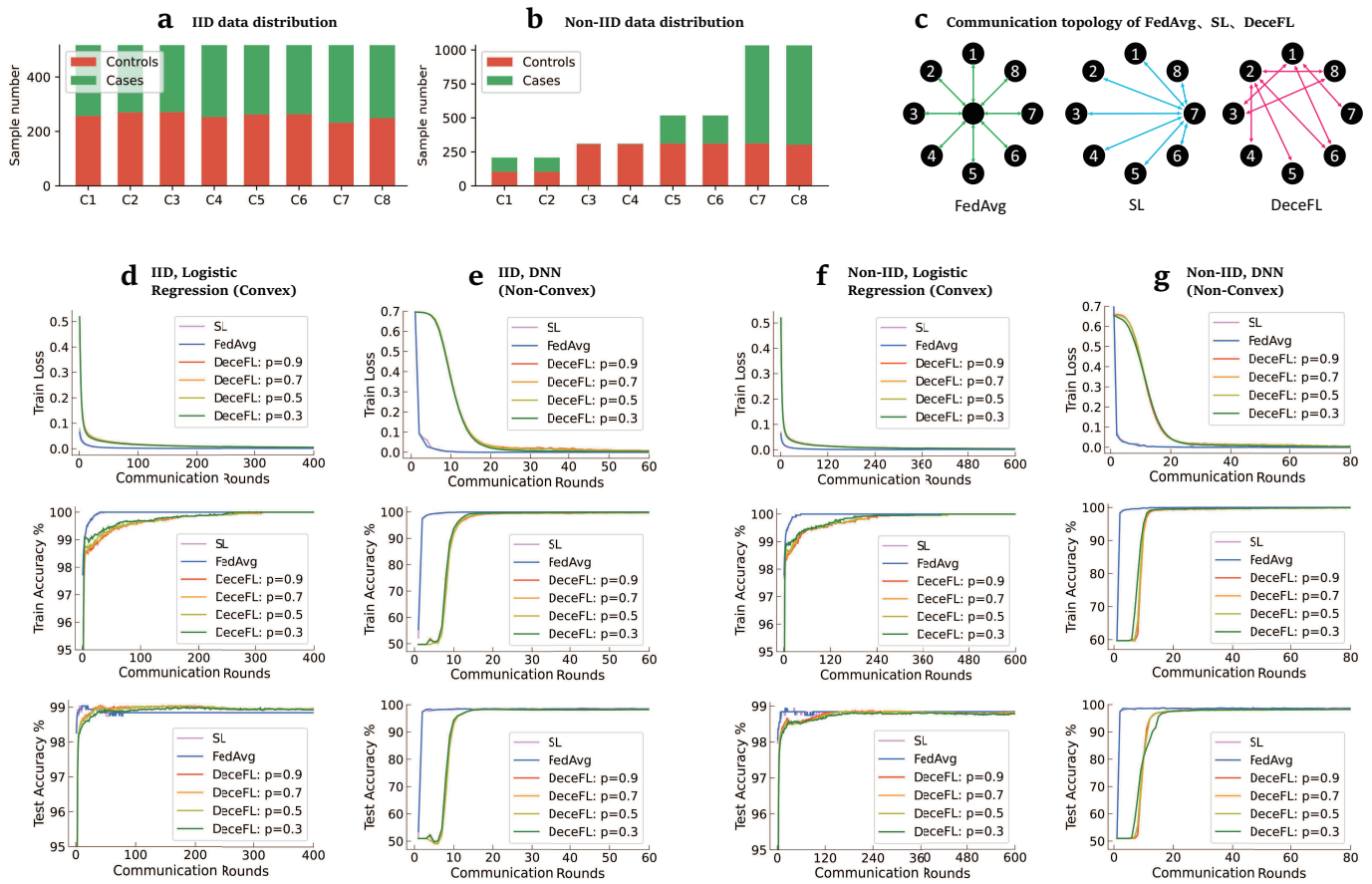


Fig. 2. DeceFL to predict leukaemias from A2 benchmark dataset [19]. **a**, Data were divided into IID samples for all clients. **b**, Data were divided into Non-IID unbalanced samples. **c**, Different topologies for FedAvg, SL and DeceFL respectively. The topology for SL must hold in every iteration when any other node is selected as a central client. **d, e, f, g**, Performance of three algorithms on IID/Non-IID setups over logistic regression/neural networks.

First, we benchmarked DeceFL against FedAvg and SL in the IID setup of dataset A2 (Fig. 2a), that is, the sample size of each node is the training set sample size divided by the number of nodes,

which ensures that each node has the same number of samples and the ratio of the positive to the negative samples is approximately 1 : 1. DeceFL applied multiple connected graphs with various connectivity probability values ($p = 0.3, 0.5, 0.7, 0.9$). This benchmark shows that DeceFL can reach the same performance as FedAvg and SL which use a (temporary) central client to gather all information from every node. FedAvg and SL only perform better during the transient period that DeceFL takes for a certain number of iterations to converge due to its decentralized nature. Second, the similar comparative study was repeated with the Non-IID setup of dataset A2 (Fig. 2b). The Non-IID setup explicitly designs, for the local data associated with each node, the sample size and the ratio between positive and negative samples (Supplementary Information). It allows us to benchmark performances on balanced/unbalanced, sufficient/deficient local training data. We obtained very similar results as in the IID setup, where DeceFL presents an equal performance to FedAvg and SL, after DeceFL reaches consensus in decentralized computation. It also shows the superiority of DeceFL over SL, which however demands huge amounts of communication costs for the selected central client at every round and relies heavily on the strong assumption of a stable fully-connected communication structure. Any bit of malfunction of clients or communication paths could melt down the whole SL process, since at each round a client is delegated to collect information from all other clients.

To show DeceFL functions well when an intervention to decentralized infrastructure happens, we conducted two experiments with time-varying graphs that take into account malfunction of clients and communication paths. First, communication structure/graph was altered in runtime (Fig. 3a), that is, the adjacency matrix that describes how nodes communicate with each other varied over time. Although being named as a decentralized framework, SL requires a fully-connected communication graph; whereas DeceFL only demands connected graphs as shown in the IID and Non-IID experiments. This time-varying experiment further shows that the conditions of DeceFL can even be weaken and generalized to such an extent that the communication graph at each time is not necessary to be connected as long as within a fixed period the information can be transmitted between any pair of nodes. Surprisingly, both experimental results Fig. 3c (IID) and Fig. 3d (Non-IID) show that DeceFL in such a scenario keeps similar performance as FedAvg. In other words, DeceFL can be so robust that random malfunction of a small portion of edges may merely deteriorate DeceFL running processes. The second experiment considers the removal and supplement of nodes, as shown in Fig. 3b: during the first 300 rounds, we used an Erdos-Renyi graph of 6 nodes; then for the 301-600 rounds, the graph was of 8 nodes by adding 2 extra nodes; and in the rest rounds, the graph was randomly removed by 2 nodes. Under such node interventions, experimental results Fig. 3e and Fig. 3f show robust performance of DeceFL which is similar to FedAvg (that does not consider node interventions). Two experiments manifest the robustness of DeceFL on interventions of computation infrastructure

in a decentralized framework.

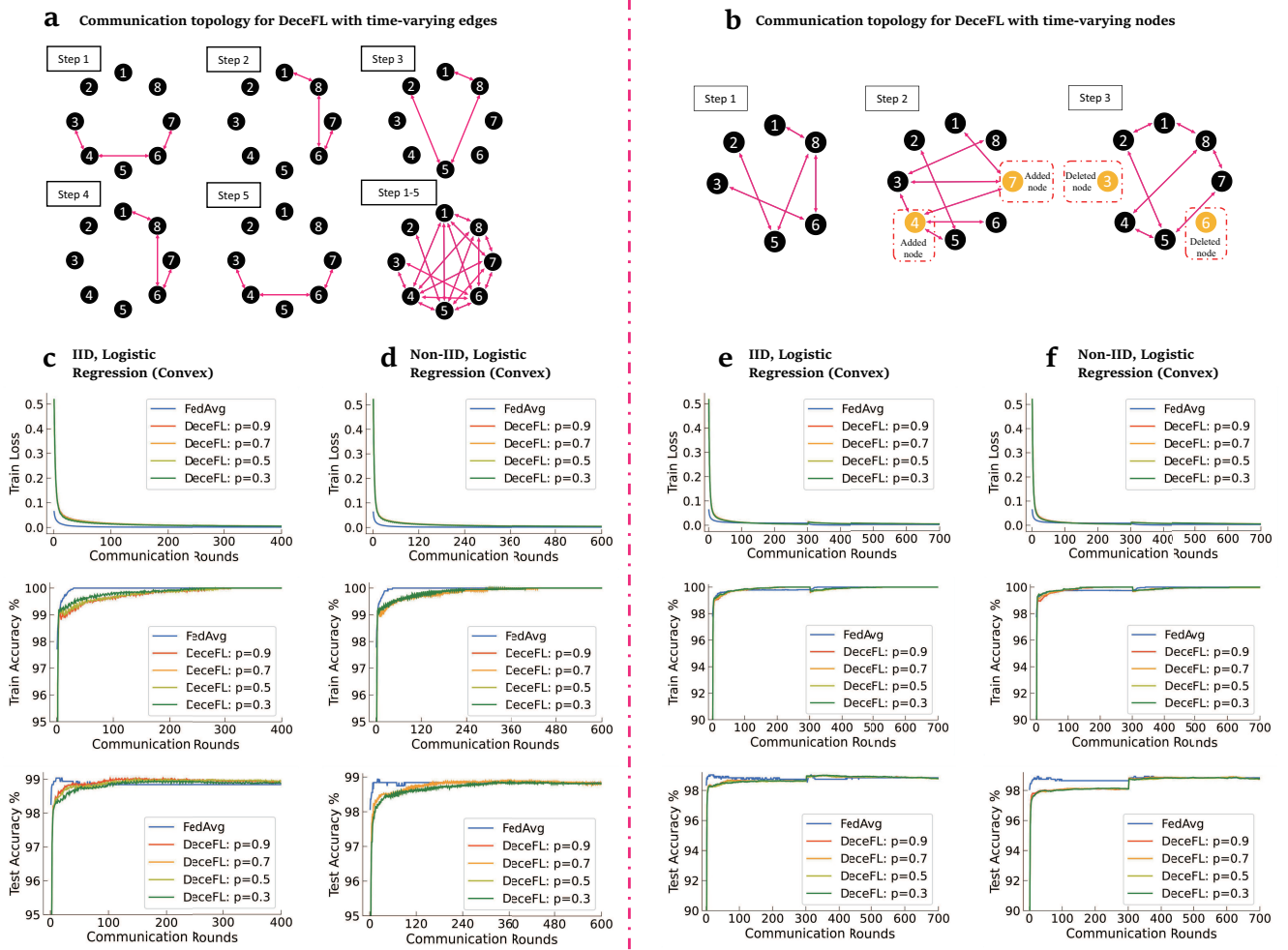


Fig. 3. DeceFL to predict leukaemias from A2 benchmark dataset [19]. **a**, Time-varying communication topology that consists of a sequence of graphs each of which is not connected while the lump-sum graph over a fixed period is connected. **b**, Time-varying communication topology that adds or removes nodes over time. **c,d**, Performance of DeceFL with edge-varying graphs on the IID and Non-IID setups of dataset A2 using logistic regression, with reference performance of FedAvg that uses full information. **e,f**, Performance of DeceFL with node-varying graphs on the IID and Non-IID setups of dataset A2 using logistic regression, with reference performance of FedAvg that uses full information.

B. Application to smart manufacturing: collaborative detection of bearing faults

Modern manufacturing is heavily influenced by AI technologies with extraordinary increase of computational power and data size. To raise productivity and reduce operational costs, a critical challenge is fault diagnosis in machining operations [25]. AI-based algorithms have the potentials to detect fault locations and even to predict faults in advance, which allow replacing regular maintenance with real-time data-driven predictive maintenance and further reduce unnecessary maintenance costs and guarantee reliability. A general fault detection framework has been proposed in [2], which,

however, needs full-cycle measurements of large amounts of machines that are most likely unavailable from a single factory. Data generated by multiple factories could be sufficient to perform preventive maintenance, while sensitive data (security or business related) are less likely to be shared in practice. The fully decentralized framework DeceFL provides a way for multiple factories to develop a global model, which generates mutual benefit from private local data without having to resort to data sharing in public.

This experiment practices such a decentralized fault diagnosis application in manufacturing, using Case Western Reserve University's (CWRU) bearing data, which comprises ball bearing test data for normal and faulty bearings, specified in the Methods Section. Specifically, we used three types of bearings data: 7 inch, 14 inch and 21 inch; and chose the drive end defects, which includes outer race defect, inner race defect, and ball defect. We chose the outer race defect appearing at the 6 o'clock (centered) position. Thus, there are in total ten distinct conditions: 9 faulty classes (3 bearing types times 3 defect types) and the normal condition. All data in use was collected at 12,000 samples/second for drive end bearing experiments. It was generated by using 4 types of motor speed: 1797 rpm, 1772 rpm, 1750 rpm and 1730 rpm. The data from 1730 rpm is reserved for test.

Assume that there are 4 factories, as clients illustrated in Fig. 4c, which collect their private full-cycle bearing data. The training data associated with each client were prepared in the IID (Fig. 4a) and the Non-IID setup (Fig. 4b). A 10-way classification problem is considered, 9 fault cases (B007, IR007, OR007, B014, IR014, OR014, B021, IR021, OR021) and 1 normal case. Learning used two methods, regularized logistic regression as a strongly convex method, and deep neural network (DNN) as a nonconvex method. In the usage of logistic regression, as guaranteed in theory, DeceFL in Fig. 4d,f confirms the same performance as FedAvg after its transient periods. For the case of DNN, as a non-convex method, although there is no theoretical guarantee, DeceFL in Fig. 4e,g shows competitive performance to FedAvg. The slight performance gap in test between DeceFL and FedAvg in Fig. 4f may be mostly caused by the chosen type of DNN, multilayer perceptrons as used in [19], which has many well-known defects; and more reasons are discussed and explored by more experiments in the Supplementary Information. Comprehensive experiments were conducted and can be found in the Supplementary Information, with more clients (that is, more factories), more learning methods, and another 4-way classification problem. Overall DeceFL manifests competitive performance on multi-class classification for industrial fault diagnosis applications, with implementations of (non-)convex methods in a fully decentralized framework that breaks through the barrier of data privacy.

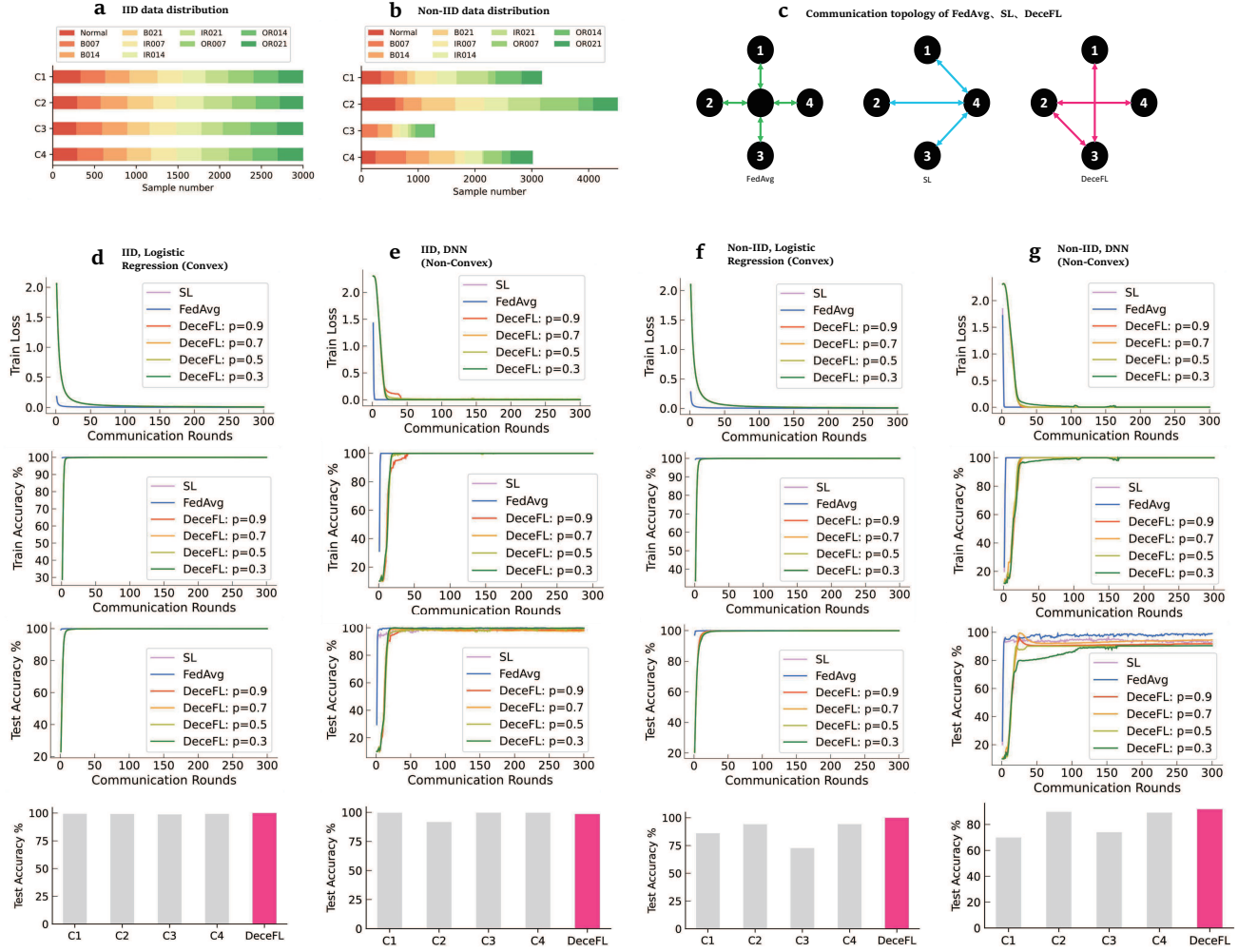


Fig. 4. DeceFL to detect bearing faults from CWRU benchmark dataset. **a,** Data were divided into IID samples for all 4 clients. **b,** Data were divided into Non-IID unbalanced samples. Each client locally specified its data size and sample distribution. **c,** Illustration of communication topology for FedAvg, SL and DeceFL. **d,e,** Performance of DeceFL on IID data using logistic regression and DNN, respectively, with reference performance of FedAvg and SL. **f,g,** Performance of DeceFL on Non-IID data using logistic regression and DNN, respectively, with reference performance of FedAvg and SL. **d,e,f,g,** The boxplots at bottom illustrate the performance comparison between DeceFL and each client trained independently (that is, each client trained its own model only using its associated local data without communicating with any other clients).

DISCUSSIONS

In this paper, we propose a new decentralized federated learning algorithm. The decentralized architecture eliminates the bandwidth bottleneck of the central client. The convergence of the DeceFL algorithm is analyzed in detail, showing that DeceFL guarantees convergence and has the same convergence rate as the centralized federated learning algorithm. The convergence performance of the algorithm is verified by training neural networks over different datasets. Compared with other state-of-the-art privacy-preserving algorithms such as FedAvg and SL [19], the proposed DeceFL algorithm is guaranteed to reach the global optimum with a similar rate as the centralized federated

learning algorithm under certain conditions. In addition, there has developed a sizable literature as surveyed in [26], which can be adapted to cope with quantization errors and noises that could happen over communication networks.

There is no doubt that decentralized federated learning framework will become increasingly popular in the nearest future for almost all AI applications given the privacy regulations. Yet our algorithm has a number of limitations that need to be taken into consideration for future development:

First of all, application of privacy algorithms (for example, blockchain or homomorphic encryption [27]) has not been considered in this study. However, similar to the centralized federated learning and swarm learning framework, it should be straightforward to apply such techniques for data privacy protection in the proposed DeceFL framework to make communication secure.

Secondly, similar to the setup of federated learning and swarm learning, all clients in the network need to know the form of the global objective function. The proposed formulation is different from those used in multi-party computation [28], where model and data can be separated [29]. Future work lies in the integration of such techniques to the proposed DeceFL algorithm to make the global objective function unknown to clients.

Finally, all clients are assumed to be collaborative, it would be interesting to further investigate whether the proposed decentralized federated learning framework is vulnerable to semi-honest or malicious clients that are not collaborative [30], which could exist in the real-world applications.

MATERIALS AND METHODS

Data pre-processing

Essential data preprocessing was performed for CWRU dataset, including class balancing and normalization, feature extraction by Fourier transform. The dataset has 10 classes in total, which vary in sample size. Hence samples in certain classes were deleted to balance sample sizes over all classes. The original data is time-series data, which was firstly divided by every 300 points and resulted in a family of time series. Each time series chose DE and FE features respectively, and produced 600 points. For every time series of each feature, we performed Fast Fourier Transform (FFT), which yielded 150 points. Thus each time series of both DE and FE has in total 300 points. The motivation to use FFT is to handling the mismatch of time stamps of sequential data. After FFT the training and test data were then normalized by removing the mean and scaling to unit variance (the test data is normalized by the normalizer of the training).

Performance metrics

The common performance metric “accuracy” is used for assessment of classification,

$$\text{accuracy} = \frac{\text{TP} + \text{TN}}{\text{TP} + \text{TN} + \text{FP} + \text{FN}} \quad (10)$$

where TP, TN, FP and FN denote the number of true positive, true negative, false positive and false negative samples, respectively.

Implementation of learning methods

To ensure in benchmark DeceFL can work well for either strongly convex learning methods or non-convex methods, we

adopted two algorithms: logistic regression with l_2 regularization, and deep neural network (DNN), as used in [19]. For logistic regression, every node runs 10 epochs in each round, with batch-size 64. It uses the SGD optimizer, with weight decay coefficient 10^{-4} for the realization of l_2 regularization. The initial learning rate (for deep learning framework) is 0.01, which is later decayed by multiplying 0.2 every 5 epochs. For DNN, every node runs 30 epochs in each round, with batch-size 64. It uses the SGD optimizer, with weight decay coefficient 10^{-4} . The initial learning rate (for deep learning framework) is 0.1, which is decayed by multiplying 0.2 every 20 epochs. This DNN has 8 hidden layers, whose dimensions are 256, 512, 512, 256, 256, 128, 128, 64, respectively. The *dropout* rate is set to 0.3. Both methods use *sigmoid* as the activation function in the output layer for binary classification (dataset A2) and *softmax* for multiclass classification (CWRU dataset). At aggregation, the gradient update coefficient for DeceFL is 0.1 (FedAvg does not use this variable). The total number of running rounds is selected by visualization effects of convergence for all methods in comparison.

Data availability

The peripheral blood mononuclear cell (PBMC)-derived transcriptome dataset, named as “dataset A2” in [19], was used, which was originally generated with Affymetrix HG-U133 2.0 microarrays (8,348 individuals), by inspection of all publicly available datasets at National Center for Biotechnology Information Gene Expression Omnibus. To perform the IID experiments, the initial preparation of dataset randomly dropped negative samples, resulting in 5,176 samples, such that the whole dataset is balanced, i.e. the ratio of the positive to the negative samples is 1 : 1. CWRU Bearing dataset refers to the data of ball bearing test for normal and faulty bearings from the Case Western Reserve University, available on <https://engineering.case.edu/bearingdatacenter>.

Code availability

All source codes are openly available on GitHub (<https://github.com/HAIRLAB/DeceFL>).

Acknowledgement

We thank Mr. Anthony Haynes, Mr. Cai Huang for editing.

Funding

This work was supported by Jiangsu Industrial Technology Research Institute (JITRI) and the National Key R&D Program of China (2018YFB1701202).

Author contributions

Idea was conceived by Y.Y.. Theory was developed by J.L., R.C., L.X., X.Y., T.Y., Y.Y.. Simulation codes were developed by D.J., C.S., M.W. and were reviewed by Z.Y.. Experiments were designed by Y.Y., Z.Y., and were performed by D.J., Z.Y., C.S., M.W., Y.Y., F.H., R.C.. Projects were supervised by Y.Y., S.S., H.D.. Funding was acquired by Y.Y., J.L., H.Z., H.D.. The original draft was written by Y.Y., Z.Y., J.L., R.C., and all authors provided critical review of the manuscript and approved the final draft.

Competing interests

The authors declare no competing interests.

REFERENCES

- [1] LeCun, Y., Bengio, Y. & Hinton, G. Deep learning. *Nature* **521**, 436–444 (2015).
- [2] Yuan, Y. *et al.* A general end-to-end diagnosis framework for manufacturing systems. *National Science Review* **7**, 418–429 (2020).
- [3] Yan, L. *et al.* An interpretable mortality prediction model for covid-19 patients. *Nature machine intelligence* **2**, 283–288 (2020).
- [4] Price, W. N. & Cohen, I. G. Privacy in the age of medical big data. *Nature medicine* **25**, 37–43 (2019).

- [5] DeGrave, A. J., Janizek, J. D. & Lee, S.-I. Ai for radiographic covid-19 detection selects shortcuts over signal. *Nature Machine Intelligence* 1–10 (2021).
- [6] Roberts, M. *et al.* Common pitfalls and recommendations for using machine learning to detect and prognosticate for covid-19 using chest radiographs and ct scans. *Nature Machine Intelligence* 3, 199–217 (2021).
- [7] Konečný, J., McMahan, B. & Ramage, D. Federated optimization: Distributed optimization beyond the datacenter. *arXiv preprint arXiv:1511.03575* (2015).
- [8] Yang, Q., Liu, Y., Chen, T. & Tong, Y. Federated machine learning: Concept and applications. *ACM Transactions on Intelligent Systems and Technology* 10, 1–19 (2019).
- [9] Konečný, J. *et al.* Federated learning: Strategies for improving communication efficiency. *arXiv preprint arXiv:1610.05492* (2016).
- [10] McMahan, B., Moore, E., Ramage, D., Hampson, S. & y Arcas, B. A. Communication-Efficient Learning of Deep Networks from Decentralized Data. In *Proceedings of the 20th International Conference on Artificial Intelligence and Statistics*, vol. 54, 1273–1282 (2017).
- [11] Bonawitz, K. *et al.* Towards federated learning at scale: System design. *arXiv preprint arXiv:1902.01046* (2019).
- [12] Gu, R., Yang, S. & Wu, F. Distributed machine learning on mobile devices: A survey. *arXiv preprint arXiv:1909.08329* (2019).
- [13] Kairouz, P. *et al.* Advances and open problems in federated learning. *arXiv preprint arXiv:1912.04977* (2019).
- [14] Li, T., Sahu, A. K., Talwalkar, A. & Smith, V. Federated learning: Challenges, methods, and future directions. *IEEE Signal Processing Magazine* 37, 50–60 (2020).
- [15] Kaassis, G. *et al.* End-to-end privacy preserving deep learning on multi-institutional medical imaging. *Nature Machine Intelligence* 3, 473–484 (2021).
- [16] Lian, X. *et al.* Can decentralized algorithms outperform centralized algorithms? A case study for decentralized parallel stochastic gradient descent. In *31th Annual Conference on Neural Information Processing Systems (NIPS 2017)*, vol. 30, 5330–5340 (2017).
- [17] Tang, Z., Shi, S. & Chu, X. Communication-efficient decentralized learning with sparsification and adaptive peer selection. *arXiv preprint arXiv:2002.09692* (2020).
- [18] Wang, S. *et al.* Adaptive federated learning in resource constrained edge computing systems. *IEEE Journal on Selected Areas in Communications* 37, 1205–1221 (2019).
- [19] Warnat-Herresthal, S. *et al.* Swarm learning for decentralized and confidential clinical machine learning. *Nature* 594, 265–270 (2021). URL <https://doi.org/10.1038/s41586-021-03583-3>.
- [20] Koloskova, A., Stich, S. U. & Jaggi, M. Decentralized stochastic optimization and gossip algorithms with compressed communication. *arXiv preprint arXiv:1902.00340* (2019).
- [21] Li, X., Huang, K., Yang, W., Wang, S. & Zhang, Z. On the convergence of FedAvg on non-IID data. *arXiv preprint arXiv:1907.02189* (2019).
- [22] Olfati-Saber, R. & Murray, R. M. Consensus problems in networks of agents with switching topology and time-delays. *IEEE Transactions on automatic control* 49, 1520–1533 (2004).
- [23] Ren, W. & Beard, R. W. Consensus seeking in multiagent systems under dynamically changing interaction topologies. *IEEE Transactions on automatic control* 50, 655–661 (2005).
- [24] Jadbabaie, A., Lin, J. & Morse, A. S. Coordination of groups of mobile autonomous agents using nearest neighbor rules. *IEEE Transactions on automatic control* 48, 988–1001 (2003).
- [25] Isermann, R. *Fault-diagnosis systems: an introduction from fault detection to fault tolerance* (Springer Science & Business Media, 2005).
- [26] Yang, T. *et al.* A survey of distributed optimization. *Annual Reviews in Control* 47, 278–305 (2019).
- [27] DeMillo, R. A. Foundations of secure computation. Tech. Rep., Georgia Institute of Technology (1978).
- [28] Yao, A. C. Protocols for secure computations. In *23rd annual symposium on foundations of computer science (sfcs 1982)*, 160–164 (IEEE, 1982).
- [29] Yu, Y. & Xie, X. Privacy-preserving computation in the post-quantum era. *National Science Review* (2021).
- [30] Lyu, L., Yu, H. & Yang, Q. Threats to federated learning: A survey. *arXiv preprint arXiv:2003.02133* (2020).

Supplementary Information

DeceFL: A Principled Decentralized Federated Learning Framework

Ye Yuan^{1,2,*}, Jun Liu^{3,*}, Dou Jin^{1,*}, Zuogong Yue^{1,*}, Ruijuan Chen¹, Maolin Wang¹, Chuan Sun¹,
Lei Xu⁴, Feng Hua², Xin He², Xinlei Yi⁵, Tao Yang⁴, Hai-Tao Zhang^{1,2}, Shaochun Sui⁶, Han Ding²

Contents

1	The Proposed Decentralized Federated Learning Algorithm	2
2	Convergence Analysis of the DeceFL Algorithm	3
3	DeceFL over Undirected Time-Varying Graphs	6
4	Consensus problem	7
4.1	FedAvg algorithm	8
4.2	SL algorithm	9
4.3	DeceFL algorithm	10
4.4	Summary	12
4.5	Example	12
5	Experiments	12
5.1	Method description	12
5.2	Dataset A2	15
5.2.1	IID experiments	15
5.2.2	Non-IID experiments	16
5.2.3	Time-varying experiments with edge changes	18
5.2.4	Time-varying experiments with node changes	21
5.3	CWRU bearing dataset	23
5.3.1	Data description	23
5.3.2	Preprocessing	25
5.3.3	Experiments	25
5.3.4	Additional Non-convex Experiments	26

¹School of Artificial Intelligence and Automation, Huazhong University of Science and Technology. ²School of Mechanical Science and Engineering, Huazhong University of Science and Technology. ³Department of Applied Mathematics, University of Waterloo. ⁴State Key Laboratory of Synthetical Automation for Process Industries, Northeastern University. ⁵School of Electrical Engineering and Computer Science, and Digital Futures, KTH Royal Institute of Technology. ⁶AVIC Chengdu Aircraft Industrial (Group) Co., Ltd.. *Equal contributions. Email: yye@hust.edu.cn.

A Appendix	33
A.1 Proof of Theorem 1	33
A.2 Proof of Proposition 1	38
A.3 Proof of Theorem 3	41

1 The Proposed Decentralized Federated Learning Algorithm

In this section, we shall propose a decentralized algorithm that removes the central server while maintaining convergence property.

Consider that there are K clients with local data in the form for standard learning tasks $\mathcal{D}_k = \{(A_{ki}, b_{ki})\}_{i=1}^{m_k}$ for $k \in \mathcal{N} \triangleq \{1, 2, \dots, K\}$, where $A_{ki} \in \mathbb{R}^n$ is the i -th sample and b_{ki} is the corresponding label in the k -th client, and $m_k = |\mathcal{D}_k|$ is defined as the number of samples on the client. The local loss function for learning $F_k(w)$ is defined as $F_k(w) \triangleq \frac{1}{m_k} \sum_{i=1}^{m_k} f(A_{ki}, b_{ki}; w)$, where $f(A_{ki}, b_{ki}; w)$ is the user-specified loss function on example (A_{ki}, b_{ki}) made with model parameters w . In such a setup, every client may have its own objective function, which could be different from and unknown to other client. Denotes that $\sum_{k=1}^K m_k = m$ which is the total number of samples in all the datasets. The following global learning problem which is the average of all local loss functions is then formulated

$$\min_{w \in \mathbb{R}^n} F(A, b; w) \triangleq \sum_{k=1}^K \frac{m_k}{m} F_k(w), \quad (1)$$

where

$$A = \begin{bmatrix} A_1 & \mathbf{O}_{m_1, n} & \cdots & \mathbf{O}_{m_1, n} \\ \mathbf{O}_{m_2, n} & A_2 & \cdots & \mathbf{O}_{m_2, n} \\ \vdots & \vdots & & \vdots \\ \mathbf{O}_{m_K, n} & \mathbf{O}_{m_K, n} & \cdots & A_K \end{bmatrix} \in \mathbb{R}^{m \times Kn}, \quad b = \begin{bmatrix} b_1 \\ \vdots \\ b_K \end{bmatrix} \in \mathbb{R}^m,$$

in which $A_k = [A_{k1}^T; \dots; A_{km_k}^T] \in \mathbb{R}^{m_k \times n}$ and $b_k = [b_{k1}; \dots; b_{km_k}] \in \mathbb{R}^{m_k}$ represents the vector of labels on all clients. From a global perspective, the global loss function can be designed in a centralized and private way, which could be unknown to all clients. A local (and possibly distinct) cost function, which is a part in the global loss function, is then designed and distributed to a local client. In such a setup, data is stored locally with high security and global loss function is protected even to any clients.

The communication network between clients can be modeled by an undirected connected¹ graph $\mathcal{G} = (\mathcal{N}, \mathcal{E}, W)$, where $\mathcal{N} := \{1, 2, \dots, K\}$ represents the set of clients, and $\mathcal{E} \subseteq \mathcal{N} \times \mathcal{N}$ represents the set of communication channels, connecting two distinct clients. For each edge $(i, j) \in \mathcal{E}$, the corresponding element in the adjacency matrix W , i.e., W_{ij} indicates whether there is a communication channel between the i -th client and the j -th client. Specifically, when $W_{ij} > 0$, there is information communication between clients i and j , while $W_{ij} = 0$ means none.

¹In this work, we consider that the information communication between clients is mutual for notational simplicity, so we can get that the matrix $W = [W_{kj}] \in \mathbb{R}^{K \times K}$ is symmetric, it is defined as the weighted connection matrix between all clients. Further we assume that all clients are connected, that is, for any two clients k and j , there is at least one path from k to j .

For client i , when $W_{ij} > 0$, then client j is called a neighbor of client i . The set of all such clients j is represented as \mathcal{N}_i , i.e., $\mathcal{N}_i = \{j | W_{ij} > 0, \forall j \in \mathcal{N}\}$.

Let the client k hold a local copy of the global variable w , which is denoted by $w_k \in \mathbb{R}^n$, and $\mathbf{w} = [w_1; \dots; w_K] \in \mathbb{R}^{Kn}$. Then, the update rule of DeceFL for solving problem (1) is, for each client $k = 1, \dots, K$,

$$w_k(t+1) = \sum_{j=1}^K W_{kj} w_j(t) - \eta_t \tilde{g}_k(w_k(t)), \quad (2)$$

where $\eta_t > 0$ is the learning rate, the initial condition $w_k(0) \in \mathbb{R}^n$ can be arbitrarily chosen, and $g_k(w_k(t))$ is the stochastic gradient on the randomly selected dataset $\mathcal{B}_k(t)$ with batch size m'_k :

$$g_k(w_k(t)) = \frac{1}{m'_k} \sum_{i \in \mathcal{B}_k(t)} \nabla f(A_{ki}, b_{ki}; w_k(t)),$$

$\tilde{g}_k(w_k(t)) = \frac{m_k}{m} g_k(w_k(t))$, which satisfies $\mathbb{E}[\tilde{g}_k(w_k(t))] = \frac{m_k}{m} \nabla F_k(w_k(t))$. For convenience, denote by $\tilde{F}_k(w_k) = \frac{m_k}{m} F_k(w_k)$. The steps of the proposed DeceFL are summarized in Algorithm 1.

Algorithm 1 DeceFL. The K clients are indexed by k , η_t is the learning rate, W is the adjacency matrix, and T is the maximum number of iterations.

```

Initialize:  $w_k(0)$  on each client  $k \in \mathcal{N}$ 
for  $t = 1, 2, \dots, T$  do
    for each client  $k = 1, 2, \dots, K$  in parallel do
         $w_k(t+1) = \sum_{j=1}^K W_{kj} w_j(t) - \eta_t \tilde{g}_k(w_k(t))$ 
    end for
end for
```

We stack the $w_k(t)$ and $\tilde{g}_k(w_k(t))$ in (2) into vectors, i.e., define $\mathbf{w}(t) = [w_1^T(t), \dots, w_K^T(t)]^T \in \mathbb{R}^{Kn}$ and $G(\mathbf{w}(t)) = [\tilde{g}_1^T(w_1(t)), \dots, \tilde{g}_K^T(w_K(t))]^T \in \mathbb{R}^{Kn}$. Then, we can compactly write (2) as:

$$\mathbf{w}(t+1) = (W \otimes \mathbf{I}_n) \mathbf{w}(t) - \eta_t G(\mathbf{w}(t)). \quad (3)$$

It is noted that classical federated learning algorithm (i.e., FedAvg) mainly focuses on the transmission of model parameters and the reception of gradients between client 0 and other clients. It not only requires the centralized topological relationship between client 0 and other clients but also leads to the high pressure of communication and computation. The algorithm (3) proposed in this paper realizes model learning by transferring model parameters between clients, in which weight matrix W means the topological relationship between clients. It can not only be designed according to the actual situation of the client but also effectively overcome the phenomenon of individual client overload.

2 Convergence Analysis of the DeceFL Algorithm

Next, we analyze the convergence of DeceFL under the following assumptions, which are standard in analyzing the convergence of FedAvg [1].

Assumption 1 The variance of stochastic gradients and the expected squared norm of stochastic gradients in each client are uniformly bounded, i.e.,

$$\mathbb{E}[\|g_k(w_k(t)) - \nabla F_k(w_k(t))\|^2] \leq \sigma_k^2, \quad (4)$$

and

$$\mathbb{E}[\|g_k(w_k(t))\|^2] \leq \chi^2, \quad (5)$$

where $k = 1, \dots, K$ and $t = 0, 1, 2, \dots$

Assumption 2 For each $k \in \mathcal{N}$, assume that F_k is L_k -smooth and μ_k -strongly convex. That is, F_k is differentiable and the gradient is L_k -Lipschitz continuous, i.e., for any $w, u \in \mathbb{R}^n$,

$$\|\nabla F_k(w) - \nabla F_k(u)\| \leq L_k \|w - u\|, \quad (6)$$

and

$$F_k(u) \geq F_k(w) + \langle \nabla F_k(w), u - w \rangle + \frac{\mu_k}{2} \|u - w\|^2. \quad (7)$$

Assumption 2 is standard and satisfied by typical loss functions in machine learning, including l_2 -regularized linear regression and l_2 -regularized logistic regression.

If Assumption 2 holds, then the global objective function $F(\cdot)$ is L -smooth and μ -strongly convex, where $L = \max\{L_k\}_{k=1}^K$ and $\mu = \min\{\mu_k\}_{k=1}^K$. Clearly, $\mu \leq L$. In addition, $\mu > 0$ can be obtained by the definition of strong convexity [2]. Additionally, $\tilde{F}_k(\cdot)$ is L_k -smooth and $\frac{\mu_k}{m}$ -strongly convex. Denote $w^* = \arg \min_{w \in \mathbb{R}^n} F(w)$, $w_k^* = \arg \min_{w_k \in \mathbb{R}^n} \tilde{F}_k(w_k)$. Furthermore, let $F^* = F(A, b; w^*) = \sum_{k=1}^K \frac{m_k}{m} F_k(w^*)$ and $\tilde{F}_k^* = \tilde{F}_k(w_k^*)$, then $F^* = \sum_{k=1}^K \tilde{F}_k(w^*)$. In addition, we define an auxiliary parameter $\tilde{F}^* = \sum_{k=1}^K \tilde{F}_k^*$, which leads to $F^* - \tilde{F}^* = \sum_{k=1}^K (\tilde{F}_k(w^*) - \tilde{F}_k(w_k^*)) \geq 0$.

In the following, we shall prove the convergence of the DeceFL algorithm (2). Without loss of generality, we consider the normalized weight setting, which means that $\sum_{j=1}^K W_{kj} = 1$, for any $k \in \mathcal{N}$. As a result, there exists $\lambda \in (0, 1)$, which is the spectral norm of $W - \frac{1}{K} \mathbf{1}_K \mathbf{1}_K^T$, such that, for any $w \in \mathbb{R}^K$, we have $\|Ww - \mathbf{1}_K \bar{w}\| \leq \lambda \|w - \mathbf{1}_K \bar{w}\|$, where $\bar{w} = \frac{1}{K} \mathbf{1}_K^T w$ [3]. For convenience, we remove K from $\mathbf{1}_K$ and abbreviate it as $\mathbf{1}$ in the following parts. To state the convergence results, we define the average sequences $\bar{w}(t) = \frac{1}{K} (\mathbf{1}^T \otimes \mathbf{I}_n) \mathbf{w}(t) = \frac{1}{K} \sum_{k=1}^K w_k(t)$ and $g(t) = \frac{1}{K} (\mathbf{1}_K^T \otimes \mathbf{I}_n) G(\mathbf{w}(t)) = \frac{1}{K} \sum_{k=1}^K \tilde{g}_k(w_k(t))$. Then by multiplying $\frac{1}{K} (\mathbf{1}^T \otimes \mathbf{I}_n)$ to both sides of (3), the average iteration can be obtained as follows,

$$\begin{aligned} \bar{w}(t+1) &= \frac{1}{K} (\mathbf{1}^T \otimes \mathbf{I}_n) \mathbf{w}(t+1) = \frac{1}{K} ((\mathbf{1}^T \otimes \mathbf{I}_n)(W \otimes \mathbf{I}_n)) \mathbf{w}(t) - \frac{\eta_t}{K} (\mathbf{1}^T \otimes \mathbf{I}_n) G(\mathbf{w}(t)) \\ &= \frac{1}{K} ((\mathbf{1}^T W) \otimes \mathbf{I}_n) \mathbf{w}(t) - \frac{\eta_t}{K} (\mathbf{1}^T \otimes \mathbf{I}_n) G(\mathbf{w}(t)) = \frac{1}{K} (\mathbf{1}^T \otimes \mathbf{I}_n) \mathbf{w}(t) - \frac{\eta_t}{K} (\mathbf{1}^T \otimes \mathbf{I}_n) G(\mathbf{w}(t)) \\ &= \bar{w}(t) - \eta_t g(t), \end{aligned} \quad (8)$$

where the third equality is established by using the property $(A \otimes B)(C \otimes D) = (AC) \otimes (BD)$ of Kronecker product, and the fourth equality uses the fact that $\mathbf{1}^T W = \mathbf{1}^T$, and the first and

last equalities use the definition of the average sequence. We first introduce a lemma on the properties of eigenvalues of the Kronecker product of matrices.

Lemma 1 ([4]) Consider the polynomial $P(u, v) = \sum_{i=0}^p \sum_{j=0}^q c_{ij} u^i v^j$, $u, v \in \mathbb{R}$, where c_{ij} is the polynomial coefficient. Given $A \in \mathbb{R}^{m \times m}$ and $D \in \mathbb{R}^{n \times n}$, let $P(A, D) = \sum_{i=0}^p \sum_{j=0}^q c_{ij} (A^i \otimes D^j)$. Then, the eigenvalues of matrices $P(A, D)$ are $P(\lambda_i, \theta_j)$, $i = 1, \dots, m$, $j = 1, \dots, n$, where $\{\lambda_i\}_{i=1}^m$ and $\{\theta_j\}_{j=1}^n$ are eigenvalue sequences of A and D , respectively.

We summarize our convergence result here.

Theorem 1 Let Assumptions 1 and 2 hold. Consider algorithm (2), where the learning rate given by $\eta_t = \frac{\delta}{t+\Gamma}$, $\delta > \frac{m}{\mu}$ and $\Gamma \geq \frac{\sqrt{2(1+\lambda^2)}+1+\lambda^2}{1-\lambda^2}$ satisfies $\frac{\delta}{\Gamma} \leq \frac{1}{2L}$, in which $\lambda \in (0, 1)$ is the spectral norm of $W - \frac{1}{K}\mathbf{1}\mathbf{1}^T$. Denote the gap between the average local optimal value and the global average optimal value as $\epsilon \triangleq \frac{1}{K}(F^* - \bar{F}^*) \geq 0$. Then the following inequality can be obtained,

$$\mathbb{E}[\|\bar{w}(t) - w^*\|^2] \leq \frac{\tilde{\zeta}}{t + \Gamma}, \quad (9)$$

where $\zeta \triangleq \max \left\{ \Gamma^2 \cdot \mathbb{E}[\|\mathbf{w}(0) - \mathbf{1}\bar{w}(0)\|^2], \frac{\delta^2 K \chi^2}{\frac{r^2(\lambda^2)}{(\Gamma+1)^2(1+\lambda^2)} - \frac{\lambda^2}{2}} \right\}$, $\tilde{\zeta} \triangleq \max \left\{ \frac{(6\epsilon L + \sigma^2)\delta^2 m + \frac{2\tilde{\zeta}m}{K}}{\mu\delta - m}, \Gamma \cdot \mathbb{E}[\|\bar{w}(0) - w^*\|^2] \right\}$, and $\sigma^2 = \frac{1}{K} \sum_{k=1}^K \sigma_k^2$.

Proof: The proof can be found in Appendix A.1. ■

Remark 1 In [5], the authors studied the convergence of FedAvg and established the convergence rate $O(1/T)$ for strongly convex and smooth problems, where T is the number of SGDs. According to Theorem 1, under the same assumption of the objective function, the proposed algorithm DeceFL achieves the same convergence rate as FedAvg.

Remark 2 In addition, it is worth noting that the proposed algorithm also has some advantages in privacy protection. As we mentioned, the DeceFL communicates in a decentralized framework, and the model is exchanged between clients instead of gradient or training data samples, which has been proved to be effective in reducing the risk of privacy leakage [6].

Note the definition that w_k^* , it is obvious that $w_k^* = \arg \min_{w_k \in \mathbb{R}^n} F_k(w_k)$. Denoted by $F_k^* = \min_{w \in \mathbb{R}^n} F_k(w)$, $\bar{F}^* = \sum_{k=1}^K F_k^*$, and $\zeta = \frac{1}{K}(F^* - \bar{F}^*)$. According to Theorem 1, we can directly get the following convergence results when the learning rate is fixed.

Proposition 1 Let Assumptions 1 and 2 hold. Consider algorithm (2), where the learning rate given by $\eta_t = \eta$ which satisfies that $\eta \leq \frac{K}{2mL}$. Then the following inequality can be obtained,

$$\begin{aligned} & \mathbb{E}[F(\bar{w}(t)) - F(w^*)] \\ & \leq (1 - \frac{\mu\eta}{m})^t (F(\bar{w}(0)) - F(w^*)) + \frac{m}{\eta\mu} \left(\frac{\eta K^2 L^2 + \eta^2 L^2 \mu}{K} \Xi + \eta K^2 \sigma^2 + \eta^2 L(\sigma^2 + 2\mu\zeta) \right), \end{aligned} \quad (10)$$

where $\Xi = \mathbb{E}[\|\mathbf{w}(0) - \mathbf{1} \otimes \bar{w}(0)\|^2] + \frac{2\eta^2 K \chi^2 (1+\lambda^2)}{(1-\lambda^2)^2}$, $\sigma^2 = \frac{1}{K} \sum_{k=1}^K \sigma_k^2$ and t is the current iteration.

Proof: The proof can be found in Appendix A.2. ■

3 DeceFL over Undirected Time-Varying Graphs

In this section we establish the sub-linear convergence of DeceFL over time-varying undirected graphs. Let us formally describe the assumptions we make on the graphs and on the mixing matrices $W(t)$ that are compatible with the graphs. Consider a time-varying undirected graph sequence $\{\mathcal{G}(0), \mathcal{G}(1), \dots\}$. Every graph instance $\mathcal{G}(t) = (\mathcal{N}, \mathcal{E}(t), W(t))$ consists of a time-invariant set of agents $\mathcal{N} = \{1, 2, \dots, K\}$ and a set of time-varying edges $\mathcal{E}(t)$. The unordered pair of vertices $(j, i) \in \mathcal{E}(t)$ if and only if agents j and i can exchange information at t -th iteration. The set of neighbors of agent i at t -th iteration is defined as $\mathcal{N}_i(t) = \{j | (j, i) \in \mathcal{E}(t)\}$.

For time-varying case, DeceFL algorithm (2) can be rewritten as,

$$w_k(t+1) = \sum_{j=1}^K W_{kj}(t) w_j(t) - \eta_t \tilde{g}_k(w_k(t)), \quad (11)$$

where $i = 1, \dots, K$.

Next, we analyze the convergence of DeceFL under the following assumptions, which are standard in analyzing the convergence of FedAvg [1].

Assumption 3 For any $t \in \mathbb{N}_+$, the directed graph $\mathcal{G}(t)$ satisfies the following conditions:

- (i) The mixing matrix $W(t)$ is doubly stochastic, i.e., $\sum_{i=1}^K W_{ij}(t) = \sum_{j=1}^K W_{ij}(t) = 1, \forall i, j \in \mathcal{N}$.
- (ii) There exists a constant $\lambda \in (0, 1)$ such that $\|W(t) - \frac{1}{K}\mathbf{1}\mathbf{1}^T\| \leq \lambda$.

One sufficient condition to guarantee the second item of Assumption 3 holds is that $\mathcal{G}(t)$ is strongly connected and there exists a constant $\omega \in (0, 1)$ such that $W_{ij}(t) \geq \omega$ if $W_{ij}(t) > 0$.

In this case, the same convergence conclusion as Theorem 1 can be obtained.

Theorem 2 Let Assumptions 1–3 hold. Consider algorithm (11), where the learning rate given by $\eta_t = \frac{\delta}{t + \Gamma}$, $\delta > \frac{m}{\mu}$ and $\Gamma \geq \frac{\sqrt{2(1+\lambda^2)}+1+\lambda^2}{1-\lambda^2}$ satisfies $\frac{\delta}{\Gamma} \leq \frac{1}{2L}$. Then

$$\mathbb{E}[\|\bar{w}(t) - w^*\|^2] \leq \frac{\tilde{\zeta}}{t + \Gamma}, \quad (12)$$

where $\tilde{\zeta}$ is defined in Theorem 1.

Proof: The proof of the above theorem is exactly the same as that of Theorem 1, except that W needs to be replaced by $W(t)$, and the proof can be completed according to Assumption 3. ■

As mentioned earlier, Assumption 3 requires that the undirected graph at each iteration time is connected, which is relatively strong. Next, we consider the topology of the graph in a more general case. In the sequel, we use the following notation, for any $t = 0, 1, \dots$ and any $b = 1, 2, \dots$,

$$\mathcal{G}_b(t) \triangleq \{\mathcal{N}, \mathcal{E}(t) \bigcup \mathcal{E}(t+1) \bigcup \dots \bigcup \mathcal{E}(t+b-1)\}, \quad (13)$$

and

$$W_b(t) \triangleq W(t)W(t-1)\dots W(t-b+1), \quad (14)$$

with the convention that $W_b(t) = I$ for any needed $t < 0$ and $W_0(t) = I$ for any t .

Next, we give the assumption that we impose on the weight matrices as [7].

Assumption 4 For any $t \in \mathbb{N}_+$, the mixing matrix $W(t) = [W_{ij}(t)] \in \mathbb{R}^{K \times K}$ satisfies the following relations:

$$(i) W(t)\mathbf{1} = \mathbf{1}, \mathbf{1}^T W(t) = \mathbf{1}^T;$$

(ii) (Joint spectrum property) There exists a positive integer B such that $\lambda = \max_{t \geq B} \lambda(t) < 1$, where $\lambda(t) = \sigma_{\max}\{W_B(t) - \frac{1}{n}\mathbf{1}\mathbf{1}^T\}$ is the largest singular value of $W_B(t) - \frac{1}{n}\mathbf{1}\mathbf{1}^T$.

We summarize our convergence results in the case of time-varying graphs as follows.

Theorem 3 Let Assumptions 1–2 and 4 hold. Consider algorithm (11), where the learning rate given by $\eta_t = \frac{\delta}{t + \Gamma}$, $\delta > \frac{m}{\mu}$ and $\Gamma \geq \frac{B(2 + \sqrt{2(1 + \lambda^2)})}{1 - \lambda^2} - 1$ satisfies $\frac{\delta}{\Gamma} \leq \frac{1}{2L}$ in which $\lambda \in (0, 1)$. Then

$$\mathbb{E}[\|\bar{w}(t) - w^*\|^2] \leq \frac{\tilde{\zeta}_B}{t + \Gamma}, \quad (15)$$

where $\zeta_B \triangleq \max \left\{ \Gamma^2 \cdot \mathbb{E}[\|\mathbf{w}(0) - \mathbf{1} \otimes \bar{w}(0)\|^2], \frac{1}{1 - \lambda^2} \cdot \frac{\delta^2 B^2 K \lambda^2}{\frac{(\Gamma+1-B)^2}{(\Gamma+1)^2(\lambda^2+1)} - \frac{1}{2}} \right\}$, $\tilde{\zeta}_B \triangleq \max \left\{ \Gamma \cdot \mathbb{E}[\|\bar{w}(0) - w^*\|^2], \frac{(6\epsilon L + \sigma^2)\delta^2 m + \frac{2\zeta_B m}{K}}{\mu\delta - m} \right\}$, $\sigma^2 = \frac{1}{K} \sum_{k=1}^K \sigma_k^2$, and ϵ as defined in Theorem 1.

Proof: The proof can be found in Appendix A.3. ■

Remark 3 Note that Assumption 4 is equivalent to Assumption 3 when $B = 1$, as in the analysis of time-varying graphs in [7]. Furthermore, Theorem 3 and Theorem 2 are the same in this case.

4 Consensus problem

For the global optimization problem as following,

$$\min_{w \in \mathbb{R}} F(\mathcal{D}; w) \triangleq \frac{1}{2} \sum_{k=1}^K (X_k w - w_k(0))^2, \quad (16)$$

where $\mathcal{D} = (X, y)$, in which $X = [X_k] = \mathbf{1}_K \in \mathbb{R}^K$ is features vector and $y = [w_k(0)] \in \mathbb{R}^K$ is the label vector, and $w_k(0)$ is the local label of client k .

Consider solving problem (16) using algorithms FedAvg, swarm learning (SL) in [8] and the proposed DeceFL respectively. Table 1 illustrates the comparison of algorithms FedAvg, SL and DeceFL.

Table 1: Comparison between FedAvg, SL and DeceFL

Study	Approach	Central sever	Communication	Aggregate average
[9]	FedAvg	✓	client $w_k(t) \rightleftharpoons$ sever	$\frac{1}{K} (\sum_{k \notin S_i} w_k(t) + \sum_{k \in S_i} w_k(t))$
[8]	SL	✓ pseudo central sever	client $w_k(t) \rightleftharpoons$ pseudo central sever	$\sum_{k=1}^K p_k w_k(t)$
Ours	DeceFL	$O(1/T)$	client $w_k(t) \rightleftharpoons$ neighbor client	$\sum_{k=1}^K W_{ki} w_k(t)$

According to $F(\mathcal{D}; w)$ in (16), then gradient $\nabla F(\mathcal{D}; w) = \sum_{k=1}^K (w - w_k(0))$ can be obtained. it can be obtained that the optimal value point of problem (16) is $w^* = \frac{1}{K} \sum_{k=1}^K w_k(0)$. Denoted

$w_k \in \mathbb{R}$ is local copy of the global variable w on client k , and the local loss function on the k -th client is denoted as $f_k(w) = \frac{1}{2}(w - w_k(0))^2$. Next, algorithms FedAvg, SL and DeceFL on k -th client at t -th iteration will be considered respectively, where $k = 1, \dots, K$ and $t \in \mathbb{N}_+$.

4.1 FedAvg algorithm

In the FedAvg algorithm, there is a central server to collect the local parameter information of each client for average aggregation, and assign it to each client,

$$\begin{aligned} w_k(t+1) &= \frac{1}{K} \sum_{j=1}^K w_j(t) - \eta \nabla f_k(w_k(t)) \\ &= \frac{1}{K} \sum_{j=1}^K w_j(t) - \eta(w_k(t) - w_k(0)), \end{aligned} \quad (17)$$

where η is step-size. We can compactly write (17) as:

$$\mathbf{w}(t+1) = \frac{1}{K} \mathbf{1}_K \mathbf{1}_K^T \mathbf{w}(t) - \eta(\mathbf{w}(t) - \mathbf{w}(0)). \quad (18)$$

Let the virtual sequences $\bar{w}(t) = \frac{1}{K} \mathbf{1}_K^T \mathbf{w}(t)$ and $\bar{w}(0) = \frac{1}{K} \mathbf{1}_K^T \mathbf{w}(0)$, then we have

$$\bar{w}(t+1) = \bar{w}(t) - \eta \bar{w}(t) + \eta \bar{w}(0), \quad (19)$$

note that $\bar{w}(0) = w^*$, thus we have,

$$\bar{w}(t+1) - w^* = (1 - \eta)(\bar{w}(t) - w^*), \quad (20)$$

the following can be obtained by subtracting the two sides of (18) by (19) respectively,

$$\mathbf{w}(t+1) - \mathbf{1}_K \bar{w}(t+1) = \left(\frac{1}{K} \mathbf{1}_K \mathbf{1}_K^T - \eta \mathbf{I}_K \right) (\mathbf{w}(t) - \mathbf{1}_K \bar{w}(t)) + \eta(\mathbf{w}(0) - \mathbf{1}_K w^*). \quad (21)$$

Furthermore, let $\sigma = \rho(\frac{1}{K} \mathbf{1}_K \mathbf{1}_K^T - \eta \mathbf{I}_K)$, where $\rho(\cdot)$ is the spectral norm. Then, from (21), we have

$$\|\mathbf{w}(t+1) - \mathbf{1}_K \bar{w}(t+1)\| \leq \sigma \|\mathbf{w}(t) - \mathbf{1}_K \bar{w}(t)\| + \eta \|\mathbf{w}(0) - \mathbf{1}_K w^*\|. \quad (22)$$

From (20) and (22), we have

$$\begin{aligned} &\begin{bmatrix} \|\mathbf{w}(t+1) - \mathbf{1}_K \bar{w}(t+1)\| \\ \|\bar{w}(t+1) - w^*\| \end{bmatrix} \\ &\leq \begin{bmatrix} \sigma & 0 \\ 0 & 1 - \eta \end{bmatrix} \begin{bmatrix} \|\mathbf{w}(t) - \mathbf{1}_K \bar{w}(t)\| \\ \|\bar{w}(t) - w^*\| \end{bmatrix} + \begin{bmatrix} \eta \|\mathbf{w}(0) - \mathbf{1}_K w^*\| \\ 0 \end{bmatrix}. \end{aligned} \quad (23)$$

On the convergence analysis of the algorithm, on the one hand, when $\eta > 0$ is fixed and $\sigma < 1$ is satisfied, then sequence $\{\|\mathbf{w}(t) - \mathbf{1}_K \bar{w}(t)\|\}_{t>0}$ linearly converges to a neighborhood of $\|\mathbf{w}(0) - \mathbf{1}_K w^*\|$. On the other hand, when $\eta \triangleq \eta_t = \frac{\delta}{t+\Gamma}$ is diminishing and $\frac{\delta}{\Gamma} < 1$ is satisfied

for any $\delta, \Gamma > 0$, then

$$\begin{bmatrix} \|\mathbf{w}(t+1) - \mathbf{1}_K \bar{w}(t+1)\| \\ \|\bar{w}(t+1) - w^*\| \end{bmatrix} \rightarrow \begin{bmatrix} 0 \\ 0 \end{bmatrix},$$

as $t \rightarrow \infty$ with converge rate $O(\frac{1}{t})$ can be obtained.

To sum up, when $\eta_t < 1$ is diminishing, it is easy to know that $\bar{w}(t) \rightarrow w^*$ and $\mathbf{w}(t) \rightarrow \mathbf{1}_K \bar{w}(t)$ as $t \rightarrow \infty$, that is, each client achieve consensus by converging to the average of the initial conditions.

4.2 SL algorithm

In the SL algorithm, the situation that without a central server is considered, in each iteration a leader is dynamically selected from the members to aggregate the model parameters in each client and assign them to each client. Specifically, the randomly selected leader in t -th iteration is denoted as j_t -th client, and the weighted average aggregation is as follows,

$$\tilde{w}_{K_t}(t) = \sum_{j=1}^K p_j w_j(t), \quad (24)$$

the remaining clients receive $\tilde{w}_{K_t}(t)$ from the leader and update as follows,

$$\begin{aligned} w_k(t+1) &= \tilde{w}_{K_t}(t) - \eta \nabla f_k(w_k(t)) \\ &= \sum_{j=1}^K p_j w_j(t) - \eta \nabla f_k(w_k(t)) \\ &= \sum_{j=1}^K p_j w_j(t) - \eta (w_k(t) - w_k(0)), \end{aligned} \quad (25)$$

where p_k is the weight of the k -th client. Then, denotes $\mathbf{P}' = [p_1; \dots; p_K] \in \mathbb{R}^K$, then (25) can be written as

$$\mathbf{w}(t+1) = (\mathbf{1}_K \mathbf{P}'^T) \mathbf{w}(t) - \eta (\mathbf{w}(t) - \mathbf{w}(0)). \quad (26)$$

Define $\bar{w}_{sl}(t) = \mathbf{P}'^T \mathbf{w}(t)$, then we have

$$\bar{w}_{sl}(t+1) = \bar{w}_{sl}(t) - \eta \bar{w}_{sl}(t) + \eta \bar{w}_{sl}(0), \quad (27)$$

subtract w^* from both sides of the above equation,

$$\bar{w}_{sl}(t+1) - w^* = (1 - \eta)(\bar{w}_{sl}(t) - w^*) + \eta(\bar{w}_{sl}(0) - w^*). \quad (28)$$

Then, from (26) and (28), we have

$$\mathbf{w}(t+1) - \mathbf{1}_K \bar{w}_{sl}(t+1) = (\mathbf{1}_K \mathbf{P}'^T - \eta \mathbf{I}_K)(\mathbf{w}(t) - \mathbf{1}_K \bar{w}_{sl}(t)) + \eta(\mathbf{w}(0) - \mathbf{1}_K \bar{w}_{sl}(0)). \quad (29)$$

The following inequality can be obtained through the matrix spectral norm,

$$\|\mathbf{w}(t+1) - \mathbf{1}_K \bar{w}_{sl}(t+1)\| \leq \min\{|1-\eta|, \eta\} \|\mathbf{w}(t) - \mathbf{1}_K \bar{w}_{sl}(t)\| + \eta \|\mathbf{w}(0) - \mathbf{1}_K \bar{w}_{sl}(0)\|. \quad (30)$$

Then, from (28) and (30), we have

$$\begin{aligned} & \begin{bmatrix} \|\mathbf{w}(t+1) - \mathbf{1}_K \bar{w}_{sl}(t+1)\| \\ \|\bar{w}_{sl}(t+1) - w^*\| \end{bmatrix} \\ & \leq \begin{bmatrix} \min\{|1-\eta|, \eta\} & 0 \\ 0 & 1-\eta \end{bmatrix} \begin{bmatrix} \|\mathbf{w}(t) - \mathbf{1}_K \bar{w}_{sl}(t)\| \\ \|\bar{w}_{sl}(t) - w^*\| \end{bmatrix} + \begin{bmatrix} \eta \|\mathbf{w}(0) - \mathbf{1}_K \bar{w}_{sl}(0)\| \\ \eta \|\bar{w}_{sl}(0) - w^*\| \end{bmatrix}. \end{aligned} \quad (31)$$

Similarly, on the convergence of SL, when $0 < \eta \leq 1$ is a fixed constant then sequence $\{\|\mathbf{w}(t) - \mathbf{1}_K \bar{w}_{sl}(t)\|\}_{t>0}$ linearly converges to a neighborhood of $\|\mathbf{w}(0) - \mathbf{1}_K \bar{w}_{sl}(0)\|$. On the other hand, if $\eta \triangleq \eta_t$ is diminishing, such as $\eta_t = \frac{\delta}{t+\Gamma}$ and $\frac{\delta}{\Gamma} \leq 1$ is satisfied for some $\delta, \Gamma > 0$, then

$$\begin{bmatrix} \|\mathbf{w}(t+1) - \mathbf{1}_K \bar{w}_{sl}(t+1)\| \\ \|\bar{w}_{sl}(t+1) - w^*\| \end{bmatrix} \rightarrow \begin{bmatrix} 0 \\ 0 \end{bmatrix},$$

as $t \rightarrow \infty$ with converge rate $O(\frac{1}{t})$ can be obtained.

To sum up, when η_t is diminishing and $\eta_t < 1$, it's easy to know that $\bar{w}_{sl}(t+1) \rightarrow w^*$ and $\mathbf{w}(t) \rightarrow \mathbf{1}_K \bar{w}_{sl}(t)$ as $t \rightarrow \infty$, that is, each client consensus convergence to the weighted average of the initial conditions.

4.3 DeceFL algorithm

Decentralization is considered in DeceFL. Each client communicates parameters through the topology of the time-varying undirected connected graph. According to the weighted aggregation of information obtained from neighbor clients, the local update is completed according to the following iteration,

$$w_k(t+1) = \sum_{j=1}^K W_{kj}(t) w_j(t) - \eta \nabla f_k(w_k(t)) = \sum_{j=1}^K W_{kj}(t) w_j(t) - \eta (w_k(t) - w_k(0)), \quad (32)$$

where $W \in \mathbb{R}^{K \times K}$ is the weighted matrix of undirected connected graph. Then (32) can be rewritten as:

$$\mathbf{w}(t+1) = W(t) \mathbf{w}(t) - \eta (\mathbf{w}(t) - \mathbf{w}(0)), \quad (33)$$

where $W(t)$ satisfies Assumption 4. According to the definition of $\bar{w}(t) = \frac{1}{K}\mathbf{1}_K^T \mathbf{w}(t)$ and $\bar{w}(0) = \frac{1}{K}\mathbf{1}_K^T \mathbf{w}(0) = w^*$, we have

$$\begin{aligned} \mathbf{w}(t+1) - \mathbf{1}_K \bar{w}(t+1) &= W(t)(\mathbf{w}(t) - \mathbf{1}_K \bar{w}(t)) - \eta(\mathbf{w}(t) - \mathbf{1}_K \bar{w}(t)) + \eta(\mathbf{w}(0) - \mathbf{1}_K w^*) \\ &= W_B(t)(\mathbf{w}(t+1-B) - \mathbf{1}_K \bar{w}(t+1-B)) \\ &\quad - \eta \sum_{\tau=1}^B W_{B-\tau}(t)(\mathbf{w}(t-B+\tau) - \mathbf{1}_K \bar{w}(t-B+\tau)) \\ &\quad + \eta \sum_{\tau=1}^B W_{B-\tau}(t)(\mathbf{w}(0) - \mathbf{1}_K w^*), \end{aligned} \quad (34)$$

and the following inequality can be obtained through the matrix spectral norm:

$$\begin{aligned} &\|\mathbf{w}(t+1) - \mathbf{1}_K \bar{w}_{sl}(t+1)\| \\ &\leq \lambda \|\mathbf{w}(t+1-B) - \mathbf{1}_K \bar{w}(t+1-B)\| \\ &\quad + \eta \sum_{\tau=1}^B \|\mathbf{w}(t-B+\tau) - \mathbf{1}_K \bar{w}(t-B+\tau)\| + \eta B \|\mathbf{w}(0) - \mathbf{1}_K w^*\| \\ &\leq (\lambda + \eta B) \max_{\tau=0,\dots,B} \{\|\mathbf{w}(t-B+\tau) - \mathbf{1}_K \bar{w}(t-B+\tau)\|\} + \eta B \|\mathbf{w}(0) - \mathbf{1}_K w^*\|. \end{aligned} \quad (35)$$

When $\eta \leq \frac{1-\lambda}{B}$, then sequence $\{\|\mathbf{w}(t) - \mathbf{1}_K \bar{w}_{sl}(t)\|\}_{t>0}$ converges to a neighborhood of $\|\mathbf{w}(0) - \mathbf{1}_K \bar{w}_{sl}(0)\|$. Notice that

$$\bar{w}(t+1) - w^* = (1-\eta)(\bar{w}(t) - w^*), \quad (36)$$

with $\eta \leq \frac{1-\lambda}{B}$, thus $\bar{w}(t+1) \rightarrow w^*$ as $t \rightarrow \infty$ can be obtained, i.e., $w_i(t)$ converges to a neighborhood of w^* as $t \rightarrow \infty$.

However, when $\eta \triangleq \eta_t = \frac{\delta}{t+\Gamma}$ is diminishing and $\frac{\delta}{\Gamma} < 1$ is satisfied for any $\delta, \Gamma > 0$. Then from (34) we have,

$$\begin{aligned} &\|\mathbf{w}(t+1) - \mathbf{1}_K \bar{w}_{sl}(t+1)\| \\ &\leq \lambda \|\mathbf{w}(t+1-B) - \mathbf{1}_K \bar{w}(t+1-B)\| \\ &\quad + \sum_{\tau=1}^B \eta_{t-B+\tau} \|\mathbf{w}(t-B+\tau) - \mathbf{1}_K \bar{w}(t-B+\tau)\| + \sum_{\tau=1}^B \eta_{t-B+\tau} \|\mathbf{w}(0) - \mathbf{1}_K w^*\| \\ &\leq \lambda \|\mathbf{w}(t+1-B) - \mathbf{1}_K \bar{w}(t+1-B)\| \\ &\quad + \eta_{t-B+1} \sum_{\tau=1}^B \|\mathbf{w}(t-B+\tau) - \mathbf{1}_K \bar{w}(t-B+\tau)\| + B \eta_{t-B+1} \|\mathbf{w}(0) - \mathbf{1}_K w^*\|. \end{aligned} \quad (37)$$

When $\frac{1}{\Gamma+1} + \delta < \frac{1-\lambda}{B}$, it can be proved by induction that

$$\|\mathbf{w}(t) - \mathbf{1}_K \bar{w}_{sl}(t)\| \leq \frac{\varrho}{t+\Gamma}, \quad (38)$$

where $\varrho = \max\{\Gamma, \frac{B}{1-\frac{B}{\Gamma+1}-(\lambda+B\delta)}\} \cdot \|\mathbf{w}(0) - \mathbf{1}_K w^*\|$. In this setting, $\eta \triangleq \eta_t$ is diminishing, such as

$\eta_t = \frac{\delta}{t+\Gamma}$ and $\frac{\delta}{\Gamma} < 1$, thus

$$\|\bar{w}(t+1) - w^*\| = (1-\eta)\|\bar{w}(t) - w^*\| = (1-\eta)^t\|\bar{w}(1) - w^*\|. \quad (39)$$

To sum up, when η_t is diminishing, $\frac{1}{\Gamma+1} + \delta < \frac{1-\lambda}{B}$ and $\frac{\delta}{\Gamma} < 1$, it's easy to know that $\bar{w}(t+1) \rightarrow w^*$ and $\mathbf{w}(t) \rightarrow \mathbf{1}_K \bar{w}(t)$ as $t \rightarrow \infty$, that is, each client consensus convergence to the average of the initial conditions.

4.4 Summary

In FedAvg, the model parameters of each client are aggregated through the central server and communicated to each client to update the local model, and finally achieve consistency between each client, and the optimally of problem (16) is realized. .

In SL, though it is not considered a central server settings, but it always randomly select a leader as a central server from all participating members, which weighted aggregation client-side model parameters and communicate with other clients to complete the clients' update. Finally, the optimally of problem (16) and the consistency that the model parameters of each client converge to the optimal value point are realized.

In DeceFL, the communication and aggregation between the central server and multiple clients are not required, but the update of local model parameters is completed through the communication and weighted average between each client and neighbor clients, so as to finally realize the consistency among clients and the optimally of problem (16) is realized.

4.5 Example

This toy example shows the behaviours of parameter convergence associated with each node in DeceFL. The setup uses undirected graphs of 8 nodes with connectivity probability $p = 0.5$ (Figure 1(a)) and $p = 0.3$ (Figure 1(c)), where a graph of smaller p has a sparser structure (i.e. its adjacency matrix has more zero elements). And every node gets one simple sample $(1, 1)$ (the 1st is the feature, and the 2nd is the label). It intends to show that in DeceFL parameters associated each node satisfying $w_k \rightarrow w^*$ ($k = 1, \dots, 8$). FedAvg in Figure 1 shows as a single curve due to the existence of a centre node and hence has no issue of consensus; while DeceFL is intrinsically decentralised and each node has its own convergence curve that finally reaches a consensus and the global optima.

5 Experiments

5.1 Method description

FedAvg framework FedAvg is a centralized framework introduced in [10, 11], as in Figure 2(a), which uses a central client to collect information from all other nodes. At aggregation, FedAvg collects model parameters from every node at the central client, takes average and then distributes the global model to every node. It is equivalent to an all-to-all network without such a central center, i.e., every client in the network can receive information from all other clients.

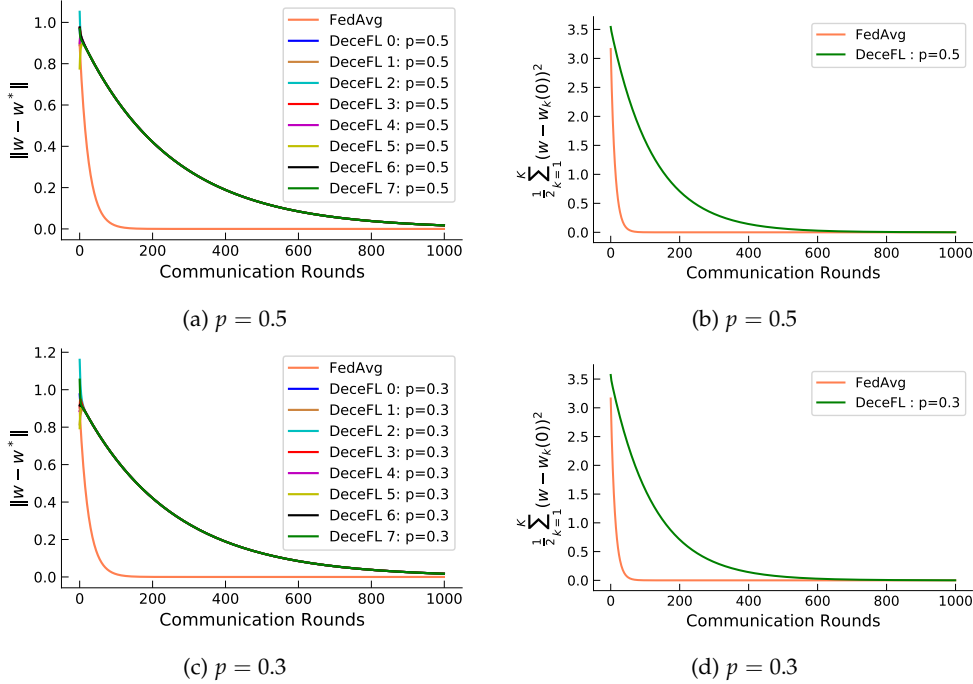


Figure 1: An example of consensus behaviours of DeceFL, intrinsically decentralised algorithm on sparse graphs. It illustrates the behaviour that all nodes in DeceFL reach a consensus on parameter estimates.

SL framework Swarm learning is introduced in [12] as a “decentralized” machine-learning approach that maintains confidentiality without the need for a central coordinator. There is no such a universal central client, but a potentially different central client is selected in every iteration, as in Figure 2(b). Mathematically, it is equivalent to FedAvg with varying central clients. In the benchmark, it will be only used in the case of 8-node graphs.

DeceFL framework DeceFL is a intrinsically decentralized framework, as in Figure 2(c), which runs on a graph (IID and Non-IID experiments) and a sequence of graphs (time-varying experiments) that is not as strong as equivalent graphs in FedAvg and SL. Our experiments use the *Erdos-Renyi* (ER) graph in DeceFL, with various connectivity probability values (controlled by an index p that specifies the probability of whether an edge exists; the graph of n nodes with index p has, in probability, $pn(n - 1)/2$ edges). With the number of nodes n and connectivity probability p specified, a connected ER graph is generated by *Erdős-Rényi model* from [13]; in particular, we use Laplacian method to choose weight matrix (see [14, 15]).

Convex and non-convex learning algorithms To ensure in benchmark DeceFL can work well for either strongly convex learning methods or non-convex methods, we adopts two algorithms:

- strongly convex: logistic regression (LR) with l_2 regularization. Every node runs 10 epochs in each round, with batch-size 64. It uses the SGD optimizer, with weight decay coefficient 10^{-4} for the realization of l_2 regularization. The initial learning rate (for deep learning framework) is 0.01, which is later decayed by multiplying 0.2 every 5 epochs.

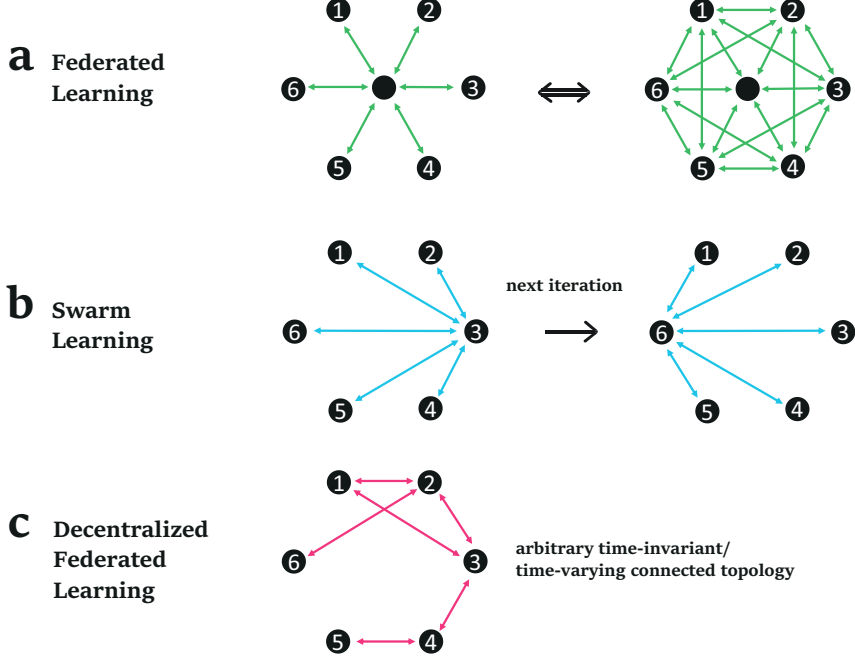


Figure 2: Illustration of key concepts in different state-of-the-art federated learning frameworks.

- non-convex: multilayer perceptrons (MLP), a type of deep neural network (DNN). Every node runs 30 epochs in each round, with batch-size 64. It uses the cross entropy loss and the SGD optimizer, with weight decay coefficient 10^{-4} . The initial learning rate (for deep learning framework) is 0.1, which is decayed by multiplying 0.2 every 20 epochs. This DNN has 8 hidden layers with ReLU activation function, whose dimensions are 256, 512, 512, 256, 256, 128, 128, 64, respectively. The *dropout* rate is set to 0.3.

Both methods use *sigmoid* as the activation function in the output layer for binary classification (dataset A2) and *softmax* for multiclass classification (4-way and 10-way problems for CWRU dataset). At aggregation, the gradient update coefficient for DeceFL is 0.1 (FedAvg does not use this variable). The total number of running rounds is selected by considering the visualization effects for all methods in comparison.

Loss and accuracy computation

- FedAvg, SL: In training, the loss/accuracy is the averaged value of the loss/accuracy values of the global model on local training datasets associated with each node. In test, the accuracy is the value of the global model on the test dataset.
- DeceFL: In training, DeceFL takes average of all the local loss/accuracy values, which are computed by the local models on the corresponding local datasets associated with each node. In test, the accuracy is the average of the accuracy values of local models at each node on the test dataset.

5.2 Dataset A2

The peripheral blood mononuclear cell (PBMC)-derived transcriptome dataset, named as “dataset A2” in [12], is used, which was originally generated with Affymetrix HG-U133 2.0 microarrays (8,348 individuals), by inspection of all publicly available datasets at National Center for Biotechnology Information Gene Expression Omnibus. To perform IID experiments, the initial preparation randomly drops negative samples, resulting in 5,176 samples, such that the whole dataset is balanced, i.e. the ratio of the positive to the negative samples is 1 : 1.

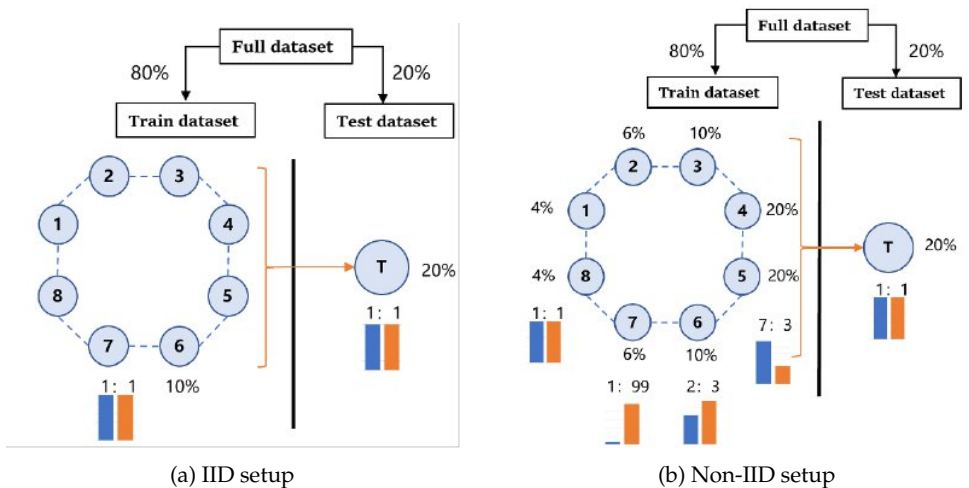


Figure 3: Preparation of training and test datasets in IID and Non-IID setups for dataset A2 in the federated learning framework of 8 nodes.

5.2.1 IID experiments

IID setup Samples from dataset A2 were split into non-overlapping training datasets for each node and a global test dataset that will be used for model testing built by DeceFL and FedAvg, SL. Dataset A2 is randomly divided into a training set (for the whole nodes) and a test set by the ratio of 8 : 2 (4140 samples for training and 1036 samples for test). In IID setup, the samples associated with each node is uniformly randomly drawn from the whole training set, such that the sample size of each node is equal and the samples keeps balanced (the ratio of the positive to the negative is approximately 1 : 1) and non-overlapped, as illustrated in Figure 3(a) for 8-node graphs.

In the IID experiments, we use datasets prepared in the IID setup. To show DeceFL works well on various graph scales and sparsity, we consider graphs of $n = 4, 8, 16$ nodes, and connectivity probability $p = 0.3, 0.5, 0.7, 0.9$. The loss and accuracy values of DeceFL are computed and compared to FedAvg in different setups (n, p). The results for logistic regression are given in Figure 4 and that for DNN are given in Figure 5. The experimental results show that, even without a central node, DeceFL can converge to the same level of training loss and test accuracy as FedAvg framework. DeceFL has a longer transient period than FedAvg (i.e. converging slower than FedAvg), which may attribute to the missing of a central node for information collection. Convergence speed could be affected by the choice of graph

connectivity and the updating step size (i.e. η_t). The choice of updating step size balances between convergence stability and speed, where the increase of step size increases convergence speed but deteriorate convergence stability. And the increase of graph connectivity can also increase convergence speed.

Table 2: The summary of accuracy values of DeceFL and FedAvg at the last rounds for the test dataset with the IID setup.

Setup	Graph	FedAvg	SL	DeceFL			
				$p = 0.9$	$p = 0.7$	$p = 0.5$	$p = 0.3$
LR	4-node	0.9874	-	0.9879	0.9879	0.9879	0.9882
	8-node	0.9874	0.9874	0.9884	0.9884	0.9884	0.9884
	16-node	0.9884	-	0.9884	0.9883	0.9884	0.9884
DNN	4-node	0.9865	-	0.9845	0.9845	0.9848	0.9833
	8-node	0.9845	0.9855	0.9826	0.9836	0.9826	0.9832
	16-node	0.9845	-	0.9839	0.9847	0.9837	0.9839

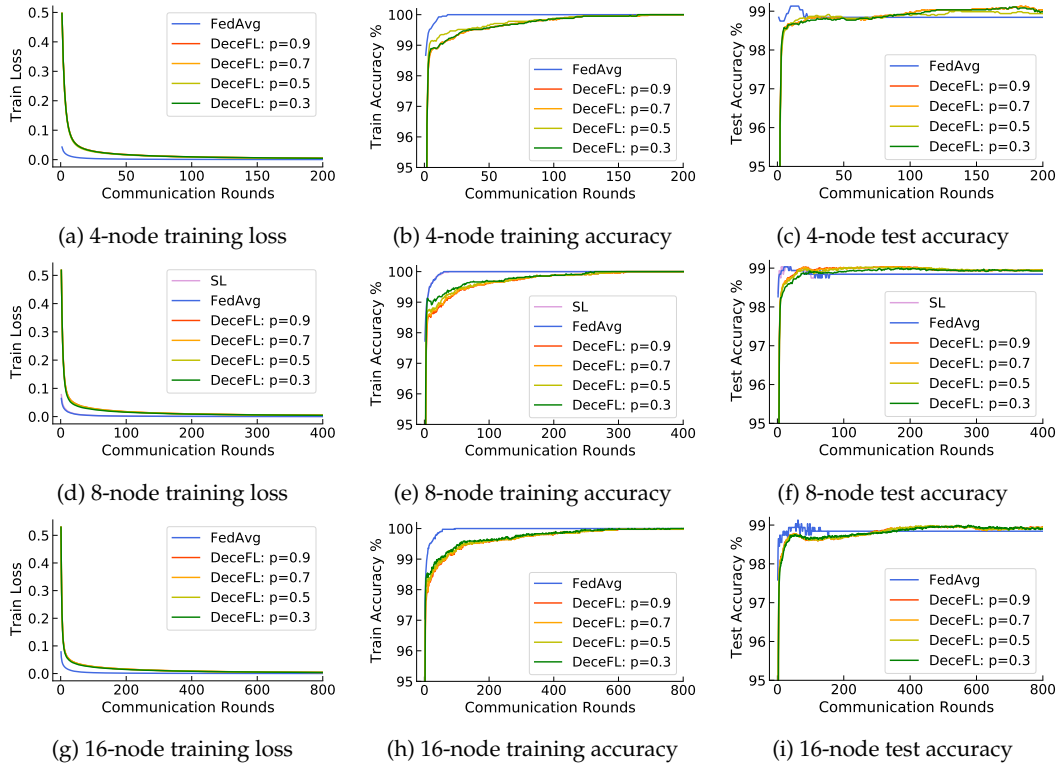


Figure 4: Comparative studies of DeceFL, FedAvg and SL (only for 8-node case) with logistic regression in the IID setup.

5.2.2 Non-IID experiments

Non-IID setup The Non-IID setup explicitly designs training datasets for each node the sample size and the sample distribution, which is summarized in detail in Table 3. The setup for 8-node graphs is illustrated in Figure 3(b). To ensure the ratio between positive and negative

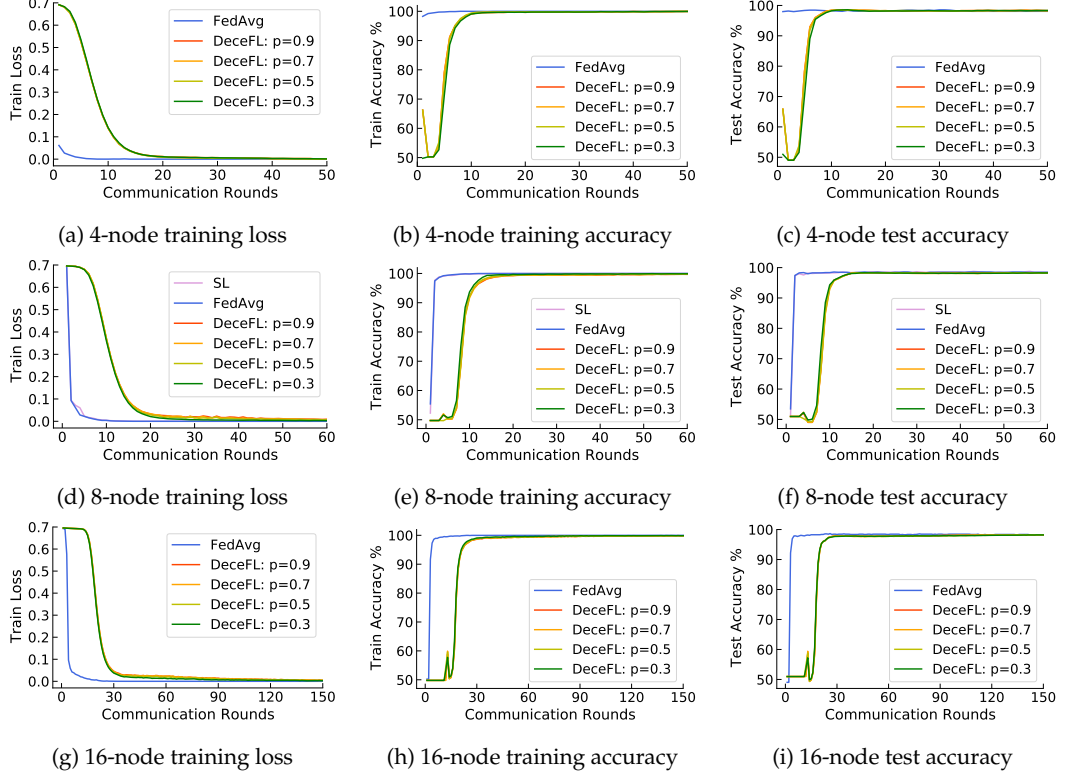


Figure 5: Comparative studies of DeceFL, FedAvg and SL (only for 8-node case) with DNN in the IID setup.

samples for each node complying with the designed value, we draw the specific amounts of positive and negative samples separately and then combine them to form the dataset.

Table 3: The Non-IID setup details for experiments with node 4, 8 and 16. The percents tell the sample sizes for each node in training, and the ratios specify the percentages of positive and negative samples among each dataset associated with every node.

4-node graph	Node 1		Node 2		Node 3		Node 4	
	10%	1:99	10%	99:1	20%	3:7	40%	6:4
8-node graph	Node 1,2		Node 3,4		Node 5,6		Node 7,8	
	4%	1:1	6%	1:99	10%	4:6	20%	7:3
16-node graph	Node 1,2,3,4		Node 5,6,7,8		Node 9,10,11,12		Node 13,14,15,16	
	2%	1:1	3%	1:99	5%	4:6	10%	7:3

In practice, the ratio between positive and negative samples may not always be balanced. To show that DeceFL functions well in practice, we explicitly design such Non-IID scenarios as shown in Table 3. It includes extremely unbalanced cases (e.g., 1:99), balanced cases (i.e. 1:1), and in-between cases (e.g., 4:6, 3:7). The results of logistic regression are shown in Figure 6 and DNN in Figure 7. In the scenario of 8-node graphs, SL is taken into account and has the similar performance as FedAvg. For both strongly convex (LR) and non-convex models (DNN), DeceFL reaches the similar accuracy as FedAvg and SL in both training and testing, although DeceFL demands certain rounds to allow nodes to reach consensus. In comparison with LR,

DNN allows nodes in DeceFL to reach consensus within less communication rounds.

Table 4: The summary of accuracy values of DeceFL and FedAvg at the last rounds for the test dataset with the Non-IID setup.

Setup	Graph	FedAvg	SL	DeceFL			
				$p = 0.9$	$p = 0.7$	$p = 0.5$	$p = 0.3$
LR	4-node	0.9874	-	0.9884	0.9884	0.9884	0.9887
	8-node	0.9874	0.9874	0.9884	0.9882	0.9882	0.9879
	16-node	0.9874	-	0.9877	0.9877	0.9877	0.9876
DNN	4-node	0.9836	-	0.9845	0.9845	0.9845	0.9841
	8-node	0.9865	0.9865	0.9836	0.9837	0.9840	0.9844
	16-node	0.9855	-	0.9864	0.9865	0.9861	0.9865

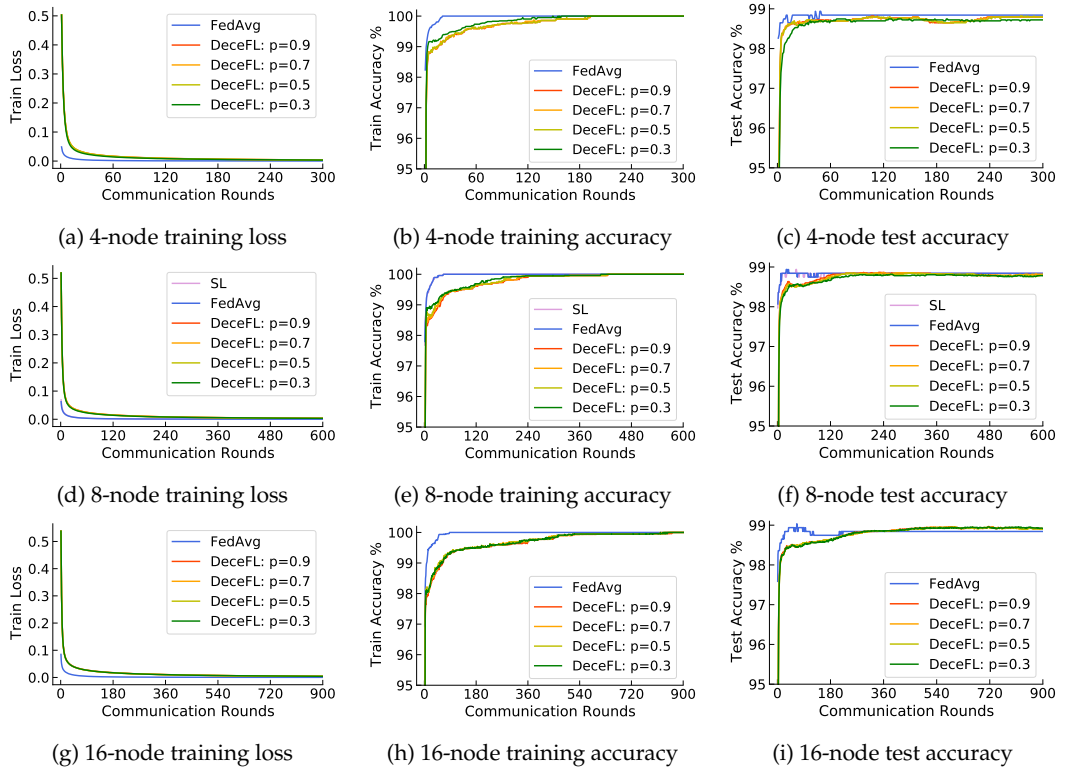


Figure 6: Comparative studies of DeceFL and FedAvg. The figure consists of nine subplots arranged in a 3x3 grid. The columns represent training loss, training accuracy, and test accuracy respectively. The rows represent 4-node, 8-node, and 16-node cases. Each subplot compares FedAvg (blue), SL (purple), and five variants of DeceFL (p=0.9, p=0.7, p=0.5, p=0.3) across communication rounds. FedAvg and SL show slow convergence, while DeceFL variants converge much faster, often within 100 rounds.

5.2.3 Time-varying experiments with edge changes

This time-varying experiment aims to simulate the scenario when certain nodes randomly malfunction in communication for the federated learning, where FedAvg or SL fails to collect information of all nodes. It intends to show that DeceFL can function well even when the chosen graph at each time is not connected as long as within a fixed time length the information can be transmitted between any pair of nodes. The key in the setup of time-varying experiments is the design of such a sequence of graphs.

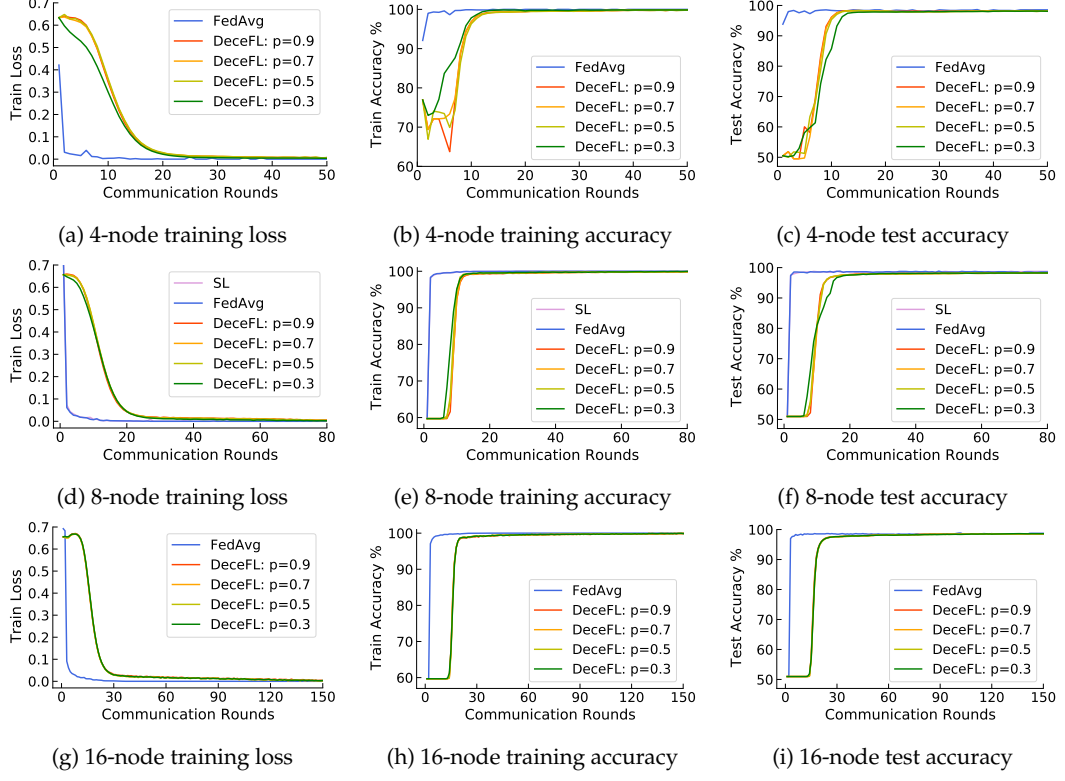


Figure 7: Comparative studies of DeceFL and FedAvgDeceFL, FedAvg and SL (only for 8-node case) with DNN in the Non-IID setup.

We use 8-node graph as an example to present the strategy for graph construction. Choose any 4 nodes for updating and, supposing $p = 0.3$, which uses the following random matrix for communication and weighting

$$W' = \begin{bmatrix} 0.6667 & 0.3333 & 0 & 0 \\ 0.3333 & 0.3333 & 0.3333 & 0 \\ 0 & 0.3333 & 0.3333 & 0.3333 \\ 0 & 0 & 0.3333 & 0.6667 \end{bmatrix};$$

and the other nodes are not involved in communication and use stochastic gradient descent (SGD) to make updates locally. In detail, we may choose the following procedure to run DeceFL:

- STEP 1: Choosing node 3,4,6,7 for communication, while node 1,2,5,8 make updates locally

by SGD, as shown in Figure 8 (Step 1). The weight matrix is

$$W_1 = \begin{bmatrix} 1.0000 & 0 & 0 & 0 & 0 & 0 & 0 & 0 \\ 0 & 1.0000 & 0 & 0 & 0 & 0 & 0 & 0 \\ 0 & 0 & 0.6667 & 0.3333 & 0 & 0 & 0 & 0 \\ 0 & 0 & 0.3333 & 0.3333 & 0 & 0.3333 & 0 & 0 \\ 0 & 0 & 0 & 0 & 1.0000 & 0 & 0 & 0 \\ 0 & 0 & 0 & 0.3333 & 0 & 0.3333 & 0.3333 & 0 \\ 0 & 0 & 0 & 0 & 0 & 0.3333 & 0.6667 & 0 \\ 0 & 0 & 0 & 0 & 0 & 0 & 0 & 1.0000 \end{bmatrix}.$$

- STEP 2: Choosing node 1,6,7,8 for communication, while node 2-5 make updates locally by SGD, as shown in Figure 8 (Step 2). The weight matrix is

$$W_2 = \begin{bmatrix} 0.6667 & 0 & 0 & 0 & 0 & 0 & 0 & 0.3333 \\ 0 & 1.0000 & 0 & 0 & 0 & 0 & 0 & 0 \\ 0 & 0 & 1.0000 & 0 & 0 & 0 & 0 & 0 \\ 0 & 0 & 0 & 1.0000 & 0 & 0 & 0 & 0 \\ 0 & 0 & 0 & 0 & 1.0000 & 0 & 0 & 0 \\ 0 & 0 & 0 & 0 & 0 & 0.3333 & 0.3333 & 0.3333 \\ 0 & 0 & 0 & 0 & 0 & 0.3333 & 0.6667 & 0 \\ 0.3333 & 0 & 0 & 0 & 0 & 0.3333 & 0 & 0.3333 \end{bmatrix}.$$

- STEP 3: Choosing node 1,2,5,8 for communication, while node 3,4,6,7 make updates locally by SGD, as shown in Figure 8 (Step 3). The whole weight matrix is

$$W_3 = \begin{bmatrix} 0.6667 & 0 & 0 & 0 & 0 & 0 & 0 & 0.3333 \\ 0 & 0.6667 & 0 & 0 & 0.3333 & 0 & 0 & 0 \\ 0 & 0 & 1.0000 & 0 & 0 & 0 & 0 & 0 \\ 0 & 0 & 0 & 1.0000 & 0 & 0 & 0 & 0 \\ 0 & 0.3333 & 0 & 0 & 0.3333 & 0 & 0 & 0.3333 \\ 0 & 0 & 0 & 0 & 0 & 1.0000 & 0 & 0 \\ 0 & 0 & 0 & 0 & 0 & 0 & 1.0000 & 0 \\ 0.3333 & 0 & 0 & 0 & 0.3333 & 0 & 0 & 0.3333 \end{bmatrix}.$$

- STEP 4: Repeat STEP 2.
- STEP 5: Repeat STEP 1.

After these five steps, in total, the lump-sum graph will be connected, Figure 8 (Step 1-5), with

the equivalent weight matrix

$$W = \begin{bmatrix} 0.4815 & 0 & 0 & 0.0370 & 0.1111 & 0.0370 & 0.0370 & 0.2963 \\ 0 & 0.6667 & 0 & 0 & 0.3333 & 0 & 0 & 0 \\ 0 & 0 & 0.5556 & 0.3333 & 0 & 0.1111 & 0 & 0 \\ 0.0370 & 0 & 0.3333 & 0.2510 & 0.0370 & 0.1770 & 0.1029 & 0.0617 \\ 0.1111 & 0.3333 & 0 & 0.0370 & 0.3333 & 0.0370 & 0.0370 & 0.1111 \\ 0.0370 & 0 & 0.1111 & 0.1770 & 0.0370 & 0.2757 & 0.2634 & 0.0988 \\ 0.0370 & 0 & 0 & 0.1029 & 0.0370 & 0.2634 & 0.4239 & 0.1358 \\ 0.2963 & 0 & 0 & 0.0617 & 0.1111 & 0.0988 & 0.1358 & 0.2963 \end{bmatrix}.$$

Hence, we ensure that every 5 steps the information can flow between any pair of nodes. For 8-node and 16-node time-varying graphs with various connectivity probability p , we can generate them for our experiments in the same manner.

The experiments choose, for FedAvg and DeceFL, the batch size 64, the local epoch 30 and the learning rate 0.1, which is used to implement l_2 -regularized logistic regression in the *Pytorch* framework. FedAvg uses arithmetic averaging for aggregation. It keeps using the complete information of the whole graph, as its algorithm required; and, with no doubt, it fails to handle the scenario and only provides a reference line for performance comparison. DeceFL uses W -weighted averaging with step size 0.1, where the weight matrix W is designed for time-varying graph generation to guarantee the resultant “overlapped” graph being connected. During the running time, every round takes a part of nodes in aggregation while the other nodes keep updating by their own local information.

Experiment results are given in Figure 9. It clearly manifests that, in such a scenario that certain nodes randomly dismiss communications, DeceFL is able to guarantee performance as well. This decentralized framework allows us to deal with practical cases, where not all nodes get involved at every round and random nodes can be malfunctioned in communication, as long as essential conditions are guaranteed.

5.2.4 Time-varying experiments with node changes

In practice there may be server nodes dropping out or being supplemented in federated learning. Theorems in Section 3 imply that DeceFL is able to handle such interventions of learning infrastructure. This experiment is designed to show that DeceFL can hold same accuracy and stability even when the topology of networked servers is varying, in specific, the addition or the deletion of nodes. Indeed it is also a type of time-varying experiments, which focuses on the impact of node changes.

The experiment uses dataset A2 with two setups, IID and Non-IID, where 20% data are reserved for test. For the case of node addition, we prepare 8 local datasets, of which 2 datasets are used for the possibly added nodes. The IID setup uniformly chooses 414 samples as a local dataset for each node, where no overlap happens between local datasets. The Non-IID setup, for each local dataset, randomly chooses a ratio of the positive to the negative samples and a sample size within a prescribed range; and then draws samples from dataset A2 to each prepare

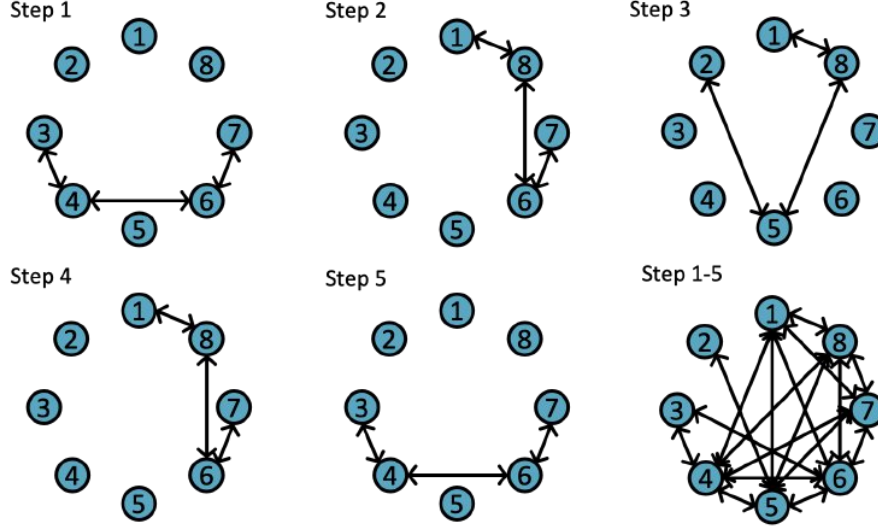


Figure 8: Time-varying communication topology that consists of a sequence of graphs each of which is not connected while the lump-sum graph over a fixed period is connected.

local dataset. The resultant local datasets in the Non-IID setup will have various sample sizes and sample distributions. The setup of two modeling methods, logistic regression and DNN, is the same, and the implementation keeps unchanged.

In experiment design, FedAvg use a central server to collect information from all available nodes (at most 8 nodes) at every round. The procedure of DeceFL is detailed as follows:

1. First 300 epochs: DeceFL randomly generates a connected ER graph of 6 nodes (among 8 nodes) as the initial. DeceFL is responsible for updating local models associated with this ER graph (6 nodes), while the other 2 nodes are updated independently.
2. 301-600 epochs: At the 301st epoch, the addition of 2 nodes happens. DeceFL will use a new connected ER graph by adding 2 more nodes. Then DeceFL keeps updating with the new ER graph of 8 nodes.
3. Last epochs: At the 601st epoch, the deletion of 2 nodes happens, which results in a new ER graph of 6 nodes that keeps connected. DeceFL continues updating using the new graph.

Performance of DeceFL in the IID and Non-IID setups is given in Figure 11. In both IID and Non-IID setups, logistic regression and DNN methods, node interventions (addition or deletion) do not deteriorate the functioning of DeceFL in the decentralized manner, which converges to the reference performance of FedAvg. It shows that DeceFL is able to preserve algorithmic stability even when the topological intervention happens, which apparently is catastrophic for centralized federated learning (including SL that requires the full connectness of graphs).

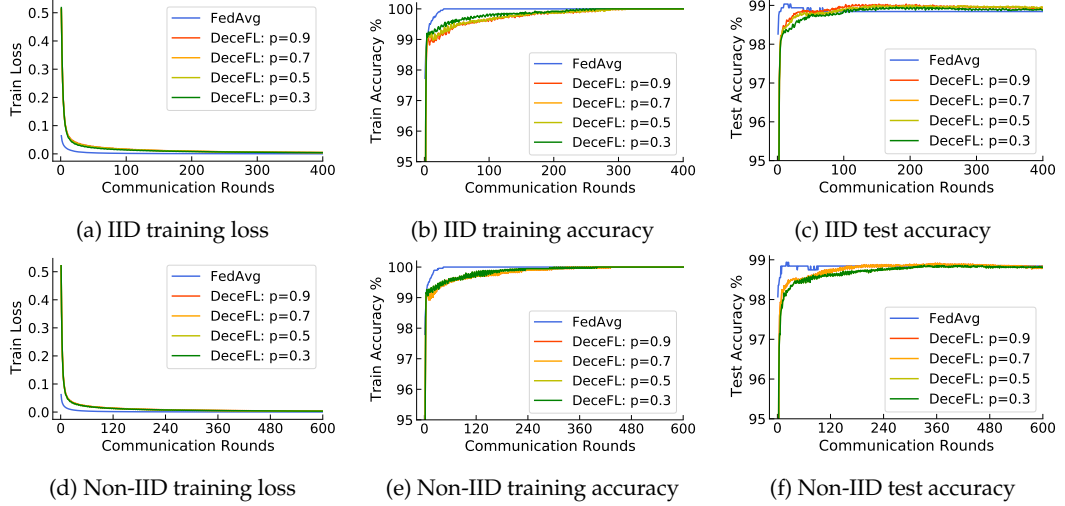


Figure 9: Performance of DeceFL with logistic regression for dataset A2 in the IID and Non-IID setups in the experiment of 8-node edge-varying graphs, with FedAvg as the reference using the complete information.

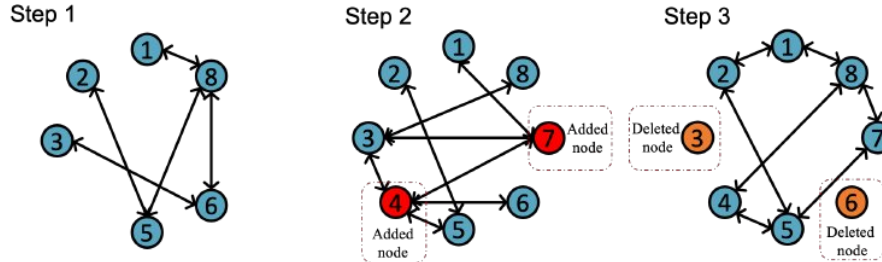


Figure 10: Time-varying communication topology that adds or removes nodes over time.

5.3 CWRU bearing dataset

5.3.1 Data description

CWRU Bearing dataset refers to the data of ball bearing test for normal and faulty bearings from the Case Western Reserve University, available on <https://engineering.case.edu/bearingdatacenter>. Experiments were conducted using 2hp Reliance Electric motor. Each data file contains fan and drive end vibration data and motor rotational speed, where acceleration was measured at locations near to and remote from the motor bearings.

Our experiment uses 3 types of bearings data, 7 inch, 14 inch and 21 inch; and chooses the drive end defects, which includes outer race defect, inner race defect, and ball defect. The outer race defect appears at three positions: the 3 (centered), 6 (orthogonal) and 12 (opposite) o'clock. Thus, our problem has in total 10 classes: 9 faulty classes (3 bearing types times 3 defect types) and the normal class. The data with these 9 defects appears in the data webpage as Figure 12. All data in use was collected at 12,000 samples/second for drive end bearing experiments. It includes 4 types of motor speed: 1797 rpm, 1772 rpm, 1750 rpm and 1730 rpm, in which the data of 1730 rpm is reserved for test. There are 2 types of features used in our experiment: DE (drive end accelerometer data), FE (fan end accelerometer data).

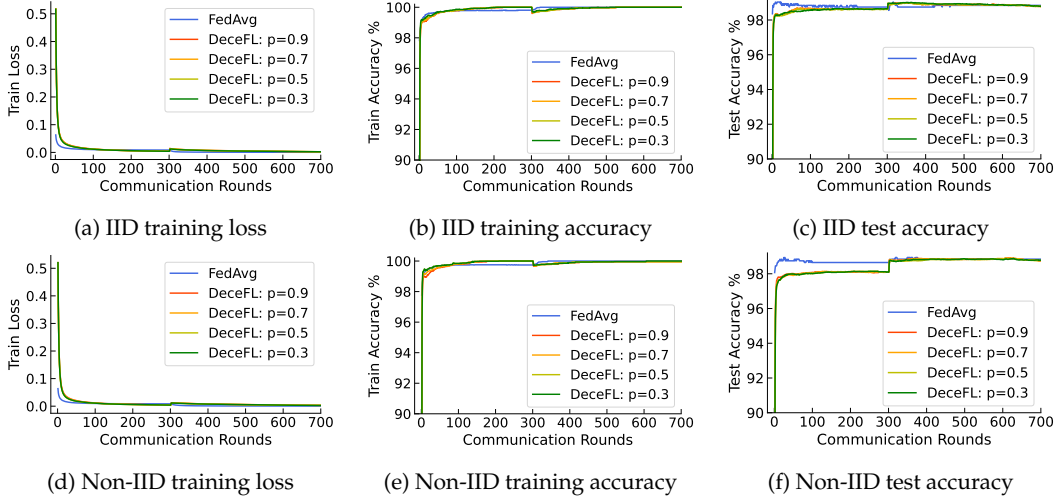


Figure 11: Performance of DeceFL with logistic regression for dataset A2 in the IID and Non-IID setups in the experiment of node-varying graphs, with FedAvg as the reference using the complete information.

12k Drive End Bearing Fault Data

* = Data not available

Fault Diameter	Motor Load (HP)	Approx. Motor Speed (rpm)	Inner Race	Ball	Outer Race Position Relative to Load Zone (Load Zone Centered at 6:00)		
					Centered @6:00	Orthogonal @3:00	Opposite @12:00
0.007"	0	1797	IR007_0	B007_0	OR007@6_0	OR007@3_0	OR007@12_0
	1	1772	IR007_1	B007_1	OR007@6_1	OR007@3_1	OR007@12_1
	2	1750	IR007_2	B007_2	OR007@6_2	OR007@3_2	OR007@12_2
	3	1730	IR007_3	B007_3	OR007@6_3	OR007@3_3	OR007@12_3
0.014"	0	1797	IR014_0	B014_0	OR014@6_0	*	*
	1	1772	IR014_1	B014_1	OR014@6_1	*	*
	2	1750	IR014_2	B014_2	OR014@6_2	*	*
	3	1730	IR014_3	B014_3	OR014@6_3	*	*
0.021"	0	1797	IR021_0	B021_0	OR021@6_0	OR021@3_0	OR021@12_0
	1	1772	IR021_1	B021_1	OR021@6_1	OR021@3_1	OR021@12_1
	2	1750	IR021_2	B021_2	OR021@6_2	OR021@3_2	OR021@12_2
	3	1730	IR021_3	B021_3	OR021@6_3	OR021@3_3	OR021@12_3
0.028"	0	1797	IR028_0	B028_0	*	*	*
	1	1772	IR028_1	B028_1	*	*	*
	2	1750	IR028_2	B028_2	*	*	*
	3	1730	IR028_3	B028_3	*	*	*

Figure 12: Webpage snapshot of fault data, where the 9 fault classes in use are marked in red.

5.3.2 Preprocessing

Essential data preprocessing is performed, including class balancing and normalization, feature extraction by Fourier transform. The dataset has 10 classes in total, which vary in sample size. Hence samples in certain classes were deleted to balance sample sizes over all classes. The original data is time-series data, which is firstly divided by every 300 points and results in a family of time series. Each time series chooses DE and FE features respectively, and produces 600 points. For every time series of each feature, we perform Fast Fourier Transform (FFT), which yields 150 points. Thus each time series of both DE and FE has in total 300 points. The motivation to use FFT is to handling the mismatch of time stamps of sequential data, which could affect MLP and LR fairly. With FFT the physical information of every particular point in data is fixed. After FFT the training and test data are normalized by removing the mean and scaling to unit variance (the test data is normalized by the normalizer of the training).

5.3.3 Experiments

Experiments consider both 4-way classification (the normal case, and fault cases B007, IR007, OR007) and 10-way classification (the normal case, and fault cases B007, IR007, OR007, B014, IR014, OR014, B021, IR021, OR021) problems. Training data are prepared in both the IID and the Non-IID setups. Communication graphs of 4, 8 and 16 nodes with $p = 0.3, 0.5, 0.7, 0.9$ are used in DeceFL, FedAvg and SL (used only in 10-way classification), which run DNN (MLP in specific) and logistic regression. For example, communication graphs of 4 nodes in DeceFL are given in Figure 13, and the associated training data in the IID and Non-IID setups are illustrated in Figure 14.

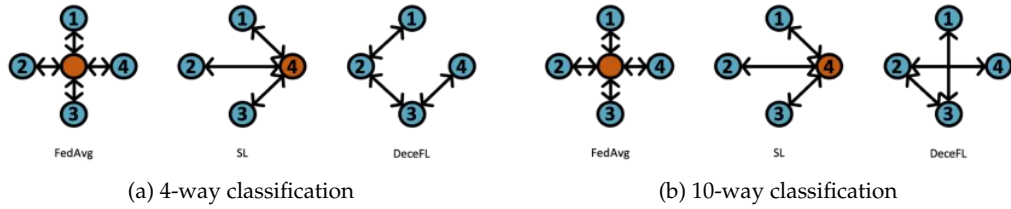


Figure 13: Communication topology of 4-node graphs used in DeceFL, FedAvg and SL for 4-way and 10-way classification problems.

Results for CWRU Bearing Dataset are given in Figure 15 and 16 for 4-way classification problems, Figure 17 and 18 for 10-way classification problems. In the usage of logistic regression, as guaranteed in theory, DeceFL in Figure 17(a)-17(i) and Figure 18(a)-18(g) confirms the same performance as FedAvg after its transient periods, in both 4-way and 10-way classification problems. For the case of DNN, as a non-convex method, although there is no theoretical guarantee, DeceFL in Figure 17(j)-17(r) and Figure 18(j)-18(p) shows competitive performance to FedAvg. They show that, in the practice of analyzing CWRU Bearing Dataset, DeceFL, as a fully decentralized framework, can reach the same performance as centralized FedAvg, which demands stronger conditions on graphs, that is, heavier communications between node servers and weaker stability against network interventions. The slight performance gap in test between DeceFL and FedAvg in Figure 18(l), 18(o), 18(r) may be mostly caused by the usage of MLP

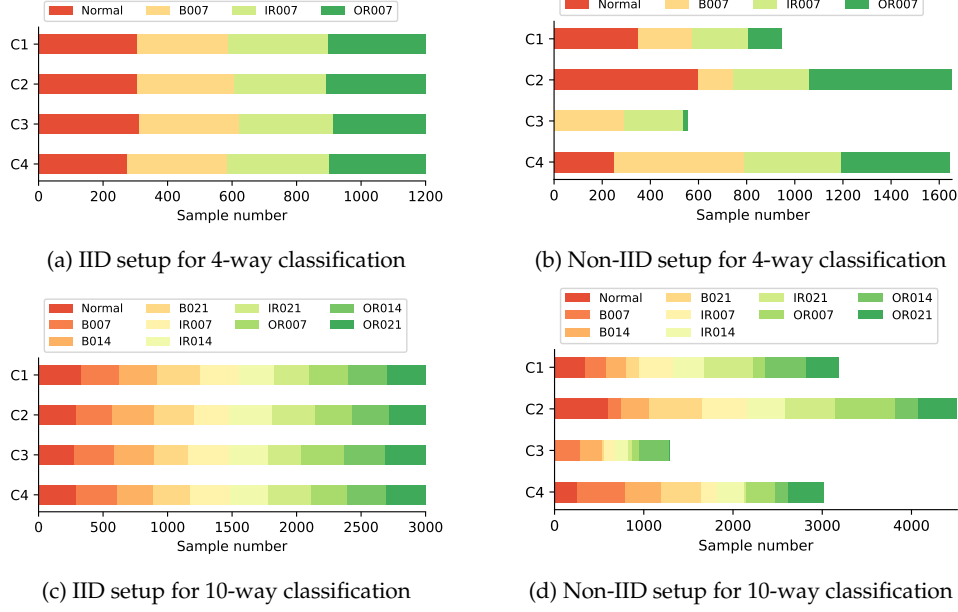


Figure 14: Training data prepared for 4-node graphs for 4-way and 10-way classification problems.

(for fair comparison with SL in [12]), which has many well-known defects; and reasons are discussed and explored by experiments in the next section.

5.3.4 Additional Non-convex Experiments

Due to no theoretical guarantees, the performance gap in Figure 18(l), 18(o), 18(r). It could be possibly caused by the defects of MLP used in [12], which is a type of DNN but is difficult to be trained and hence deteriorates generalization performance. To confirm this speculation, we perform experiments by replacing MLP used in [12] with a better DNN method, *ResNet*. Results for ResNet used for data in the Non-IID setup are presented in Figure 19, which clearly much smaller performance gap of test accuracy between DeceFL and FedAvg. It implies that the performance of the chosen non-convex learning methods could affect the performance of DeceFL. Unfortunately, neither DeceFL nor FedAvg has no guarantees in theory for non-convex learning methods.

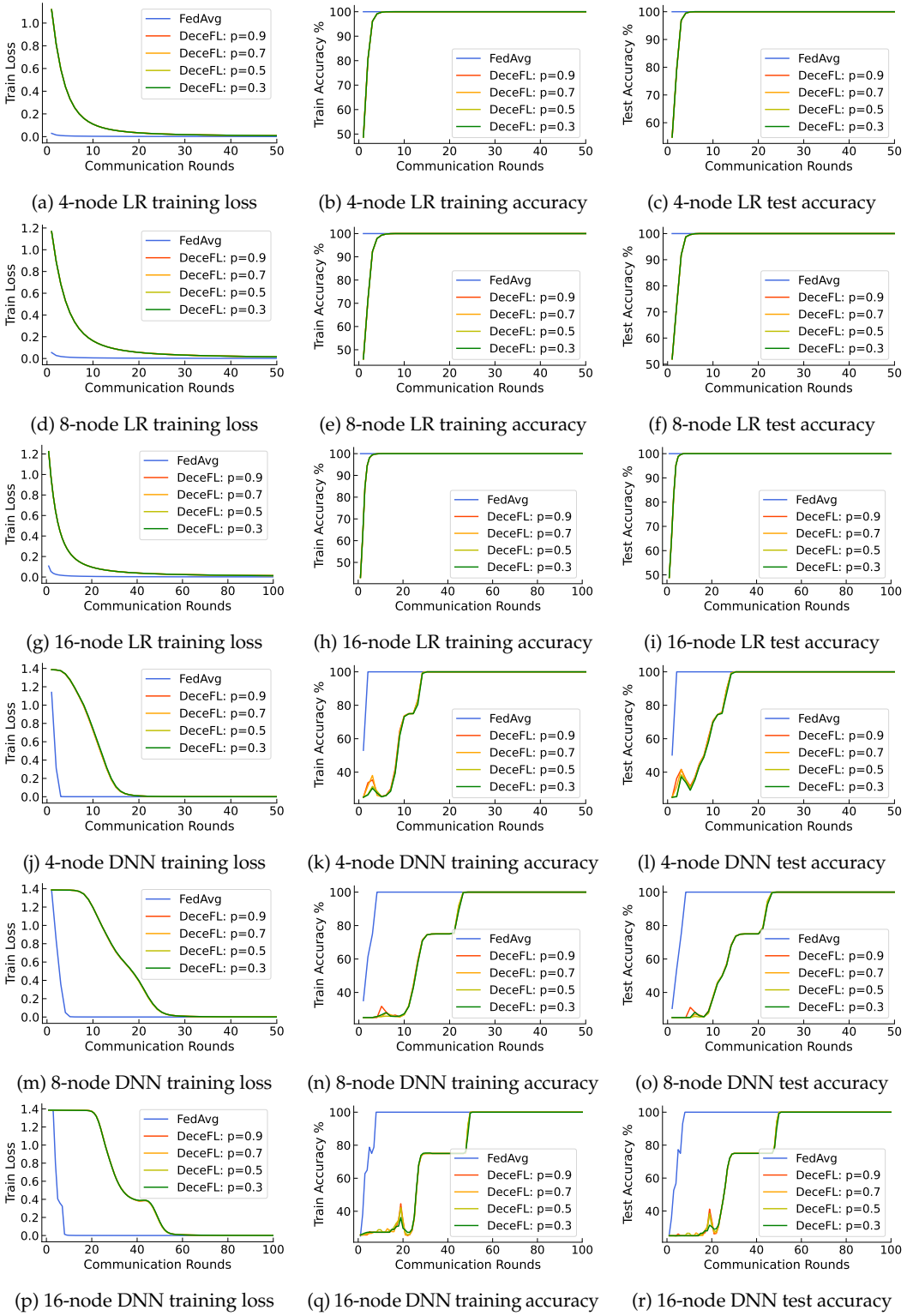


Figure 15: Application of DeceFL to CWRU Bearing data in the IID setup, with FedAvg as the reference, using logistic regression (LR) and DNN for 4-way classification problems.

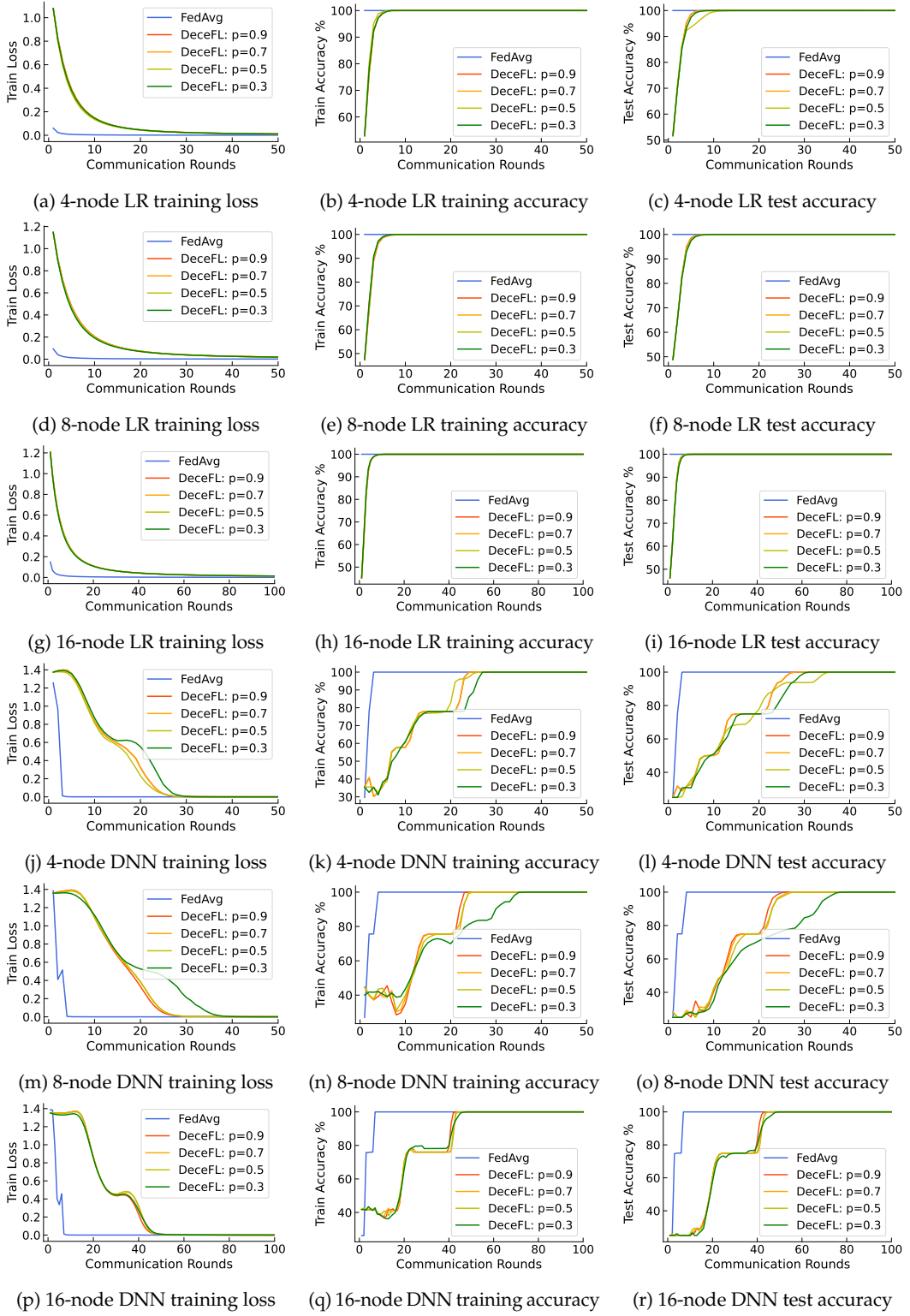


Figure 16: Application of DeceFL to CWRU Bearing data in the Non-IID setup, with FedAvg as the reference, using logistic regression (LR) and DNN for 4-way classification problems.

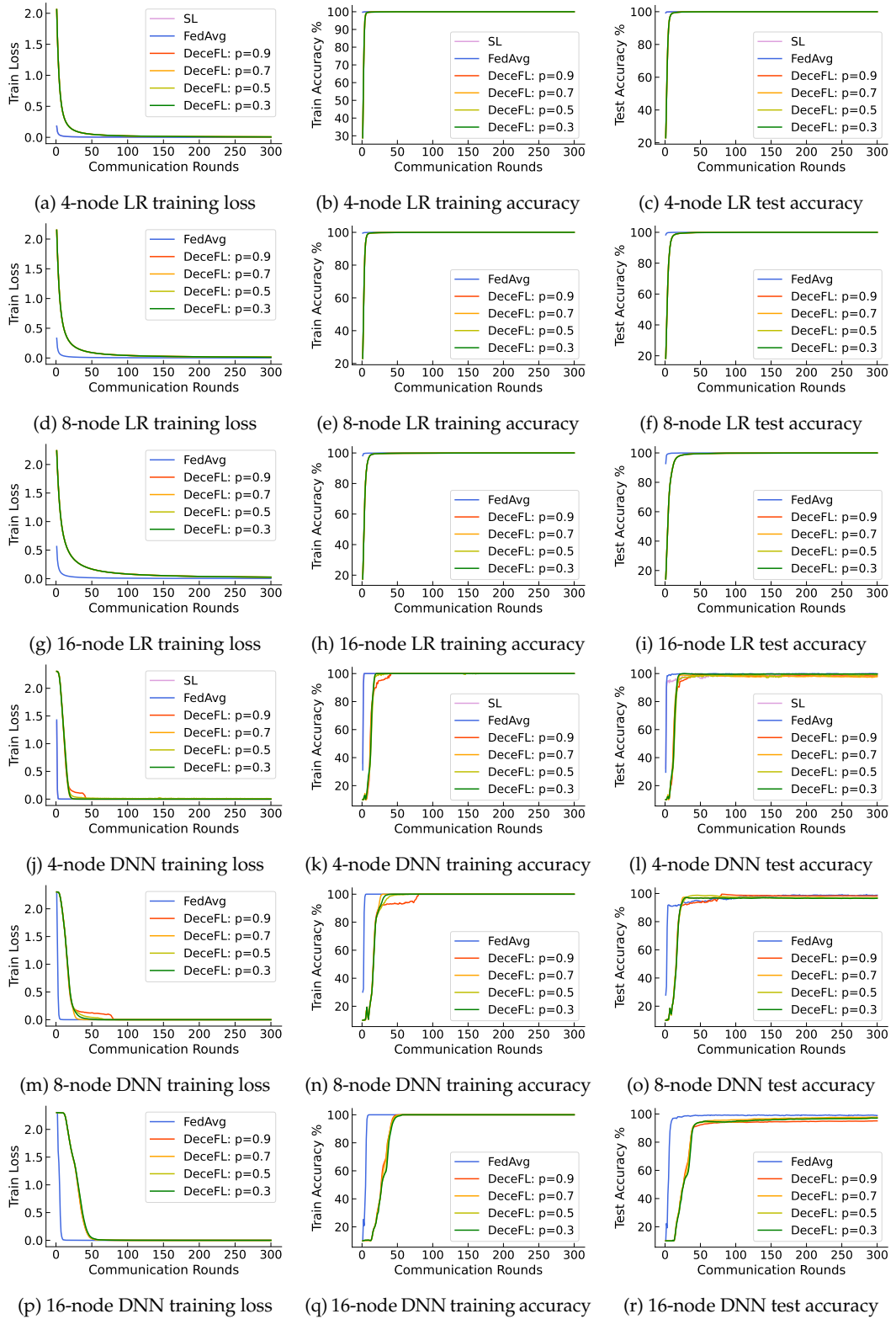


Figure 17: Application of DeceFL to CWRU Bearing data in the IID setup, with FedAvg and SL as the reference, using logistic regression (LR) and DNN for 10-way classification problems.

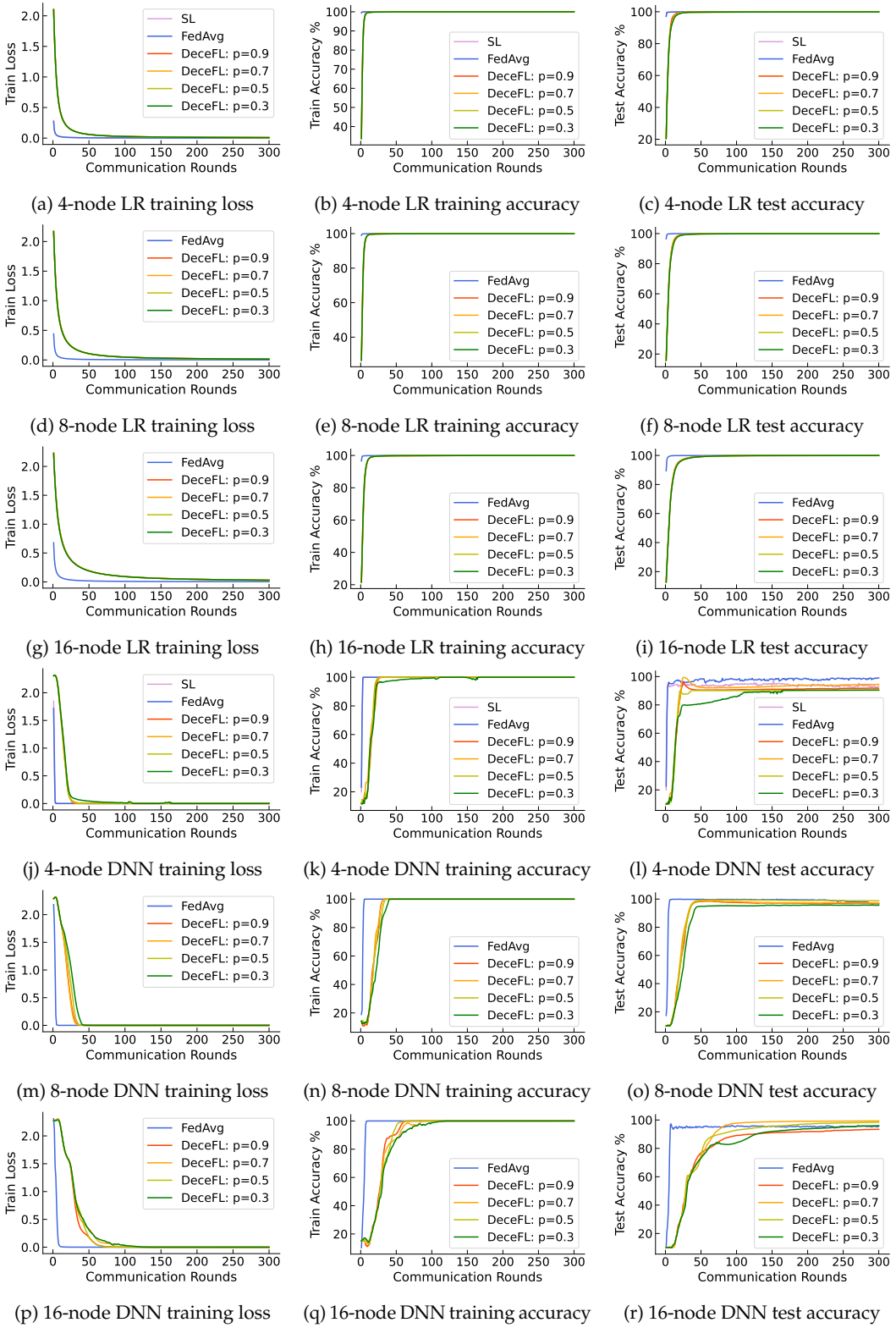


Figure 18: Application of DeceFL to CWRU Bearing data in the Non-IID setup, with FedAvg and SL as the reference, using logistic regression (LR) and DNN for 10-way classification problems.

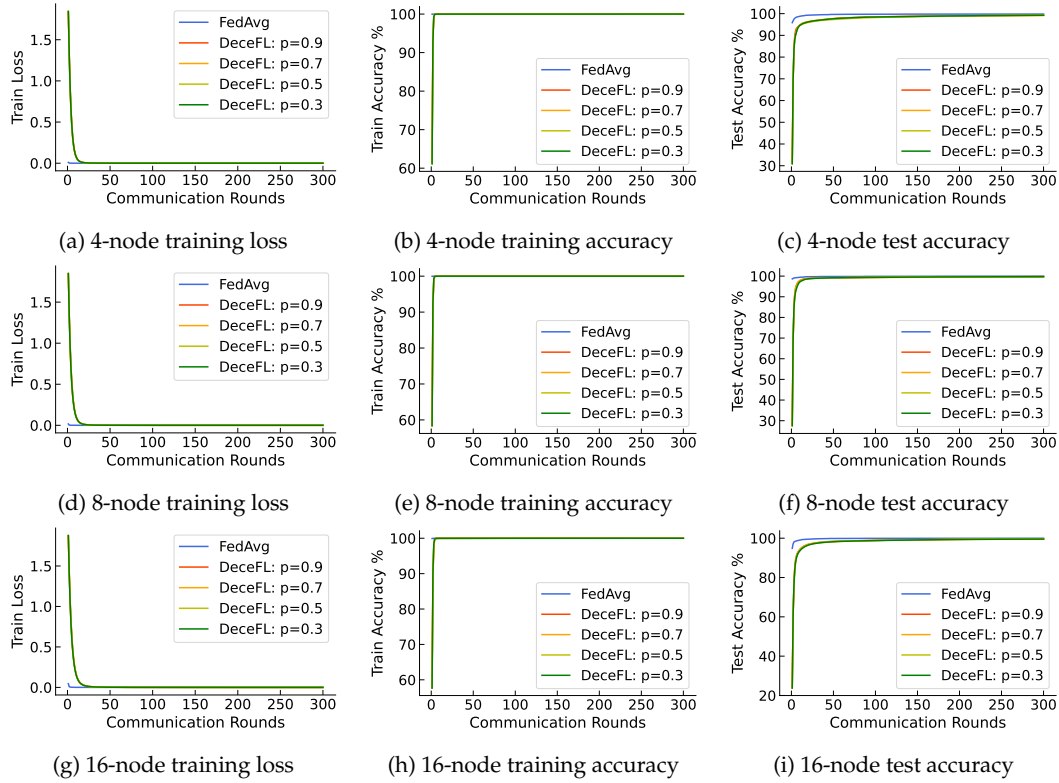


Figure 19: Application of DeceFL to CWRU Bearing data in the Non-IID setup, with FedAvg as the reference, using ResNet for 10-way classification problems.

References

- [1] Koloskova, A., Stich, S. U. & Jaggi, M. Decentralized stochastic optimization and gossip algorithms with compressed communication. *arXiv preprint arXiv:1902.00340* (2019).
- [2] Nesterov, Y. E. *Introductory Lectures on Convex Optimization-A Basic Course*, vol. 87 (Springer, 2004).
- [3] Olshevsky, A. & Tsitsiklis, J. N. Convergence speed in distributed consensus and averaging. *SIAM Review* **53**, 747–772 (2011).
- [4] Lancaster, P. & Tismenetsky, M. *The Theory of Matrices: With Applications* (Orlando: Academic Press, 1985).
- [5] Li, X., Huang, K., Yang, W., Wang, S. & Zhang, Z. On the convergence of FedAvg on non-IID data. *arXiv preprint arXiv:1907.02189* (2019).
- [6] Bellet, A., Guerraoui, R., Taziki, M. & Tommasi, M. Personalized and private peer-to-peer machine learning. *arXiv preprint arXiv:1705.08435* (2017).
- [7] Nedic, A., Olshevsky, A. & Shi, W. Achieving geometric convergence for distributed optimization over time-varying graphs. *SIAM Journal on Optimization* **27**, 2597–2633 (2017).
- [8] S, W.-H. *et al.* Swarm learning for decentralized and confidential clinical machine learning. *Nature* **594**, 265–270 (2021).
- [9] McMahan, B., Moore, E., Ramage, D., Hampson, S. & y Arcas, B. A. Communication-Efficient Learning of Deep Networks from Decentralized Data. In *Proceedings of the 20th International Conference on Artificial Intelligence and Statistics*, vol. 54, 1273–1282 (2017).
- [10] Konečný, J. *et al.* Federated learning: Strategies for improving communication efficiency. *arXiv preprint arXiv:1610.05492* (2016).
- [11] McMahan, B., Moore, E., Ramage, D., Hampson, S. & y Arcas, B. A. Communication-efficient learning of deep networks from decentralized data. In *Artificial intelligence and statistics*, 1273–1282 (PMLR, 2017).
- [12] Warnat-Herresthal, S. *et al.* Swarm Learning for decentralized and confidential clinical machine learning. *Nature* **594**, 265–270 (2021). URL <https://doi.org/10.1038/s41586-021-03583-3>.
- [13] Erdős, P. & Rényi, A. On random graphs. i. *Publicationes Mathematicae* **4**, 3286–3291 (1959).
- [14] Wei, S., Qing, L., Gang, W. & Wotao, Y. EXTRA: An exact first-order algorithm for decentralized consensus optimization. *SIAM Journal on Optimization* **25**, 944–966 (2015).
- [15] Qu, G. & Li, N. Accelerated distributed nesterov gradient descent. *IEEE Transactions on Automatic Control* **65**, 2566–2581 (2020).

A Appendix

A.1 Proof of Theorem 1

Proof: Note that $\bar{w}(t+1) = \bar{w}(t) - \eta_t g(t)$. Let the average gradient $h(t) = \frac{1}{K} \sum_{k=1}^K \nabla \tilde{F}_k(w_k(t))$. Then

$$\begin{aligned} & \|\bar{w}(t+1) - w^*\|^2 \\ &= \|\bar{w}(t) - w^* - \eta_t g(t) + \eta_t h(t) - \eta_t h(t)\|^2 \\ &= \|\bar{w}(t) - w^* - \eta_t h(t)\|^2 + \eta_t^2 \|h(t) - g(t)\|^2 + 2\eta_t \langle \bar{w}(t) - w^* - \eta_t h(t), h(t) - g(t) \rangle. \end{aligned} \quad (40)$$

For the first term on the right side of (40),

$$\|\bar{w}(t) - w^* - \eta_t h(t)\|^2 = \|\bar{w}(t) - w^*\|^2 - 2\eta_t \langle \bar{w}(t) - w^*, h(t) \rangle + \eta_t^2 \|h(t)\|^2. \quad (41)$$

For the term $\eta_t^2 \|h(t)\|^2$, we have

$$\eta_t^2 \|h(t)\|^2 = \eta_t^2 \left\| \frac{1}{K} \sum_{k=1}^K \nabla \tilde{F}_k(w_k(t)) \right\|^2 \leq \frac{\eta_t^2}{K} \sum_{k=1}^K \|\nabla \tilde{F}_k(w_k(t))\|^2 \leq \frac{2\eta_t^2 L}{K} \sum_{k=1}^K (\tilde{F}_k(w_k(t)) - \tilde{F}_k^*),$$

where the convexity of $\|\cdot\|^2$ is used in the first inequality, and the L_k -Lipschitz continuity of $\tilde{F}_k(\cdot)$ and the definition of L are used in the second inequality. In addition, note that

$$\begin{aligned} & -2\eta_t \langle \bar{w}(t) - w^*, h(t) \rangle \\ &= -\frac{2\eta_t}{K} \sum_{k=1}^K \langle \bar{w}(t) - w^*, \nabla \tilde{F}_k(w_k(t)) \rangle \\ &= -\frac{2\eta_t}{K} \sum_{k=1}^K \langle \bar{w}(t) - w_k(t), \nabla \tilde{F}_k(w_k(t)) \rangle - \frac{2\eta_t}{K} \sum_{k=1}^K \langle w_k(t) - w^*, \nabla \tilde{F}_k(w_k(t)) \rangle \\ &\leq \frac{\eta_t}{K} \sum_{k=1}^K \left[\frac{1}{\eta_t} \|w_k(t) - \bar{w}(t)\|^2 + \eta_t \|\nabla \tilde{F}_k(w_k(t))\|^2 \right] - \frac{2\eta_t}{K} \sum_{k=1}^K [\tilde{F}_k(w_k(t)) - \tilde{F}_k(w^*) + \frac{\mu_k}{2m} \|w_k(t) - w^*\|^2], \end{aligned}$$

where the inequality is established by using the convexity of $\|\cdot\|^2$ for the first term, and the $\frac{\mu_k}{m}$ -strongly convex of $\tilde{F}_k(\cdot)$ for the second term.

Therefore, it can be concluded from (41) that,

$$\begin{aligned}
& \|\bar{w}(t) - w^* - \eta_t h(t)\|^2 \\
& \leq \|\bar{w}(t) - w^*\|^2 + \frac{2\eta_t^2 L}{K} \sum_{k=1}^K (\tilde{F}_k(w_k(t)) - \tilde{F}_k^*) + \frac{\eta_t}{K} \sum_{k=1}^K \left[\frac{1}{\eta_t} \|w_k(t) - \bar{w}(t)\|^2 + \eta_t \|\nabla \tilde{F}_k(w_k(t))\|^2 \right] \\
& \quad - \frac{2\eta_t}{K} \sum_{k=1}^K (\tilde{F}_k(w_k(t)) - \tilde{F}_k(w^*)) - \frac{\mu\eta_t}{Km} \sum_{k=1}^K \|w_k(t) - w^*\|^2 \\
& \leq (1 - \frac{\mu\eta_t}{m}) \|\bar{w}(t) - w^*\|^2 + \frac{2\eta_t^2 L}{K} \sum_{k=1}^K (\tilde{F}_k(w_k(t)) - \tilde{F}_k^*) + \frac{1}{K} \sum_{k=1}^K \|w_k(t) - \bar{w}(t)\|^2 \\
& \quad + \frac{\eta_t^2}{K} \sum_{k=1}^K \|\nabla \tilde{F}_k(w_k(t))\|^2 - \frac{2\eta_t}{K} \sum_{k=1}^K (\tilde{F}_k(w_k(t)) - \tilde{F}_k(w^*)) \\
& \leq (1 - \frac{\mu\eta_t}{m}) \|\bar{w}(t) - w^*\|^2 + \frac{2\eta_t^2 L}{K} \sum_{k=1}^K (\tilde{F}_k(w_k(t)) - \tilde{F}_k^*) + \frac{1}{K} \sum_{k=1}^K \|w_k(t) - \bar{w}(t)\|^2 \\
& \quad + \frac{2\eta_t^2 L}{K} \sum_{k=1}^K (\tilde{F}_k(w_k(t)) - \tilde{F}_k^*) - \frac{2\eta_t}{K} \sum_{k=1}^K (\tilde{F}_k(w_k(t)) - \tilde{F}_k(w^*)),
\end{aligned}$$

where the definition of $\mu = \min\{\mu_i\}_{i=1}^K$ is used in the first inequality, the inequality of arithmetic and geometric means is used in the second inequality, and the L_k -Lipschitz continuity of $\tilde{F}_k(\cdot)$ and the definition of L are used in the third inequality.

This gives us,

$$\begin{aligned}
& \|\bar{w}(t) - w^* - \eta_t h(t)\|^2 \\
& \leq (1 - \frac{\mu\eta_t}{m}) \|\bar{w}(t) - w^*\|^2 + \frac{1}{K} \sum_{k=1}^K \|w_k(t) - \bar{w}(t)\|^2 \\
& \quad + \frac{4\eta_t^2 L}{K} \sum_{k=1}^K (\tilde{F}_k(w_k(t)) - \tilde{F}_k(w^*) + \tilde{F}_k(w^*) - \tilde{F}_k^*) - \frac{2\eta_t}{K} \sum_{k=1}^K (\tilde{F}_k(w_k(t)) - \tilde{F}_k(w^*)) \\
& = (1 - \frac{\mu\eta_t}{m}) \|\bar{w}(t) - w^*\|^2 + \frac{1}{K} \sum_{k=1}^K \|w_k(t) - \bar{w}(t)\|^2 - \frac{2\eta_t(1 - 2\eta_t L)}{K} \sum_{k=1}^K (\tilde{F}_k(w_k(t)) - F^*) \\
& \quad + \frac{4\eta_t^2 L}{K} (F^* - \tilde{F}^*),
\end{aligned}$$

Note that when $\eta_t = \frac{\delta}{t+\Gamma}$, where $\frac{\delta}{\Gamma} \leq \frac{1}{2L}$, we have that $1 - 2\eta_t L \geq 0$ and $1 - \frac{\mu\eta_t}{m} \geq 0$. Furthermore,

$$\begin{aligned}
\|\bar{w}(t) - w^* - \eta_t h(t)\|^2 & \leq (1 - \frac{\mu\eta_t}{m}) \|\bar{w}(t) - w^*\|^2 + \frac{1}{K} \sum_{k=1}^K \|w_k(t) - \bar{w}(t)\|^2 + \frac{4\eta_t^2 L}{K} (F^* - \tilde{F}^*) \\
& \quad - \frac{2\eta_t(1 - 2\eta_t L)}{K} \sum_{k=1}^K [\tilde{F}_k(w_k(t)) - \tilde{F}_k(\bar{w}(t)) + \tilde{F}_k(\bar{w}(t)) - F^*].
\end{aligned}$$

Furthermore, with the fact that \tilde{F}_k is convex, we have

$$\begin{aligned}
& \|\bar{w}(t) - w^* - \eta_t h(t)\|^2 \\
\leq & (1 - \frac{\mu\eta_t}{m}) \|\bar{w}(t) - w^*\|^2 + \frac{1}{K} \sum_{k=1}^K \|w_k(t) - \bar{w}(t)\|^2 - \frac{2\eta_t(1 - 2\eta_t L)}{K} \sum_{k=1}^K \langle \nabla \tilde{F}_k(\bar{w}(t)), w_k(t) - \bar{w}(t) \rangle \\
& - \frac{2\eta_t(1 - 2\eta_t L)}{K} \sum_{k=1}^K (\tilde{F}_k(\bar{w}(t)) - F^*) + \frac{4\eta_t^2 L}{K} (F^* - \tilde{F}^*) \\
\leq & (1 - \frac{\mu\eta_t}{m}) \|\bar{w}(t) - w^*\|^2 + \frac{1}{K} \sum_{k=1}^K \|w_k(t) - \bar{w}(t)\|^2 + \frac{2\eta_t(1 - 2\eta_t L)}{K} \left[\frac{\eta_t}{2} \sum_{k=1}^K \|\nabla \tilde{F}_k(\bar{w}(t))\|^2 \right. \\
& \left. + \frac{1}{2\eta_t} \sum_{k=1}^K \|w_k(t) - \bar{w}(t)\|^2 \right] - \frac{2\eta_t(1 - 2\eta_t L)}{K} \sum_{k=1}^K (\tilde{F}_k(\bar{w}(t)) - F^*) + \frac{4\eta_t^2 L}{K} (F^* - \tilde{F}^*),
\end{aligned}$$

where the second inequality uses the inequality of arithmetic and geometric means.

Moreover,

$$\begin{aligned}
& \|\bar{w}(t) - w^* - \eta_t h(t)\|^2 \\
\leq & (1 - \frac{\mu\eta_t}{m}) \|\bar{w}(t) - w^*\|^2 + \frac{1}{K} \sum_{k=1}^K \|w_k(t) - \bar{w}(t)\|^2 + \frac{2\eta_t(1 - 2\eta_t L)}{K} \cdot \frac{\eta_t}{2} \sum_{k=1}^K 2L_k (\tilde{F}_k(\bar{w}(t)) - \tilde{F}_k^*) \\
& + \frac{2\eta_t(1 - 2\eta_t L)}{K} \cdot \frac{1}{2\eta_t} \sum_{k=1}^K \|w_k(t) - \bar{w}(t)\|^2 - \frac{2\eta_t(1 - 2\eta_t L)}{K} \sum_{k=1}^K (\tilde{F}_k(\bar{w}(t)) - F^*) + \frac{4\eta_t^2 L}{K} (F^* - \tilde{F}^*) \\
\leq & (1 - \frac{\mu\eta_t}{m}) \|\bar{w}(t) - w^*\|^2 + \frac{1}{K} \sum_{k=1}^K \|w_k(t) - \bar{w}(t)\|^2 + \frac{2\eta_t^2 L(1 - 2\eta_t L)}{K} \sum_{k=1}^K (\tilde{F}_k(\bar{w}(t)) - F^* + F^* - \tilde{F}_k^*) \\
& + \frac{1 - 2\eta_t L}{K} \sum_{k=1}^K \|w_k(t) - \bar{w}(t)\|^2 + \frac{4\eta_t^2 L}{K} (F^* - \tilde{F}^*) - \frac{2\eta_t(1 - 2\eta_t L)}{K} \sum_{k=1}^K (\tilde{F}_k(\bar{w}(t)) - F^*) \\
= & (1 - \frac{\mu\eta_t}{m}) \|\bar{w}(t) - w^*\|^2 + \frac{1}{K} \sum_{k=1}^K \|\bar{w}(t) - w_k(t)\|^2 + \frac{1 - 2\eta_t L}{K} \sum_{k=1}^K \|w_k(t) - \bar{w}(t)\|^2 \\
& + 2\eta_t(1 - 2\eta_t L)(\eta_t L - 1) \cdot \frac{1}{K} \sum_{k=1}^K (\tilde{F}_k(\bar{w}(t)) - F^*) + \frac{2\eta_t^2 L(3 - 2\eta_t L)}{K} (F^* - \tilde{F}^*),
\end{aligned}$$

where the first inequality uses the fact that the function $\tilde{F}_k(\cdot)$ is convex and L_k -Lipschitz smooth, and the third inequality uses the definition of L , respectively.

Then from (40) we have

$$\begin{aligned}
& \|\bar{w}(t+1) - w^*\|^2 \\
\leq & (1 - \frac{\mu\eta_t}{m}) \|\bar{w}(t) - w^*\|^2 + \eta_t^2 \|h(t) - g(t)\|^2 + \frac{6\eta_t^2 L}{K} (F^* - \tilde{F}^*) \\
& + \frac{2(1 - \eta_t L)}{K} \sum_{k=1}^K \|w_k(t) - \bar{w}(t)\|^2 + 2\eta_t \langle \bar{w}(t) - w^* - \eta_t h(t), h(t) - g(t) \rangle. \quad (42)
\end{aligned}$$

For the last term of (42), $\mathbb{E}[\langle \bar{w}(t) - w^* - \eta_t h(t), h(t) - g(t) \rangle] = 0$. Taking the expectation on

both sides of (42), we can get the following inequality

$$\begin{aligned}\mathbb{E}[\|\bar{w}(t+1) - w^*\|^2] &\leq (1 - \frac{\mu\eta_t}{m})\mathbb{E}[\|\bar{w}(t) - w^*\|^2] + \frac{6\eta_t^2 L}{K}(F^* - \tilde{F}^*) \\ &\quad + \frac{2(1 - \eta_t L)}{K} \sum_{k=1}^K \mathbb{E}[\|w_k(t) - \bar{w}(t)\|^2] + \eta_t^2 \mathbb{E}[\|h(t) - g(t)\|^2].\end{aligned}\quad (43)$$

In order to prove the boundedness of $\mathbb{E}[\|\bar{w}(t) - w^*\|^2]$, we analyze the bounds of $\mathbb{E}[\|\mathbf{w}(t) - \mathbf{1} \otimes \bar{w}(t)\|^2]$. From (8),

$$\begin{aligned}\sum_{k=1}^K \mathbb{E}[\|w_k(t+1) - \bar{w}(t+1)\|^2] &= \mathbb{E}[\|\mathbf{w}(t+1) - \mathbf{1} \otimes \bar{w}(t+1)\|^2] \\ &= \mathbb{E}[\|(W \otimes \mathbf{I}_n)\mathbf{w}(t) - \eta_t G(\mathbf{w}(t)) - \mathbf{1} \otimes (\bar{w}(t) - \eta_t g(t))\|^2] \\ &= \mathbb{E}[\|(W \otimes \mathbf{I}_n)\mathbf{w}(t) - \mathbf{1} \otimes \bar{w}(t)\|^2] + \mathbb{E}[\eta_t^2 \|G(\mathbf{w}(t)) - \mathbf{1} \otimes g(t)\|^2] \\ &\quad - 2\eta_t \mathbb{E}[\langle (W \otimes \mathbf{I}_n)\mathbf{w}(t) - \mathbf{1} \otimes \bar{w}(t), G(\mathbf{w}(t)) - \mathbf{1} \otimes g(t) \rangle].\end{aligned}$$

Notice that

$$\begin{aligned}(W \otimes \mathbf{I}_n)\mathbf{w} - \mathbf{1} \otimes \bar{w} &= (W \otimes \mathbf{I}_n)\mathbf{w} - \frac{1}{K}\mathbf{1} \otimes (\mathbf{1}^T \otimes I_n)\mathbf{w} = (W \otimes \mathbf{I}_n)\mathbf{w} - \frac{1}{K}((\mathbf{1} \otimes \mathbf{1}^T) \otimes I_n)\mathbf{w} \\ &= (W \otimes \mathbf{I}_n - \frac{1}{K}\mathbf{1}\mathbf{1}^T \otimes \mathbf{I}_n)\mathbf{w} = ((W - \frac{1}{K}\mathbf{1}\mathbf{1}^T) \otimes \mathbf{I}_n)\mathbf{w} = ((W - \frac{1}{K}\mathbf{1}\mathbf{1}^T) \otimes \mathbf{I}_n)(\mathbf{w} - \mathbf{1} \otimes \bar{w}),\end{aligned}\quad (44)$$

where the first equality used the definition of \bar{w} , the second equality is obtained directly by calculation, and the fifth equality uses Kronecker's property that $A \otimes C + D \otimes C = (A + D) \otimes C$, and in the last equality we have used the fact that $((W - \frac{1}{K}\mathbf{1}\mathbf{1}^T) \otimes \mathbf{I}_n)(\mathbf{1} \otimes \bar{w}) = ((W - \frac{1}{K}\mathbf{1}\mathbf{1}^T)\mathbf{1}) \otimes (\mathbf{I}_n\bar{w}) = (\mathbf{1} - \frac{1}{K}\mathbf{1}\mathbf{1}^T\mathbf{1}) \otimes \bar{w} = (\mathbf{1} - \mathbf{1}) \otimes \bar{w} = \mathbf{0}_{nK}$.

With the fact that $\rho(W - \frac{1}{K}\mathbf{1}\mathbf{1}^T) < 1$. Let $A = (W - \frac{1}{K}\mathbf{1}\mathbf{1}^T)$ and $D = \mathbf{I}_n$ in Lemma 1, we have $\rho((W - \frac{1}{K}\mathbf{1}\mathbf{1}^T) \otimes \mathbf{I}_n) = \rho(W - \frac{1}{K}\mathbf{1}\mathbf{1}^T) = \lambda < 1$. Moreover, $\|(W \otimes \mathbf{I}_n)\mathbf{w} - \mathbf{1} \otimes \bar{w}\| = \|((W - \frac{1}{K}\mathbf{1}\mathbf{1}^T) \otimes \mathbf{I}_n)(\mathbf{w} - \mathbf{1} \otimes \bar{w})\| \leq \rho(W - \frac{1}{K}\mathbf{1}\mathbf{1}^T)\|\mathbf{w} - \mathbf{1} \otimes \bar{w}\| = \lambda\|\mathbf{w} - \mathbf{1} \otimes \bar{w}\|$. Then, we have

$$\begin{aligned}&\mathbb{E}[\|\mathbf{w}(t+1) - \mathbf{1} \otimes \bar{w}(t+1)\|^2] \\ &\leq \lambda^2 \mathbb{E}[\|\mathbf{w}(t) - \mathbf{1} \otimes \bar{w}(t)\|^2] + \eta_t^2 \mathbb{E}[\|G(\mathbf{w}(t)) - \mathbf{1} \otimes g(t)\|^2] + Y\mathbb{E}[\|(W \otimes \mathbf{I}_n)\mathbf{w}(t) - \mathbf{1} \otimes \bar{w}(t)\|^2] \\ &\quad + \frac{\eta_t^2}{Y} \mathbb{E}[\|G(\mathbf{w}(t)) - \mathbf{1} \otimes g(t)\|^2] \\ &= \lambda^2(1 + Y)\mathbb{E}[\|\mathbf{w}(t) - \mathbf{1} \otimes \bar{w}(t)\|^2] + \eta_t^2(1 + \frac{1}{Y})\mathbb{E}[\|G(\mathbf{w}(t))\|^2 - K\|g(t)\|^2] \\ &\leq \lambda^2(1 + Y)\mathbb{E}[\|\mathbf{w}(t) - \mathbf{1} \otimes \bar{w}(t)\|^2] + \eta_t^2(1 + \frac{1}{Y})K\chi^2,\end{aligned}\quad (45)$$

where in the first inequality we have used the the inequality of arithmetic and geometric means, in the equality we have used the fact that,

$$\begin{aligned}\|G(\mathbf{w}(t)) - \mathbf{1} \otimes g(t)\|^2 &= \|G(\mathbf{w}(t))\|^2 + \|\mathbf{1} \otimes g(t)\|^2 - 2\langle G(\mathbf{w}(t)), \mathbf{1} \otimes g(t) \rangle \\ &= \|G(\mathbf{w}(t))\|^2 + \|\mathbf{1} \otimes g(t)\|^2 - 2\sum_{k=1}^K \tilde{g}_k^T(w_k(t))g(t) = \|G(\mathbf{w}(t))\|^2 - K\|g(t)\|^2,\end{aligned}$$

where the third equality holds used the definition of $g(t)$. And Assumption 1 is used to obtain the last inequality, in which $Y = \frac{1}{2}(\frac{1}{\lambda^2} - 1)$ such that $\lambda^2(1 + Y) = \lambda^2(1 + \frac{1}{2}(\frac{1}{\lambda^2} - 1)) = \frac{1}{2}(\lambda^2 + 1) < 1$.

Next, we will analyze the boundedness of $\mathbb{E}[\|\mathbf{w}(t) - \mathbf{1} \otimes \bar{w}(t)\|^2]$ and prove

$$\mathbb{E}[\|\mathbf{w}(t) - \mathbf{1} \otimes \bar{w}(t)\|^2] \leq \frac{\zeta}{(t + \Gamma)^2}, \quad (46)$$

by induction, where $\zeta := \max \left\{ \Gamma^2 \cdot \mathbb{E}[\|\mathbf{w}(0) - \mathbf{1} \otimes \bar{w}(0)\|^2], \frac{1}{1-\lambda^2} \cdot \frac{\delta^2 K \lambda^2}{\frac{\Gamma^2}{(\Gamma+1)^2(\lambda^2+1)} - \frac{1}{2}} \right\}$ and Γ satisfies that $\frac{\Gamma}{\Gamma+1} \geq \sqrt{\frac{1+\lambda^2}{2}}$. Firstly, when $t = 0$, it is obvious that $\mathbb{E}[\|\mathbf{w}(0) - \mathbf{1} \otimes \bar{w}(0)\|^2] \leq \frac{\zeta}{\Gamma^2}$ holds according to the definition of ζ . Secondly, suppose that for any $t > 0$, there is always $\mathbb{E}[\|\mathbf{w}(t) - \mathbf{1} \otimes \bar{w}(t)\|^2] \leq \frac{\zeta}{(t+\Gamma)^2}$. Finally, for $(t+1)$ -th iteration from (45), we have

$$\begin{aligned} \mathbb{E}[\|\mathbf{w}(t+1) - \mathbf{1} \otimes \bar{w}(t+1)\|^2] &\leq \lambda^2(1 + Y) \cdot \frac{\zeta}{(t+\Gamma)^2} + \eta_t^2 \cdot \frac{1}{\delta^2} \left(\frac{\Gamma^2}{(\Gamma+1)^2} - \lambda^2(1 + Y) \right) \zeta \\ &\leq \lambda^2(1 + Y) \cdot \frac{\zeta}{(t+\Gamma)^2} + \frac{1}{(t+\Gamma)^2} \cdot \left(\frac{(t+\Gamma)^2}{(t+\Gamma+1)^2} - \lambda^2(1 + Y) \right) \zeta \\ &= \frac{\zeta}{(t+1+\Gamma)^2}, \end{aligned} \quad (47)$$

where in the second inequality we used the definition of ζ , and in the third one we used that $\phi(t) = \frac{(t+\Gamma)^2}{(t+1+\Gamma)^2}$ is a monotone increasing function with $t \geq 0$ and the definition of $\eta_t = \frac{\delta}{t+\Gamma}$.

To sum up, the boundedness (46) can be obtained, when $\zeta := \max \left\{ \Gamma^2 \cdot \mathbb{E}[\|\mathbf{w}(0) - \mathbf{1} \otimes \bar{w}(0)\|^2], \frac{1}{1-\lambda^2} \cdot \frac{K \lambda^2 \delta^2}{\frac{\Gamma^2}{(\Gamma+1)^2(\lambda^2+1)} - \frac{1}{2}} \right\}$ and Γ satisfies that $\frac{\Gamma}{\Gamma+1} \geq \sqrt{\frac{1+\lambda^2}{2}}$.

Similarly, when $\frac{\delta}{\Gamma} \leq \frac{1}{L}$ and $\delta > \frac{m}{\mu}$, it can be proved by induction that

$$\mathbb{E}[\|\bar{w}(t) - w^*\|^2] \leq \frac{\tilde{\zeta}}{t + \Gamma}, \quad (48)$$

where $\tilde{\zeta} \triangleq \max \left\{ \frac{(6\epsilon L + \sigma^2)\delta^2 m + 2\zeta m}{\mu\delta - m}, \Gamma \cdot \mathbb{E}[\|\bar{w}(0) - w^*\|^2] \right\}$ and $\epsilon \triangleq \frac{1}{K}F^* - \tilde{F}_k^*$.

When $t = 0$, it is obvious that $\mathbb{E}[\|\bar{w}(0) - w^*\|^2] \leq \frac{\tilde{\zeta}}{\Gamma}$ holds according to the definition of $\tilde{\zeta}$. Suppose that for any $t > 0$, there is always $\mathbb{E}[\|\bar{w}(t) - w^*\|^2] \leq \frac{\tilde{\zeta}}{(t+\Gamma)^2}$. Finally, according

to the assumption conditions and (47), from (43), we have

$$\begin{aligned}
\mathbb{E}[\|\bar{w}(t+1) - w^*\|^2] &\leq \left(1 - \frac{\mu\eta_t}{m}\right) \cdot \frac{\tilde{\zeta}}{t+\Gamma} + 6\eta_t^2\varepsilon L + \eta_t^2\sigma^2 + \frac{2(1-\eta_t L)}{K} \cdot \frac{\zeta}{(t+\Gamma)^2} \\
&= \left(1 - \frac{\mu\delta}{m(t+\Gamma)}\right) \frac{\tilde{\zeta}}{t+\Gamma} + \frac{\delta^2}{(t+\Gamma)^2} (6\varepsilon L + \sigma^2) + \frac{2(1-\eta_t L)}{K} \cdot \frac{\zeta}{(t+\Gamma)^2} \\
&\leq \left(1 - \frac{\mu\delta}{m(t+\Gamma)}\right) \frac{\tilde{\zeta}}{t+\Gamma} + \frac{\delta^2(6\varepsilon L + \sigma^2) + \frac{2\zeta}{K}}{(t+\Gamma)^2} \\
&\leq \left(1 - \frac{\mu\delta}{m(t+\Gamma)}\right) \frac{\tilde{\zeta}}{t+\Gamma} + \frac{(\mu\delta - m)\tilde{\zeta}}{m(t+\Gamma)^2} \\
&= \left(1 - \frac{1}{t+\Gamma}\right) \frac{\tilde{\zeta}}{t+\Gamma} \leq \frac{\tilde{\zeta}}{t+1+\Gamma},
\end{aligned}$$

where in the third inequality we used the definition of $\tilde{\zeta}$.

To sum up, (48) holds, when $\tilde{\zeta} \triangleq \max\left\{\frac{(6\varepsilon L + \sigma^2)\delta^2 m + \frac{2\zeta m}{K}}{\mu\delta - m}, \Gamma \cdot \mathbb{E}[\|\bar{w}(0) - w^*\|^2]\right\}$ and $\delta > \frac{m}{\mu}$. ■

A.2 Proof of Proposition 1

Proof: According to the averaging iteration $\bar{w}(t+1) = \bar{w}(t) - \eta_t g(t)$, with $\eta_t = \eta$. From the fact that $F(\cdot)$ is L -Lipschitz smooth, we can get

$$F(\bar{w}(t+1)) \leq F(\bar{w}(t)) - \eta g(t)^T \nabla F(\bar{w}(t)) + \frac{\eta^2 L}{2} \|g(t)\|^2. \quad (49)$$

The following inequality can be obtained by taking the expectation of (49),

$$\begin{aligned}
&\mathbb{E}[F(\bar{w}(t+1))] \\
&\leq \mathbb{E}[F(\bar{w}(t))] - \eta \mathbb{E}[g(t)^T \nabla F(\bar{w}(t))] + \frac{\eta^2 L}{2} \mathbb{E}[\|g(t)\|^2] \\
&= \mathbb{E}[F(\bar{w}(t))] - \eta \mathbb{E}[\|\nabla F(\bar{w}(t))\|^2] + \eta \mathbb{E}[\langle \nabla F(\bar{w}(t)), \nabla F(\bar{w}(t)) - g(t) \rangle] + \frac{\eta^2 L}{2} \mathbb{E}[\|g(t)\|^2] \\
&\leq \mathbb{E}[F(\bar{w}(t))] - \eta \mathbb{E}[\|\nabla F(\bar{w}(t))\|^2] + \frac{\eta}{2} \mathbb{E}[\|\nabla F(\bar{w}(t))\|^2] + \frac{\eta}{2} \mathbb{E}[\|\nabla F(\bar{w}(t)) - g(t)\|^2] + \frac{\eta^2 L}{2} \mathbb{E}[\|g(t)\|^2] \\
&\leq \mathbb{E}[F(\bar{w}(t))] - \frac{\eta}{2} \mathbb{E}[\|\nabla F(\bar{w}(t))\|^2] + \frac{\eta}{2} \mathbb{E}[\|\nabla F(\bar{w}(t)) - \sum_{k=1}^K \nabla F_k(w_k(t))\|^2] \\
&\quad + \frac{\eta}{2} \mathbb{E}[\|\sum_{k=1}^K \nabla F_k(w_k(t)) - g(t)\|^2] + \frac{\eta^2 L}{2} \mathbb{E}[\|g(t)\|^2] \\
&\leq \mathbb{E}[F(\bar{w}(t))] - \frac{\eta}{2} \mathbb{E}[\|\nabla F(\bar{w}(t))\|^2] + \frac{\eta K}{2} \sum_{k=1}^K \mathbb{E}[\|\nabla F_k(\bar{w}(t)) - \nabla F_k(w_k(t))\|^2] \\
&\quad + \frac{\eta K}{2} \sum_{k=1}^K \mathbb{E}[\|\nabla F_k(w_k(t)) - \tilde{g}(w_k(t))\|^2] + \frac{\eta^2 L}{2} \mathbb{E}[\|g(t)\|^2] \\
&\leq \mathbb{E}[F(\bar{w}(t))] - \frac{\eta}{2} \mathbb{E}[\|\nabla F(\bar{w}(t))\|^2] + \frac{\eta K}{2} \sum_{k=1}^K L_k^2 \|\bar{w}(t) - w_k(t)\|^2 + \frac{\eta K}{2} \sum_{k=1}^K \sigma_k^2 + \frac{\eta^2 L}{2} \mathbb{E}[\|g(t)\|^2] \\
&= \mathbb{E}[F(\bar{w}(t))] - \frac{\eta}{2} \mathbb{E}[\|\nabla F(\bar{w}(t))\|^2] + \frac{\eta^2 L}{2} \mathbb{E}[\|g(t)\|^2] + \frac{\eta K L^2}{2} \|\mathbf{1}_K \otimes \bar{w}(t) - \mathbf{w}_k(t)\|^2 + \frac{\eta K^2 \sigma^2}{2} \quad (50)
\end{aligned}$$

where

$$\mathbb{E}[\|g(t)\|^2] = \mathbb{E}\left[\left\|\frac{1}{K} \sum_{k=1}^K \tilde{g}_k(w_k(t))\right\|^2\right] \leq \frac{1}{K} \sum_{k=1}^K \mathbb{E}[\|\tilde{g}_k(w_k(t))\|^2] \leq \frac{1}{K} \sum_{k=1}^K \mathbb{E}[\|g_k(w_k(t))\|^2],$$

From (4) in Assumption 1, we have

$$\mathbb{E}[\|g_k(w_k(t))\|^2] \leq \sigma_k^2 + \|\nabla F_k(w_k(t))\|^2,$$

this gives us

$$\frac{1}{K} \sum_{k=1}^K \mathbb{E}[\|g_k(w_k(t))\|^2] \leq \frac{1}{K} \sum_{k=1}^K \sigma_k^2 + \frac{1}{K} \sum_{k=1}^K \|\nabla F_k(w_k(t))\|^2. \quad (51)$$

Note the definition that $w_k^* = \arg \min_{w \in \mathbb{R}^n} \tilde{F}_k(w)$, so it is obvious that w_k^* is the minimum of $F_k(w)$. Denoted by $F_k^* = \min_{w \in \mathbb{R}^n} F_k(w)$ and $\bar{F}^* = \sum_{k=1}^K F_k^*$, $\zeta = \frac{1}{K}(F^* - \bar{F}^*)$. Then for the second term on the right of (51),

$$\begin{aligned} \frac{1}{K} \sum_{k=1}^K \|\nabla F_k(w_k(t))\|^2 &\leq \frac{1}{K} \sum_{k=1}^K 2\mu_k(F_k(w_k(t)) - F_k^*) \\ &\leq \frac{2\mu}{K} \sum_{k=1}^K (F_k(w_k(t)) - F_k(\bar{w}(t)) + F_k(\bar{w}(t)) - F_k(w^*) + F_k(w^*) - F_k^*) \\ &\leq \frac{2\mu}{K}(F(\bar{w}(t)) - F^*) + \frac{2\mu}{K} \sum_{k=1}^K (F_k(w_k(t)) - F_k(\bar{w}(t))) + \frac{2\mu}{K}(F_k(w^*) - \bar{F}^*) \\ &\leq \frac{2\mu}{K}(F(\bar{w}(t)) - F^*) + \frac{\mu L}{K} \|\mathbf{w}(t) - \mathbf{1} \otimes \bar{w}(t)\|^2 + 2\mu\zeta, \end{aligned} \quad (52)$$

where for the first inequality we used the fact that $F_k(\cdot)$ is μ_k -strongly convex and in the second inequality have used the definition of $\mu = \min_k \{\mu_k\}_{k=1}^K$. The inequality of arithmetic and geometric means is used for the last inequality.

Substituting (52) into (51), then the following can be obtained,

$$\frac{1}{K} \sum_{k=1}^K \mathbb{E}[\|g_k(w_k(t))\|^2] \leq \sigma^2 + \frac{2\mu}{K}(F(\bar{w}(t)) - F^*) + \frac{\mu L}{K} \|\mathbf{w}(t) - \mathbf{1} \otimes \bar{w}(t)\|^2 + 2\mu\zeta.$$

Then, from (50), we have

$$\begin{aligned}
& \mathbb{E}[F(\bar{w}(t+1))] \\
& \leq \mathbb{E}[F(\bar{w}(t))] - \frac{\eta}{2} \mathbb{E}[\|\nabla F(\bar{w}(t))\|^2] + \frac{\eta^2 L}{2} \mathbb{E}[\|g(t)\|^2] + \frac{\eta K L^2}{2} \|\mathbf{1}_K \otimes \bar{w}(t) - \mathbf{w}_k(t)\|^2 + \frac{\eta K^2 \sigma^2}{2} \\
& \leq \mathbb{E}[F(\bar{w}(t))] - \frac{\mu\eta}{m} \mathbb{E}[F(\bar{w}(t)) - F^*] + \frac{\eta^2 L}{2} (\sigma^2 + \frac{2\mu}{K} (F(\bar{w}_k(t)) - F^*)) + \frac{\mu L}{K} \|\mathbf{w}(t) - \mathbf{1} \otimes \bar{w}(t)\|^2 + 2\mu\zeta \\
& \quad + \frac{\eta K L^2}{2} \|\mathbf{1}_K \otimes \bar{w}(t) - \mathbf{w}_k(t)\|^2 + \frac{\eta K^2 \sigma^2}{2} \\
& = \mathbb{E}[F(\bar{w}(t))] - \mu\eta \left(\frac{1}{m} - \frac{\eta L}{K} \right) \mathbb{E}[F(\bar{w}(t)) - F^*] + \frac{\eta K^2 L^2 + \eta^2 L^2 \mu}{2K} \|\mathbf{1}_K \otimes \bar{w}(t) - \mathbf{w}_k(t)\|^2 \\
& \quad + \frac{\eta K^2 \sigma^2 + \eta^2 L(\sigma^2 + 2\mu\zeta)}{2},
\end{aligned}$$

can be obtained, where the inequality used the fact that $F(\cdot)$ is $\frac{\mu}{m}$ -strongly convex with $\|\nabla F(\bar{w}(t))\|^2 \geq \frac{2\mu}{m} (F(\bar{w}(t)) - F^*)$. According to (45), it can be obtained by recursive calculation, for any $t \geq 0$

$$\mathbb{E}[\|\mathbf{w}(t+1) - \mathbf{1} \otimes \bar{w}(t+1)\|^2] \tag{53}$$

$$\begin{aligned}
& \leq \lambda^2 (1 + Y) \mathbb{E}[\|\mathbf{w}(t) - \mathbf{1} \otimes \bar{w}(t)\|^2] + \eta^2 \left(1 + \frac{1}{Y}\right) K \chi^2 \\
& \leq (\lambda^2 (1 + Y))^{t+1} \mathbb{E}[\|\mathbf{w}(0) - \mathbf{1} \otimes \bar{w}(0)\|^2] + \eta^2 \left(1 + \frac{1}{Y}\right) K \chi^2 \sum_{\tau=0}^t (\lambda^2 (1 + Y))^{\tau} \\
& \leq \mathbb{E}[\|\mathbf{w}(0) - \mathbf{1} \otimes \bar{w}(0)\|^2] + \left(1 + \frac{1}{Y}\right) \frac{\eta^2 K \chi^2}{1 - \lambda^2 (1 + Y)} \\
& = \mathbb{E}[\|\mathbf{w}(0) - \mathbf{1} \otimes \bar{w}(0)\|^2] + \frac{2\eta^2 K \chi^2 (1 + \lambda^2)}{(1 - \lambda^2)^2} \triangleq \Xi. \tag{54}
\end{aligned}$$

Subtracting F^* from both sides, we get

$$\begin{aligned}
\mathbb{E}[F(\bar{w}(t+1)) - F^*] & \leq \mathbb{E}[F(\bar{w}(t)) - F^*] - \mu\eta \left(\frac{1}{m} - \frac{\eta L}{K} \right) \mathbb{E}[F(\bar{w}_k(t)) - F^*] \\
& \quad + \frac{\eta K^2 L^2 + \eta^2 L^2 \mu}{2K} \Xi + \frac{\eta K^2 \sigma^2 + \eta^2 L(\sigma^2 + 2\mu\zeta)}{2}.
\end{aligned}$$

When $\eta \leq \frac{K}{2mL}$, we subtracting the fixed constant from both sides gives us

$$\begin{aligned}
& \mathbb{E}[F(\bar{w}(t+1)) - F^*] - \Xi_1 \\
& \leq \left(1 - \frac{\eta\mu}{2m}\right) \mathbb{E}[F(\bar{w}(t)) - F^*] + \frac{\eta K^2 L^2 + \eta^2 L^2 \mu}{2K} \Xi + \frac{\eta K^2 \sigma^2 + \eta^2 L(\sigma^2 + 2\mu\zeta)}{2} - \Xi_1 \\
& = \left(1 - \frac{\eta\mu}{2m}\right) (\mathbb{E}[F(\bar{w}(t)) - F^*] - \Xi_1),
\end{aligned}$$

where $\Xi_1 = \frac{m}{\eta\mu} \left(\frac{\eta K^2 L^2 + \eta^2 L^2 \mu}{K} \Xi + \eta K^2 \sigma^2 + \eta^2 L(\sigma^2 + 2\mu\zeta) \right)$. Applying this recursively,

$$\mathbb{E}[F(\bar{w}(t+1)) - F^*] - \Xi_1 \leq \left(1 - \frac{\eta\mu}{2m}\right)^{t+1} (\mathbb{E}[F(\bar{w}(0)) - F^*] - \Xi_1),$$

then we have that

$$\begin{aligned}\mathbb{E}[F(\bar{w}(t)) - F^*] &\leq (1 - \frac{\eta\mu}{2m})^t (\mathbb{E}[F(\bar{w}(0)) - F^*] - \Xi_1) + \Xi_1 \\ &\leq (1 - \frac{\eta\mu}{2m})^t (F(\bar{w}(0)) - F^*) + \Xi_1.\end{aligned}$$

Substituting Ξ_1 for the above equation shows that (10) holds. \blacksquare

A.3 Proof of Theorem 3

The proof of this theorem is the same as the proof of Theorem 1 up to (43). We will not repeat it here, but continue to prove the following parts.

Now we analyze the bounds of $\mathbb{E}[\|\mathbf{w}(t) - \mathbf{1} \otimes \bar{w}(t)\|^2]$. From (11),

$$\begin{aligned}&\sum_{k=1}^K \mathbb{E}[\|w_k(t+1) - \bar{w}(t+1)\|^2] \\ &= \mathbb{E}[\|\mathbf{w}(t+1) - \mathbf{1} \otimes \bar{w}(t+1)\|^2] \\ &= \mathbb{E}[\|(W(t) \otimes \mathbf{I}_n)\mathbf{w}(t) - \eta_t G(\mathbf{w}(t)) - \mathbf{1} \otimes (\bar{w}(t) - \eta_t g(t))\|^2] \\ &= \mathbb{E}[\|(W_B(t) \otimes \mathbf{I}_n)(\mathbf{w}(t+1-B) - \mathbf{1} \otimes \bar{w}(t+1-B)) \\ &\quad - \sum_{\tau=1}^B \eta_{t-B+\tau} (W_{B-\tau}(t) \otimes \mathbf{I}_n)(G(\mathbf{w}(t-B+\tau)) - \mathbf{1} \otimes g(t-B+\tau))\|^2] \\ &= \mathbb{E}[\|(W_B(t) \otimes \mathbf{I}_n)\mathbf{w}(t+1-B) - \mathbf{1} \otimes \bar{w}(t+1-B)\|^2] \\ &\quad + \mathbb{E}[\|\sum_{\tau=1}^B \eta_{t-B+\tau} (W_{B-\tau}(t) \otimes \mathbf{I}_n)(G(\mathbf{w}(t-B+\tau)) - \mathbf{1} \otimes g(t-B+\tau))\|^2] \\ &\quad - 2\mathbb{E}[\langle (W_B(t) \otimes \mathbf{I}_n)\mathbf{w}(t+1-B) - \mathbf{1} \otimes \bar{w}(t+1-B), \\ &\quad \sum_{\tau=1}^B \eta_{t-B+\tau} (W_{B-\tau}(t) \otimes \mathbf{I}_n)(G(\mathbf{w}(t-B+\tau)) - \mathbf{1} \otimes g(t-B+\tau)) \rangle].\end{aligned}$$

Notice that for any $b = 1, \dots, B$, $W_b(t)$ is doubly stochastic, then similar to (44), we have

$$\begin{aligned}(W_b(t) \otimes \mathbf{I}_n)\mathbf{w}(t) - \mathbf{1} \otimes \bar{w}(t) &= (W_b(t) \otimes \mathbf{I}_n)\mathbf{w}(t) - \frac{1}{K}\mathbf{1} \otimes (\mathbf{1}^T \otimes I_n)\mathbf{w}(t) \\ &= (W_b(t) \otimes \mathbf{I}_n)\mathbf{w}(t) - \frac{1}{K}((\mathbf{1} \otimes \mathbf{1}^T) \otimes I_n)\mathbf{w}(t) = (W_b(t) \otimes \mathbf{I}_n - \frac{1}{K}\mathbf{1}\mathbf{1}^T \otimes \mathbf{I}_n)\mathbf{w}(t) \\ &= ((W_b(t) - \frac{1}{K}\mathbf{1}\mathbf{1}^T) \otimes \mathbf{I}_n)\mathbf{w}(t) = ((W_b(t) - \frac{1}{K}\mathbf{1}\mathbf{1}^T) \otimes \mathbf{I}_n)(\mathbf{w}(t) - \mathbf{1} \otimes \bar{w}(t)).\end{aligned}$$

With the fact that (iii) in Assumption 4 $\rho(W_B(t) - \frac{1}{K}(\mathbf{1}\mathbf{1}^T)) < 1$. Let $A = (W_B(t) - \frac{1}{K}\mathbf{1}\mathbf{1}^T)$ and $D = \mathbf{I}_n$ in Lemma 1, we have $\rho((W_B(t) - \frac{1}{K}\mathbf{1}\mathbf{1}^T) \otimes \mathbf{I}_n) = \rho(W_B(t) - \frac{1}{K}\mathbf{1}\mathbf{1}^T) \leq \lambda < 1$. Moreover, $\|(W_B(t) \otimes \mathbf{I}_n)\mathbf{w} - \mathbf{1} \otimes \bar{w}(t)\| = \|((W_B(t) - \frac{1}{K}\mathbf{1}\mathbf{1}^T) \otimes \mathbf{I}_n)(\mathbf{w}(t) - \mathbf{1} \otimes \bar{w}(t))\| \leq \rho(W_B(t) - \frac{1}{K}\mathbf{1}\mathbf{1}^T) \|(W_B(t) \otimes \mathbf{I}_n)\mathbf{w}(t) - \mathbf{1} \otimes \bar{w}(t)\| < 1$.

$\frac{1}{K}\mathbf{1}\mathbf{1}^T)\|\mathbf{w}(t) - \mathbf{1} \otimes \bar{w}(t)\| = \lambda\|\mathbf{w}(t) - \mathbf{1} \otimes \bar{w}(t)\|$. Then, we have

$$\begin{aligned}
& \|\mathbf{w}(t+1) - \mathbf{1} \otimes \bar{w}(t+1)\|^2 \\
& \leq \lambda^2\|\mathbf{w}(t+1-B) - \mathbf{1} \otimes \bar{w}(t+1-B)\|^2 + B \sum_{\tau=1}^B \eta_{t-B+\tau}^2 \mathbb{E}[\|G(\mathbf{w}(t-B+\tau)) - \mathbf{1} \otimes g(t-B+\tau)\|^2] \\
& \quad + \sum_{\tau=1}^B \left(Y\|(W_B(t) \otimes \mathbf{I}_n)\mathbf{w}(t+1-B) - \mathbf{1} \otimes \bar{w}(t+1-B)\|^2 \right. \\
& \quad \left. + \frac{\eta_{t-B+\tau}^2}{Y}\|G(\mathbf{w}(t-B+\tau)) - \mathbf{1} \otimes g(t-B+\tau)\|^2 \right) \\
& \leq \lambda^2(1+BY)\|\mathbf{w}(t+1-B) - \mathbf{1} \otimes \bar{w}(t+1-B)\|^2 \\
& \quad + \eta_{t-B+1}^2(B + \frac{1}{Y}) \sum_{\tau=1}^B (\|G(\mathbf{w}(t-B+\tau))\|^2 - K\|g(t-B+\tau)\|^2),
\end{aligned} \tag{55}$$

where in the first inequality we have used the inequality of arithmetic and geometric means, and Assumption 1 is used to obtain the last inequality, in which $Y = \frac{1}{2B}(\frac{1}{\lambda^2} - 1)$ such that $\lambda^2(1+BY) = \lambda^2(1 + \frac{1}{2}(\frac{1}{\lambda^2} - 1)) = \frac{1}{2}(\lambda^2 + 1) < 1$. Then, the expectation of (55) can be obtained as follows,

$$\begin{aligned}
& \mathbb{E}[\|\mathbf{w}(t+1) - \mathbf{1} \otimes \bar{w}(t+1)\|^2] \\
& \leq \lambda^2(1+BY)\mathbb{E}[\|\mathbf{w}(t+1-B) - \mathbf{1} \otimes \bar{w}(t+1-B)\|^2] + \eta_{t-B+1}^2(B + \frac{1}{Y})BK\chi^2.
\end{aligned} \tag{56}$$

Next, we will analyze the boundedness of $\mathbb{E}[\|\mathbf{w}(t) - \mathbf{1} \otimes \bar{w}(t)\|^2]$ and prove

$$\mathbb{E}[\|\mathbf{w}(t) - \mathbf{1} \otimes \bar{w}(t)\|^2] \leq \frac{\zeta_B}{(t+\Gamma)^2}, \tag{57}$$

by induction, where $\zeta_B := \max \left\{ \Gamma^2 \cdot \mathbb{E}[\|\mathbf{w}(0) - \mathbf{1} \otimes \bar{w}(0)\|^2], \frac{1}{1-\lambda^2} \cdot \frac{\delta^2 B^2 K \lambda^2}{\frac{(\Gamma+1-B)^2}{(\Gamma+1)^2(\lambda^2+1)} - \frac{1}{2}} \right\}$ and Γ satisfies that $\frac{\Gamma+1-B}{\Gamma+1} \geq \sqrt{\frac{1+\lambda^2}{2}}$. Firstly, when $t = 0$, it is obvious that $\mathbb{E}[\|\mathbf{w}(0) - \mathbf{1} \otimes \bar{w}(0)\|^2] \leq \frac{\zeta_B}{\Gamma^2}$ holds according to the definition of ζ_B . Secondly, suppose that for any $t > 0$, there is always $\mathbb{E}[\|\mathbf{w}(t) - \mathbf{1} \otimes \bar{w}(t)\|^2] \leq \frac{\zeta_B}{(t+\Gamma)^2}$. Finally, for $(t+1)$ -th iteration from (56), we have

$$\begin{aligned}
& \mathbb{E}[\|\mathbf{w}(t+1) - \mathbf{1} \otimes \bar{w}(t+1)\|^2] \\
& \leq \lambda^2(1+BY) \cdot \frac{\zeta_B}{(t+1-B+\Gamma)^2} + \eta_{t+1-B}^2 \cdot \frac{1}{\delta^2} \left(\frac{(\Gamma+1-B)^2}{(\Gamma+1)^2} - \lambda^2(1+BY) \right) \zeta_B \\
& \leq \lambda^2(1+BY) \cdot \frac{\zeta_B}{(t+1-B+\Gamma)^2} + \frac{1}{(t+1-B+\Gamma)^2} \cdot \left(\frac{(t+1-B+\Gamma)^2}{(t+1+\Gamma)^2} - \lambda^2(1+BY) \right) \zeta_B \\
& = \frac{\zeta_B}{(t+1+\Gamma)^2},
\end{aligned} \tag{58}$$

where in the first inequality we used the definition of ζ_B and $Y = \frac{1}{2B}(\frac{1}{\lambda^2} - 1)$, and in the second one we used that $\phi(t) = \frac{(t+1-B+\Gamma)^2}{(t+1+\Gamma)^2}$ is a monotone increasing function with $t \geq 0$ and $\eta_t = \frac{\delta}{t+\Gamma}$.

To sum up, the boundedness (57) can be obtained. Then from (43), the following inequality

similar to (48) in Theorem 1 can be obtained,

$$\mathbb{E}[\|\bar{w}(t) - w^*\|^2] \leq \frac{\tilde{\zeta}_B}{t + \Gamma}, \quad (59)$$

where $\tilde{\zeta}_B \triangleq \max\left\{\frac{(6\epsilon L + \sigma^2)\delta^2 m + \frac{2\tilde{\zeta}_B m}{K}}{\mu\delta - m}, \Gamma \cdot \mathbb{E}[\|\bar{w}(0) - w^*\|^2]\right\}$ and $\epsilon \triangleq \frac{1}{K}(F^* - \tilde{F}_k^*)$. \blacksquare